OPTIMUM DESIGN OF 3-D IRREGULAR STEEL FRAMES USING ANT COLONY OPTIMIZATION AND HARMONY SEARCH ALGORITHMS

A THESIS SUBMITTED TO
THE GRADUATE SCHOOL OF NATURAL AND APPLIED SCIENCES
OF
MIDDLE EAST TECHNICAL UNIVERSITY

BY

İBRAHİM AYDOĞDU

IN PARTIAL FULFILLMENT OF THE REQUIREMENTS
FOR
THE DEGREE OF DOCTOR OF PHILOSOPHY
IN
ENGINEERING SCIENCES

AUGUST 2010

Approval of the thesis:

OPTIMUM DESIGN OF IRREGULAR 3-D STEEL FRAMES USING ANT COLONY OPTIMIZATION AND HARMONY SEARCH ALGORITHMS

Submitted by **İBRAHİM AYDOĞDU** in partial fulfillment of the requirements for the degree of **doctor of philosophy in Engineering Sciences Department, Middle East Technical University** by,

Prof. Dr. Canan Özgen _____
Dean, Graduate School of **Natural and Applied Sciences**

Prof. Dr. Turgut Tokdemir _____
Head of Department, **Engineering Sciences**

Prof. Dr. Mehmet Polat Saka _____
Supervisor, **Engineering Sciences Dept., METU**

Prof. Dr. Turgut Tokdemir _____
Co-Supervisor, **Engineering Sciences Dept., METU**

Examining Committee Members:

Prof. Dr. Mehmet Polat Saka _____
Engineering Sciences Dept., METU

Prof. Dr. Gülin Ayşe Birlik _____
Engineering Sciences Dept., METU

Prof. Dr. Mehmet ÜLKER _____
Civil Engineering Dept., Fırat University

Assoc. Prof. Dr. Oğuzhan Hasançebi _____
Civil Engineering Dept., METU

Assoc. Prof. Dr. Ömer Civalek _____
Civil Engineering Dept., Ákdeniz University

Date:

I hereby declare that all information in this document has been obtained and presented in accordance with academic rules and ethical conduct. I also declare that, as required by these rules and conduct, I have fully cited and referenced all material and results that are not original to this work.

Name, Last name:

Signature:

ABSTRACT

OPTIMUM DESIGN OF IRREGULAR 3-D STEEL FRAMES USING ANT COLONY OPTIMIZATION AND HARMONY SEARCH ALGORITHMS

Aydoğdu, İbrahim

Ph.D, Department of Engineering Sciences

Supervisor : Prof. Dr. Mehmet Polat Saka

Co-Supervisor: Prof. Dr. Turgut Tokdemir

August 2010, 185 pages

Steel space frames having irregular shapes when subjected to lateral loads caused by wind or earthquakes undergo twisting as a result of their unsymmetrical topology. As a result, torsional moment comes out which is required to be resisted by the three dimensional frame system. The members of such frame are generally made out of steel I sections which are thin walled open sections. The simple beam theory is not adequate to predict behavior of such thin-walled sections under torsional moments due to the fact that the large warping deformations occur in the cross section of the member. Therefore, it is necessary to consider the effect of warping in the design of the steel space frames having members of thin walled steel sections is significant. In this study the optimum design problem of steel space frames is formulated according to the provisions of LRFD-AISC (Load and Resistance factor design of American Institute of Steel Construction) in which the effect of warping is also taken into account. Ant colony optimization and harmony search techniques two of the recent methods in stochastic search techniques are used to obtain the solution of the design problem. Number of space frame

examples is designed by the algorithms developed in order to demonstrate the effect of warping in the optimum design.

Keywords: optimum structural design, combinatorial optimization, stochastic search techniques, ant colony optimization, minimum weight, steel space frame, warping effect

ÖZ

DÜZENSİZ ÜÇ BOYUTLU ÇELİK ÇERÇEVELERİN KARINCA KOLONİ OPTİMİZASYONU VE HARMONİ ARAMA YÖNTEMLERİ İLE OPTİMUM BOYUTLANDIRILMASI

Aydoğdu, İbrahim

Doktora, Mühendislik Bilimleri Bölümü

Tez Yöneticisi : Prof. Dr. Mehmet Polat Saka

Ortak Tez Yöneticisi: Prof. Dr. Turgut Tokdemir

Ağustos 2010, 185 sayfa

Düzensiz şekle sahip çelik uzay çerçeveler rüzgar veya depremden oluşan yatay yüklerin etkisinde kaldıklarında simetrik olmayan topolojilerinden dolayı burulma dönmesine maruz kalırlar. Bunun sonucunda oluşan burulma momentlerine üç boyutlu çerçevenin karşı koyması gerekir. Genel olarak bu tür çerçevelerin elemanları I şeklinde, açık ve ince cidarlı kesitlerden yapılır. Basit kiriş teorisi burulma momentine maruz ince cidarlı kesitlerin davranışını elemanların kesitlerinde çarpılmadan dolayı oluşan büyük şekil değiştirmeleri nedeniyle belirlemeye yeterli değildir. Bundan dolayı ince cidarlı kesitlerden oluşan çelik uzay çerçevelerin boyutlandırılmasında çarpılmanın göz önüne alınması gerekir. Bu çalışmada çelik uzay çerçevelerin optimum boyutlandırılması problemi LRFD-AISC (Yük ve Direnç Faktörü Tasarımı - Amerikan Çelik Konstrüksiyon Enstitüsü) kurallarına göre çarpılma etkisi göz önüne alınarak formüle edilmiştir. Optimum boyutlandırma probleminin çözümü de stokastik arama yöntemlerinin yeni iki metodu olan karınca kolonisi ve harmoni arama teknikleri ile elde edilmiştir. Çarpılmanın optimum boyutlandırmadaki etkisini göstermek

için geliştirilen algoritma ile uzay çerçeve sistemleri boyutlandırılmıştır.

Anahtar kelimeler: Optimum yapı tasarımı, kombinasyönel optimizasyon, stokastik arama teknikleri, karınca kolonisi optimizasyonu, harmoni arama minimum ağırlık, uzay çelik çerçeve, çarpılma etkisi

To My Family,

For your endless support and love

ACKNOWLEDGEMENTS

I wish to express his deepest gratitude to his supervisor Prof. Dr. Mehmet Polat SAKA for his guidance, advice, criticism, encouragements and insight throughout the research.

Grateful thanks also extended to Assoc. Prof. Dr. Ömer CİVALEK and Assoc. Prof. Dr. Oğuzhan HASANÇEBİ for not only serving as members of my thesis committee but also for offering their invaluable guidance and help.

I should remark that without the sincere friendship of my roommate Alper Akın, this work would not have been come to conclusion. I aprreciate him for his amity. And strongly thanks to Zeynep Özdamar, Erkan Doğan, Serdar Çarbaş, and Ferhat Erdal for their excellent understanding and great help at every stage of my thesis study.

I would also like to appreciate to my friends, especially Semih Erhan, Hakan Bayrak, Refik Burak Taymuş, Fuat Korkut, Özlem Aydın, Hüseyin Çelik, Cihan Yıldırım, Serap Güngör Geridönmez and Kaveh Hassanzehtap for their friendship and encouragement during my thesis.

I owe appreciate to most special person in my life Gülşah Sürekli for her boundless moral support giving me joy of living.

Words cannot describe my gratitude towards the people dearest to me Havvana, Halil, Ömer and Özkan my family; my mother, my father and my brothers. Their belief in me, although at times irrational, has been vital for this work. I dedicate this thesis to them.

TABLE OF CONTENTS

ABSTRACT iv

ÖZ vi

ACKNOWLEDGEMENTS ix

TABLE OF CONTENTS x

LIST OF FIGURES xvi

LIST OF TABLES xix

CHAPTERS

1. INTRODUCTION 1

1.1 Optimization 1

1.2.1 Design variables 2

1.2.2 Objective function 2

1.2.3 Constraints 3

1.2.4 Mathematical modeling of the optimization problem 3

1.3 Structural optimization 6

1.3.1 Mathematical modeling of structural optimization 6

1.3.2 Methods of Structural optimization 7

1.4 Stochastic search methods 9

1.4.1 Genetic algorithm 10

1.4.2 Evolutionary strategies 11

1.4.3 Simulating annealing 12

1.4.4 Particle Swarm Optimization Method 12

1.4.5 Tabu Search 13

1.4.6 Ant colony optimization 14

1.4.7 Harmony search 14

1.5 Literature survey of structural optimization 15

1.6 Irregular Frames and the effect of warping 16

1.7 Literature survey on structural optimization that considers effect of warping 17

1.8 Scope of the thesis 18

2. MATRIX DISPLACEMENT METHOD FOR 3-D IRREGULAR STEEL FRAMES 20

2.1 Introduction 20

2.2 Matrix displacement method for 3-D frames 21

2.2.1 Relationship between member end forces and member end displacements 22

2.2.2 Coordinate transformation 25

2.2.3 Relationship between external loads and member end forces 36

2.2.4 Overall stiffness matrix..... 38

2.2.5 Member end conditions 40

2.2.6 General steps for 3-D frame analysis 52

2.3 The effect of warping in thin walled members 52

2.4 Numerical examples 59

2.4.1 Numerical example eight member 3-D frame..... 59

2.4.2 Two-bay two-storey three dimensional irregular frame 64

2.4.3 468 Member twenty storey three dimensional irregular frame..... 66

3. DESIGN OF STEEL BEAM-COLUMN MEMBER ACCORDING TO LRFD-AISC INCLUDING EFFECT OF WARPING..... 72

3.1 Introduction..... 72

3.2 Design of steel beam-column members 73

3.2.1 Design of steel beam-column members without considering the effect of warping..... 73

3.2.2 Strength constraints with considering the effect of warping 86

4. ANT COLONY OPTIMIZATION AND HARMONY SEARCH METHODS 88

4.1 Introduction 88

4.2 Ant colony optimization 89

4.2.1 Natural behavior of ants 89

4.2.2 Method 90

4.3 Harmony search algorithm 93

4.3.1 Initialization of harmony memory matrix: 94

4.3.2 Evaluation of harmony memory matrix: 95

4.3.3 Improvising a new harmony: 95

4.3.4 Update of harmony matrix: 96

4.3.5 Check stopping criteria: 97

4.4 Numerical Applications 99

4.4.1 Travelling Salesman Problem 99

4.4.2 Continuous Optimization Problem 1 104

4.4.3 Continuous Optimization Problem 2 106

4.4.4 Welded cantilever beam design 107

5. OPTIMUM DESIGN OF STEEL SPACE FRAMES 112

5.1 Introduction..... 112

5.2 Discrete optimum design of space steel frames to LRFD- AISC 113

5.2.1 The objective function 113

5.2.2 Constraints functions 114

5.3 Optimum Structural Design Algorithms 120

5.3.1 Ant colony optimization based optimum design algorithm..... 120

5.3.2 Improvements in ant colony optimization algorithm 124

5.3.3 Harmony search algorithm for frame design problem 128

5.3.4 Improvements in the harmony search algorithm..... 130

6. DESIGN EXAMPLES 131

6.1 Introduction..... 131

6.2 Two- story, two-bay irregular steel space frame 132

6.3 Five-story, two-bay regular steel space frame 134

6.4 Four-story, three bay 132 members space frame 138

6.5 Twenty-story, 460 members irregular space frame..... 144

6.6 Ten-story, four-bay steel space frame 149

6.7 Twenty-story, 1860–member, steel space frame 154

6.7 Discussion 162

7. SUMMARY AND CONCLUSIONS 166

7.1 Recommendations for future work 168

REFERENCES 171

CURRICULUM VITAE 185

LIST OF FIGURES

FIGURES		
Figure 2.1	3-D frame	21
Figure 2.2	Joint end displacements, end forces and end moments in frame members	22
Figure 2.3	Member forces and moments for degree of freedoms	24
Figure 2.4	Rotation of g about x axis	26
Figure 2.5	Rotation of a about y axis	28
Figure 2.6	Rotation of b about z axis	30
Figure 2.7	Coordinate transformation from local axis to global axis	32
Figure 2.8	Calculation of the length of an element	34
Figure 2.9	Local coordinates of vertical member in +Y direction	36
Figure 2.10	Local coordinates of vertical member in -Y direction	37
Figure 2.11	8 members 3-D frame	40
Figure 2.12	Position of stiffness matrix terms for 8 members 3-D frame	41
Figure 2.13	3-D frame member having a hinge connection at its first end	42
Figure 2.14	3-D frame member having a hinge connection at its second end	46
Figure 2.15	3-D frame member having a hinge connections at both ends	50
Figure 2.16	Warping effect of thin walled beam	54
Figure 2.17	Beam element subjected to the torsion	57
Figure 2.18	Twisting torque acting on beam element	58
Figure 2.19	Eight member 3-D frame	61
Figure 2.20	Beam Element subjected to the torsion	66
Figure 2.21	3-D view of twenty-story, three-bay irregular frame	69
Figure 2.22	Plan view of twenty-story, three-bay irregular frame	70
Figure 2.23	Displacements of twenty-story, three-bay irregular frame	71
Figure 2.24	Rotations of twenty-story, three-bay irregular frame	72

Figure 4.1	Natural behavior of ants.	91
Figure 4.2	Improvising new harmony memory process	97
Figure 4.3	Flowchart of harmony search algorithm.	99
Figure 4.4	A simple travelling Salesman Problem	100
Figure 4.5	Initial cities of ants at the beginning of the problem	102
Figure 4.6	Selection of second city for Ant	103
Figure 4.7	7 Position of ants at the end of first iteration	103
Figure 4.8	Position of ants at the end of (a) second, (b) third and (c) fourth iterations	104
Figure 4.9	Welded cantilever beam	109
Figure 5.1	Beam-Columns Geometric Constraints	121
Figure 6.1	Two-story, two bay irregular frame	133
Figure 6.2	Design histories of two-story, two bay irregular frame	136
Figure 6.3	Plan view of five-story, two bay steel frame	137
Figure 6.4	3D View of the five-story, two bay steel frame	137
Figure 6.5	Design histories of the five-story, two bay steel frame	139
Figure 6.6	3D view of four-story, three bay space frame	140
Figure 6.7	Side view of four-story, three bay space frame	141
Figure 6.8	Plan view of four-story, three bay space frame	141
Figure 6.9	Design histories of the 132-member space frame	143
Figure 6.10	3D view of twenty-story, irregular steel frame	146
Figure 6.11	Side view of twenty-story, irregular steel frame	147
Figure 6.12	Plan view of the twenty-story, irregular steel frame	148
Figure 6.13	Design histories of the twenty-story, irregular steel frame	150
Figure 6.14	3-D view of ten-storey, four-bay steel space frame	151
Figure 6.15	Side view of ten-storey, four-bay steel space frame	152
Figure 6.16	Side view of ten-storey, four-bay steel space frame	152
Figure 6.17	Design histories of the ten-storey, four-bay steel space frame	155
Figure 6.18	3-D view of twenty-storey, 1860 member steel space frame	157
Figure 6.19	Plan views of twenty-storey, 1860 member steel space frame	159

Figure 6.20	Design histories of the twenty-storey, 1860 member steel space frame	163
Figure 6.21	The effect of warping in the optimum design of six steel space frames	165
Figure 6.22	Comparison of the effect of warping with respect height of frame	167

LIST OF TABLES

TABLES

Table 2.1	Type of hinge conditions	42
Table 2.2	Input data of eight member 3-D frame	62
Table 2.3	Joint displacements of eight member 3-D frame	63
Table 2.4	Member end forces of eight member 3-D frame	63
Table 2.5	Joint displacements of eight member 3-D frame obtained by STRAND7	64
Table 2.6	Member end forces of eight member 3-D frame obtained by STRAND7	65
Table 2.7	Displacements (excluding warping effect)	67
Table 2.8	Displacements (including warping effect)	67
Table 2.9	Member end forces (excluding warping effect)	67
Table 2.10	Member end forces (including warping effect)	68
Table 2.11	Assigned sections for each group	70
Table 2.12	Stresses for twenty-story, three-bay irregular frame	73
Table 4.1	Distances between cities	101
Table 4.2	Visibility Matrix	101
Table 4.3	Calculation of global updates	105
Table 4.4	Optimum solutions of continuous optimization problem 1	106
Table 4.5	Optimum solutions of continuous optimization problem 1	107
Table 4.6	Optimum solutions for example 3	111
Table 5.1	Displacement limitations for steel frames	118
Table 6.1	Design results of two-story, two bay irregular frame	134
Table 6.2	Beam gravity loading of the five-story, two bay steel frame	136
Table 6.3	Design results of the five-story, two bay steel frame	138
Table 6.4	Gravity loading on the beams of 132-member space frame	142
Table 6.5	Lateral loading on the beams of 132-member space frame	142

Table 6.6	Design results of the 132-member space frame	144
Table 6.7	Design results of the twenty-story, irregular steel frame	149
Table 6.8	Horizontal forces of ten-storey, four-bay steel space frame	153
Table 6.9	Design results of the ten-storey, four-bay steel space frame	155
Table 6.10	Design results of the twenty-storey, 1860 member steel space frame	161
Table 6.11	Comparison of optimum design weights of all design examples	165

CHAPTER 1

INTRODUCTION

1.1 Optimization

Optimization is a branch of mathematics where the maximum (or the minimum) of a function is sought under number of constraints if there are any. Optimization techniques determine the best alternative among the available options while satisfying the required limitations. In nature animals or plants use optimization instinctually in such a manner that minimizes the path for finding foods or maximize energy for hunting. Human beings also use optimization several stages of their lives. The importance of optimization is permanently increasing in today's world due to limitations in available resources and increase in human population. Optimization plays important role in the large variety of fields such as applied mathematics, computer science, engineering and economics.

1.2 Optimization Problem

General optimization problems have three elements which are required to be identified in order to construct its mathematical model. The first one is design variables. The second is the objective function and the third is constraints.

1.2.1 Design variables

A design variable in an optimization problem is a quantity change of which affects the outcome of the problem. In structural engineering problems cross sectional dimensions of structural member such as width, height and thickness can be selected as design variables because when their values change behavior of the structure chance. Design variables can be divided to two categories; continuous and discrete design variables. Continuous variable is a variable that can take any value in its range. For example, a depth of a built-up steel beam can have any value between its upper and lower bounds. Hence in the optimum design problem of a built up steel beam the depth can be treated as continuous design variable. On the other hand, discrete design variables can only take certain values from a list of values. The optimum design of steel frames requires selecting steel profiles from available list in practice which contains only list of sections that are discrete. Number of bolts in the connection is also required to be an integer number. This is also a typical example of discrete variable, if number of bolts in the optimum design of beam column connection is taken as design variable. Although optimization problems with discrete design variables are more suitable for engineering design problems, they are more difficult to handle than the optimization problems with continuous design problems.

1.2.2 Objective function

Objective function is a function of design variables that determines the quality of a solution. In other words objective function determines effectiveness of the design under consideration. Optimization problem becomes either minimization or maximization problem depending on the objective of a problem. For example, if in a structural design problem deflection of a beam is required to be as small as possible, it is then necessary to maximize the stiffness of the beam. In this problem the objective function is required to be maximized. On the other hand, if the aim is to design a structure using the least amount of steel then the objective

becomes minimizing the weight of the structure. Such problems are called minimization problems.

1.2.3 Constraints

In optimization problem generally values of the design variables can not be selected arbitrarily. Solutions of the optimization problems have to satisfy some restrictions in the optimization problem. These restrictions are called as constraints. Constraints may be categorized in two groups in structural optimization problems which are behavior constraints and size constraints. Size constraints are the limitations that make sure that values of the design variables are assigned only with in a certain range. For example in a beam cross section design problem, height and width variables are limited to their upper and lower values. Such constraints are called as side constraints. In contrast to side constraints, behavior constraints impose restraints on the behavior or performance of the system. For instance in structural optimization problem, displacements are required to be not larger than certain limits in order to satisfy the serviceability conditions. Furthermore each member of a structure should have sufficient strength to be able to resist the internal forces which develop under the external loads. Hence displacement limitations and strength limitation which are taken from design code specifications are called behavior constraints.

1.2.4 Mathematical modeling of the optimization problem

After definition of the elements of optimization problem, mathematical modeling of the optimization problem is expressed as follows:

$$\text{Find values of design variables } X^T = [x_1, x_2, \ldots, x_n] \tag{1.1}$$

in order to minimize, $f(x_1, x_2, ..., x_n)$ (1.2)

subject to

$$g_1(x_1, x_2 \ldots, x_n) \le 0,\ g_2(x_1, x_2, \ldots, x_n) \le 0, \ldots g_{nic}(x_1, x_2, \ldots, x_n) \le 0$$

$$h_1(x_1, x_2 \ldots, x_n) = 0,\ h_2(x_1, x_2, \ldots, x_n) = 0, \ldots h_{nec}(x_1, x_2, \ldots, x_n) = 0 \quad (1.3)$$

where, n is the total design variables in optimization problem, $X^T = [x_1, x_2, \ldots, x_n]$ is the vector of design variables, $f(x_1, x_2, ..., x_n)$ is the objective function, $g(x_1, x_2 \ldots, x_n) \le 0$ is the inequality constraints and $h_1(x_1, x_2 \ldots, x_n) = 0$ is the equality constraints.

1.2.5 Optimization Techniques

The techniques available to find the solution of optimization problems may be traced back to the days of Lagrange, Cauchy and Newton [1]. The contributions of Newton and Leibnitz to calculus provided a development of differential calculus methods of optimization. The calculus of variations related to the minimization of a function goes back to Bernoulli, Euler, Lagrange, and Weirstrass [1]. The method of optimization for constrained problems involving addition of unknown multipliers invented by Lagrange [1]. The first application of the steepest descent method to solve unconstrained minimization problems was made by Cauchy. Despite these early contributions, it is noticed that until the middle of the twentieth century there is little improvisations in optimization. After the middle of the twentieth century emergence of high-speed digital computers made the implementation of the numerical optimization procedures possible and stimulated further research on new methods. As a result of extended research large

amount of new numerical optimization techniques are developed which made it possible to find optimum solutions of various engineering problems. In 1947, Dantzig [2] developed the simplex method for linear programming problems. In 1957, Bellman [3] developed the principle of optimality for dynamic programming problems. These developments pave the way to improvement of the methods of constrained optimization by Kuhn and Tucker [4]. Kuhn and Tucker expressed the conditions for the optimal solution of programming problems. This work laid the foundations for a great deal of numerical methods for solving the nonlinear programming problems.

During the early 1960s Zoutendijk and Rosen [5] suggested method of feasible directions which obtains the solution of nonlinear programming problems where the objectives function and the constraints are nonlinear. In the l960s, Duffin, Zener, and Peterson [6] developed the well-known technique of geometric programming which have ability of solving complex optimization problems. Carroll [7], Fiacco and McCormick [8] presented penalty function method for nonlinear programming problems. These techniques were applied to determine the solution of wide variety of engineering design problems and it is observed that while they were efficient in finding the solution of some of these design problems, they were not performing well in some others. Furthermore, in large size design problems they exhibited convergence difficulties. Their success was dependent upon the type of optimization problem. It is observed that none of these newly developed techniques were powerful enough to determine the optimum solution of any general nonlinear programming problem. These methods were particularly non-efficient in finding the solutions of nonlinear programming problems where the design variables are required to be selected from a discrete set. In practice when formulated as programming problem large number of engineering design optimization problems turn out to be discrete programming problems.

The stochastic search techniques developed by Dantzig and Charnes has provided an efficient tool for solving discrete programming problems [9-28]. Genetic

algorithm, evolutionary strategies, simulating annealing, tabu search, ant colony optimization and particle swarm optimization algorithms are some of the stochastic search techniques that are also used to develop structural optimization algorithms [29]. These techniques are nontraditional search and optimization methods and they very suitable and robust obtaining the solution of discrete optimization problems.

1.3 Structural optimization

In recent years, importance of the structural optimization has increased rapidly due to demand for economical and reliable structures. Structural optimization deals with finding the appropriate cross sectional properties of structural members such that the structure has the minimum cost and the response of the structure to external loads are within the limitations specified by design codes.

1.3.1 Mathematical modeling of structural optimization

Mathematical modeling of a structural optimization problem can be stated as in the following.

$$\text{Find cross-sectional area vectors } A^T = \left[A_1, A_2, \ldots, A_{ng}\right] \tag{1.4}$$

$$\text{in order to minimize, } W(A_1, A_2, ..., A_{ng}) = \sum_{k=1}^{ng} A_k \sum_{i=1}^{mk} \rho_i L_i \tag{1.5}$$

$$\text{subject to } g_1 \le 0,\ g_2 \le 0, \ldots g_n \le 0 \tag{1.6}$$

where, ng is the total numbers of member groups in the structural system, mk is the total number of members in group k, A_k is the cross sectional area of members in group k, L_i is the length of member i, ρ_i is the specific gravity of an element i, and $g_1, g_2, ..., g_n$ are the constraint functions. Constraint functions are described by design codes such as LRFD-AISC [30], TS648 [31]. According to LRFD-AISC design code constraint functions can be expressed as:

1. Strength Constraints. It is required that each frame member should have sufficient strength to resist the internal forces developed due to factored external loading.

2. Serviceability constraints. Deflection of beams and lateral displacement of the frame should be less than the limits specified in the code.

3. Geometric constraints. Sections that are to be selected for columns and beams at each beam-column connection and column-column connection should be compatible so that the connection can be materialized. Detailed information of these constraints will be given in the next chapter.

1.3.2 Methods of Structural optimization

There are large amount of methods developed that may be used to determine the solution of optimum design problems [8-29]. These can be collected under two broad categories. The fists one is the analytical methods and the second is the numerical optimization techniques.

1.3.2.1 Analytical methods

Analytical methods are usually used for finding minimum and maximum values of a function by using classical mathematical tools such as theory of calculus and variational methods. In structural engineering these methods are used in studies of optimal layouts or geometrical forms of structural elements [32]. These methods find the optimum solution as the exact solution of system of equations which expresses the conditions for optimality. Although analytical methods are good tools for fundamental studies of single structural components, they are not suitable to determine the optimum solution of large scale structural systems.

1.3.2.2 Numerical Optimization Methods

Numerical optimization methods that are used to develop optimum structural design algorithms are summarized in the following:

Mathematical programming

Mathematical programming attempts to determine the minimum or maximum of a function of continuous variables under certain constraint functions. Mathematical programming techniques are generally classified as linear programming and nonlinear programming. In linear programming the objective function and the constraint consist of linear functions of design variables. In nonlinear programming methods either the objective function and/or constraints are nonlinear functions of design variables. Nonlinear programming techniques initiate the search for optimum from an initial point and move along the gradient of the objective function in order to achieve reduction in the value of the objective function while satisfying the constraints. Although mathematical programming techniques show good performance in small size optimization problems, they are weak and present convergence difficulties in the large scale optimization problems [33].

Optimality criteria method

Optimality criteria method is a rigorous mathematical method that is introduced by Prager and Shield [34]. This method consists of two complimentary main parts. The first part is Kuhn-Tucker conditions of nonlinear programming and the second one is Lagrange multipliers. Optimality criteria method is based on the assumption that some characteristic will be attained at the optimum solution. The well-known application of optimality method is the fully stressed design technique. It is assumed that, in an optimum design, each member of a structure is fully stressed at least one design loading condition. Optimality criteria methods have been used effectively in structural optimization problems because they constitute an adequate compromise in order to obtain practical and efficient solutions. [35-37]. Optimality criteria method is applied as two step procedure. In first step, an optimality criteria is derived either using Kuhn-Tucker conditions or using an intuitive one such as the stipulation that the strain energy density in the structure is uniform. In the second step an algorithm is developed to resize the structure for the purpose of satisfying this optimality criterion. Again a rigorous mathematical method may be used to satify the optimality criterion, or one may devise an ad-hoc method which sometimes works and sometime does not work. In optimality criteria methods the design variables are considered to be having continuous values. However, with some alteration these methods can also be used in solving discrete optimization problems.

1.4 Stochastic search methods

The stochastic search algorithms developed recently has provided an efficient tool for solving large scale problems [9-28]. These stochastic search algorithms make use of the ideas taken from the nature and do not require gradient computations of the objective function and constraints as is the case in mathematical programming

based optimum design methods. The basic idea behind these techniques is to simulate the natural phenomena such as immune system, survival of the fittest, finding shortest path, particle swarm intelligence and the cooling process of molten metals into a numerical algorithm. These methods are nontraditional search and optimization methods and they are very efficient and robust methods obtaining the solution of large size optimization problems. They use probabilistic transition rules not deterministic rules. Large number of optimum structural design methods based on these effective, powerful and novel techniques is developed in recent years [38-52]. Some of the stochastic search methods are summarized in the following.

1.4.1 Genetic algorithm

Genetic algorithm is one of the famous stochastic search algorithms developed from evolutions theory such as crossover, inheritance, selection and mutation. Genetic algorithms are famous in evolutionary algorithms that categorized as global search heuristics. Theory of this method depends on the principle of Darwin's theory of survival fittest. This can be summarized that any individual animal or plant which succeeds in reproducing itself is "fit" and will contribute to survival of its species, not just the "fittest" ones, though some of the population will be better adapted to the circumstances than others [53, and 54]. Genetic algorithm are constituted three main phases [55]. These are,

- coding and decoding variables into strings;
- evaluating the fitness of each solution string;
- Applying genetic operators to generate the next generation of solution strings.

Genetic algorithms can be used for wide range of optimization problems, such as optimal control problems, transportation problems, economical problems, structural engineering problems, etc. This technique can be used in structural

optimization problems involving both discrete and continuous variables. Genetic algorithms have been so effective and robust method in solving both constrained and unconstrained optimization problems. Therefore this technique one of possible optimization method applied for structural engineering problems.

1.4.2 Evolutionary strategies

The evolution strategies (ES) were first developed by Rechenberg [56] and Schwefel [57] in 1964 at Technical University of Berlin as an experimental optimization technique. These algorithms were originally developed for continuous optimization problems. This optimization technique is based on ideas of adaptation and evolution has very complex mutation and replacement functions. Initial populations consisting of μ parent individuals are randomly generated in evolution strategies algorithm. It then uses recombination, mutation and selection operators to attain a new population.

Rajasekaran et al [58] used the evolutionary strategies for the solution of optimum design of large scale steel space structures. It is reported in this study that evolutionary strategies algorithms show good performance in finding the optimum design of large size structures. Ebenaua et al [59] and Hasançebi et al [60] also presented studies about optimum design of large scale structures by using the evolutionary strategies method. In these studies, it is shown that the evolutionary strategies methods are efficient methods in order to determine the optimum solutions of large scale structures. Hence, it is concluded that the evolutionary strategies method is one of the robust optimization methods for structural optimization problems.

1.4.3 Simulating annealing

Simulated annealing (SA) is one of the commonly used stochastic search techniques for the structural optimization problem. This algorithm was invented by S. Kirkpatrick et al in 1983 [61]. Name of the simulating annealing algorithm comes from annealing in metallurgy. This technique involves controlled cooling and heating processes of a material in order to expand the size of its crystals and decrease their defects. The heat causes the atoms to leave from their initial positions (a local minimum of the internal energy) and move randomly through states of higher energy; the slow cooling gives the atoms enough time to find positions that minimize a steady state is reached. Simulating Annealing algorithm starts with initial design which is randomly created. Then initial value of the temperature is set. New structure designs are generated in the close neighbor of the current structure design. Objective function values of new structure designs are calculated and temperature is decreased. This process is repeated when the system is frozen in an optimum state at a low temperature. There are many publications about simulated annealing algorithm for structural optimization problems. In 1991 and 1992, Balling [62, 63] used simulated annealing method for the discrete optimum design of three dimensional steel frames. Topping [64], Hasançebi and Erbatur [65 and 66] used this algorithm for optimum design of +truss systems. It can be concluded that this method is efficient tool for structural optimization problems.

1.4.4 Particle Swarm Optimization Method

Particle swarm optimization is one of the stochastic optimization technique based algorithm to find a solution to an optimization problem in a search space or model and predict social behavior in the presence of objectives. This method is first described in 1995 by James and Russell C. Eberhant [24] inspiring social behavior of bird flocking or fish schooling.

Particle swarm optimization algorithm can be summarized as follows. Initially populations of individuals known as particles are selected randomly. These particles generate structure designs by using random guesses. Then an iterative process is initiated in order to improve these structure designs. Particles iteratively calculate the value of the objective function of structure and the location where they had their best design is stored. Best structure design is defined as the local best or the best particle. Best particle, its design and location can be also seen from its neighbors. This information guides the movements in the design space. In the past fifteen years, there are many studies on particle swarm optimization method. Fourie and Groenwold [67] published a paper about particle swarm optimization method for optimum design of structures with sizing and shape variables. Perez and Behdinan [68] presented a study about optimum design algorithm for pin jointed steel frames problems which is based on particle swarm optimization method. It is reported from studies that particle swarm optimization method shows effective performance in structural design optimization.

1.4.5 Tabu Search

Tabu search is one of the stochastic search methods introduced by Glover [69] in 1989. This method uses a neighbor search procedure. New solution x' is obtained by moving iteratively from a solution x in the neighborhood of x. This procedure is continued by the time that one of the some stopping criteria is satisfied. Tabu search method modifies the neighborhood structure of each design as the search progresses in order to search the regions of the unused design space. The solutions admitted to $N^*(x)$, the new neighborhood, are determined through the use of memory structures. "*The search then progresses iteratively by moving from a solution x to a solution x' in* $N^*(x)$ "[70].

Degertekin et al used tabu search method to develop an optimum design algorithm for steel frames [71-75]. Hasançebi et al [60] applied tabu search method for optimum design of design of real size pin joints structures. Similar to

aforementioned stochastic search methods tabu search method is popular among researches for structural optimization problems.

1.4.6 Ant colony optimization

Ant colony algorithm is inspired from natural behavior of ants. This technique is one the robust techniques for structural optimization problems. Detailed information about this algorithm will be given in the following chapters.

1.4.7 Harmony search

Harmony search algorithm is one of the recent stochastic search algorithms adopted from composition of musical harmony. This algorithm was inspired by the observation of music improvisation. Trying to find a pleasing harmony in a musical performance is analogous to finding the optimum solution in an optimization problem. The aim of the musician is to procedure a piece of music with harmony. Similarly a designer intends to determine the best design in a structural optimization problem under the given objective and limiting constraints. Both have the same target; to determine the best. This method is also an efficient method for structural optimization problems. Detailed information about this algorithm is also provided in the following chapters.

1.5 Literature survey of structural optimization

The early studies of structural optimization problems utilized mathematical programming aalgorithms such as integer programming, branch and bound method and dynamic programming or optimality criteria method [76-78]. In some of these algorithms the design requirements of structural optimization problem are implemented from design codes. Among these Saka [79] has presented a study about optimum design of pin jointed steel structures with optimality criteria algorithm where the design requirements were imposed from Allowable Stress Design of American Institute of Steel Construction (ASD-AISC). In 1990, Grierson and Cameron [80] introduced SODA (Structural optimization design) that was the first structural optimization package software for practical structure design. This software considered the design requirements from Canadian Code of Standard Practice for Structural Steel Design (CAN/CSA-S16-01 Limit States Design of Steel Structures) and obtained optimum desogn of steel frames by using available set of steel sections.

C.M. Chan and Grierson [81] and C.M. Chan [82] pubished a study about the design of tall steel building frameworks with optimization technique based on the optimality criteria method where areas are of member sections selected from the standard steel sections. This method considers the inter storey drift, strength and sizing constraints in accordance with building code and fabrications requirements. Soegiarso and Adeli [83] developed an algorithm for the minimum weight design of steel moment resisting space frame structures with or without bracing by using the optimality criteria method according to LRFD-AISC design code. Constraints functions for moment resisting frames derived from the LRFD-AISC design code are highly nonlinear and implicit functions of design variables. In this study, the steel moment resisting space frame is subjected to the dead, live and wind loads computed according to the Unified Building Code. The algorithm is performed in optimum structural design problems of four large high-rise steel building

structures. Arora [84] published comprehensive review of the methods for discrete structural optimization problems.

The emergence of stochastic search optimization techniques has opened a new era in obtaining the solution of discrete optimization problems. In literature there are many studies have been done for structural optimization problems by using stochastic search techniques [11, 14-18, 24, 26-28, 61, 85 and 86] and these methods show good performance in structural optimization problems. Ant colony optimization algorithm (ACO) introduced by Marco Dorigo [9, 22, 87-90] is one of the stochastic search methods that locate the optimum solution of combinatorial optimization problems. This method is inspired from the behavior of ants in finding the shortest path from the nest of a colony to food source. This method is firstly used in the solution of well known traveling salesman problem (TSP). In 2000, ant colony optimization algorithm is applied optimization problem of structural system [93]. In 2004, study about ant colony optimization method for optimum design of truss systems problems was introduced by Camp and Bichon [94]. Camp and Bichon [95] also presented a study ant colony optimization method for optimum design of frame structures problems in 2005. Another recent addition to these techniques is the harmony search algorithm. This method is first developed by Geem [25, 96-101]. Harmony search algorithm is based on the musical performance process that takes place when a musician searches for a better state of harmony. Harmony search method is widely applied in structural design optimization problems since its emergence [102]. These applications have shown that harmony search algorithm is robust, effective and reliable optimization method [33].

1.6 Irregular Frames and the effect of warping

Steel buildings are preferred in residential as well as commercial buildings due to their high strength and ductility particularly in regions which are prone to

earthquakes. Some of these buildings have irregular shapes due to architectural considerations. Such three dimensional buildings when subjected to lateral loads caused by wind or earthquakes undergo twisting as a result of their unsymmetrical topology. This occurs due to the fact that the resultant of lateral loads acting on the building does not pass through the shear center of the structure. As a result, torsional moment comes out which is required to be resisted by the three dimensional framing system. The members of steel frames are generally made out of steel I sections which are thin walled open sections. The simple beam theory is not adequate to predict behavior of such thin-walled sections under torsional moments. The large warping deformations occur in the cross section of the member due to the effect of torsional moments. This causes plane sections to warp and plane sections do not remain plane. Therefore normal stresses develop in addition to shear stresses in the member. Computation of these additional stresses can easily be carried out by using the theory derived by Vlasov [103]. The simplicity of this theory is that it includes additional terms in simple bending expressions to accommodate the effect of warping. This expression requires the computation of the sectorial coordinate and warping moment of inertia of thin walled open section.

1.7 Literature survey on structural optimization that considers effect of warping

In 1961, Vlasov developed a theory which simplifies the computation of stresses caused by warping of thin walled sections. Attard [104] carried out investigation on the nonlinear analysis of thin-walled beams including warping effect. Gotluru et al [105] and Chu et al [106] studied the effect of warping on thin walled cold formed steel members. Tso [107], Trahair and Yong Lin Pi [108-110] presented a study on the nonlinear elastic analysis torsion of thin walled steel beams. However, these studies analyze the effect of warping on the basis of the element. Al-Mosawi and Saka [112] developed shape optimization algorithm for cold-

formed thin-walled steel sections that considers the effect of warping. This study also considers only single element. Saka et al later presented study on the optimum spacing design of grillage system considering the effect of warping. This study one of the few studies which investigate the effect of warping at the level of structure. However, grillage systems are small scale structures. Therefore, this study is not adequate to give information about the effect of warping for large scale structures.

1.8 Scope of the thesis

The main goal of this study is to investigate the effect of warping for optimum design of irregular steel space frames. Ant colony optimization and harmony search algorithms are the selected optimization methods in order to solve the optimization problem formulated. In this thesis, chapters are arranged as in the following. In the first chapter, general definition about optimization, elements of optimization problems, some optimization methods that are used in structural optimization problems are discussed briefly. Besides these, a literature survey on the optimum design of frame structures and the effect of warping is included in a historical order. In the second chapter, the matrix displacement method for 3-D frames and the theory of the effect of warping are described. In addition to these, a computer program written in FORTRAN which has the feature of analysis of 3-D frames excluding or including effect of warping is tested considering number of 3-D frames. The results obtained from this computer program are verified with those attained using the software STRAND7 [113]. The design of steel members that are subjected to axial force as well as bending moments according to design code LRFD-AISC [30] is described in the Chapter 3. In the fourth chapter, optimization methods of harmony search and ant colony optimization that are used in thesis are explained. Besides, performance these methods are tested with

other optimization methods using some sample mathematical optimization problems. Mathematical problem of structural optimization problem, harmony search and ant colony optimization algorithms for structural optimization problems and improvements in harmony search and ant colony optimization algorithms are described in the Chapter 5. The last two parts of this study are allocated for design examples and conclusions, respectively. In the Chapter 6, six design examples two of which are regular steel space frames and four of which are irregular steel space frame are designed by the ant colony optimization and harmony search algorithms developed and the results obtained are presented. The last chapter, Chapter 7 contains the conclusions of the study.

CHAPTER 2

MATRIX DISPLACEMENT METHOD FOR 3-D IRREGULAR STEEL FRAMES

2.1 Introduction

High-rise steel buildings are sometimes given irregular shapes and unsymmetrical floor plans so that they posses impressive images. Such three dimensional structures undergo twisting as a result of their unsymmetrical topology when they subjected to lateral loads. This occurs due to fact that the resultant of lateral forces acting on building does not passing trough to shear center of the structure. As a result, torsional moment that comes out due to this eccentricity is required to be resisted by the three dimensional frame system. The members of such frames are generally made out of steel W sections that are thin walled open sections with relatively small torsional rigidity. Consequently, when these members subjected to torsional moments, large warping deformations occurs in the cross sections these members. Plane sections does nor remain plane and normal stresses develop at cross sections of these members in addition to shear stresses. It is shown in the literature that the values of these stresses are significant and they are required to be considered in predicting the realistic behavior of thin walled members [114].

In this chapter, firstly the classical matrix displacement method for 3-D frames is described and later it is extended to cover the inclusion of the effect of warping. A computer program is coded in FORTRAN which has the feature of analysis of 3-D frames excluding or including effect of warping. The program written is tested

considering number of 3-D frames the results obtained are verified with those attained using the software STRAND7 [113].

2.2 Matrix displacement method for 3-D frames

In matrix displacement method, a 3-D frame considered to be system consists of connecting one-dimensional elements to each other at joints as shown in figure 2.1. The joint coordinates are defined according to the XYZ Cartesian system which is called global axis system. There are six degree of freedoms located in a joint of 3-D frame. These are the usual three translations (d_1 , d_2 , d_3) along X, Y, and Z axes and three rotations (d_4 , d_5 , d_6) about these axes shown Figure 2.1. Therefore, the displacement vector of any joint i, can be represented in a vector form as $\{D_i\} = \{d_1\ d_2\ d_3\ d_4\ d_5\ d_6\}$ in the global axis. The corresponding loading vector applied on joint i is demonstrated as $\{P_i\} = \{P_1\ P_2\ P_3\ P_4\ P_5\ P_6\}$. In this vector; P_1 , P_2 , P_3 are forces acting on joint i along X, Y, and Z axis respectively and P_4 , P_5 , P_6 are moments acting on this joint along X, Y, and Z axis, respectively.

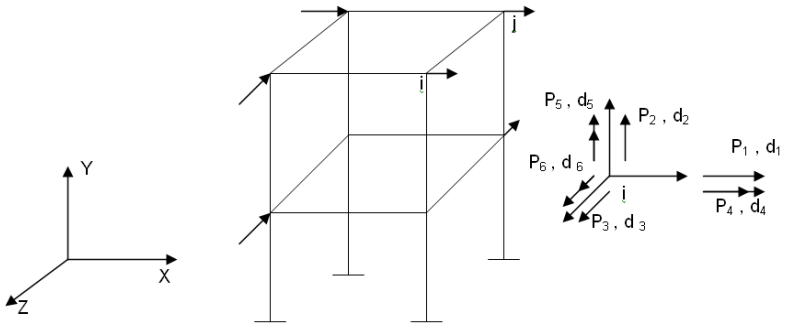

Figure 2.1 3-D frame

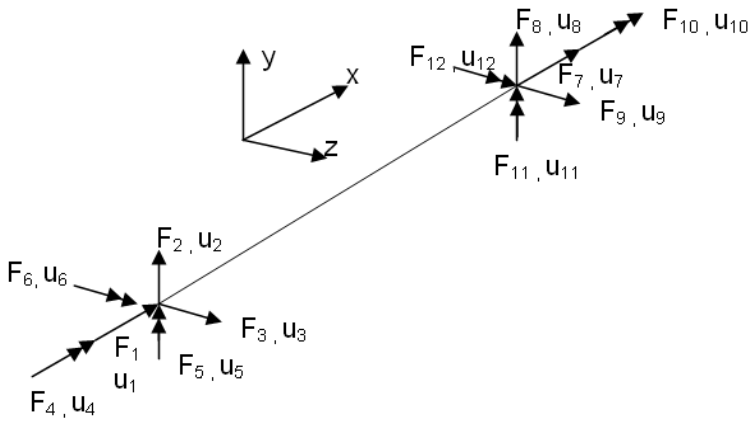

Figure 2.2 Joint end displacements, end forces and end moments in frame members

When structure is subjected to external forces, joint displacements and end forces occur in its members. Joint displacements and end forces are defined in local axis as shown in Figure 2.2. In this figure, first end forces and moments of the member k, are represented as vector $\{F_k\} = \{F_1\ F_2\ F_3\ F_4\ F_5\ F_6\}$ where; F_1 , F_2 , F_3 are the axial force, shear forces y and z axis respectively and F_4 , F_5 , F_6 are end moments of the first end of the member k . The member end displacement vector in the first end of member k is described as $\{U_k\} = \{u_1\ u_2\ u_3\ u_4\ u_5\ u_6\}$ in the local coordinate system. Consequently, six joint displacement and six end forces develop at each end of the member.

2.2.1 Relationship between member end forces and member end displacements

The relationship between member end forces and member end deformations is described as follows.

$$\{F_i\} = [k_i]\{U_i\} \tag{2.1}$$

where; $[k_i]$ is the stiffness matrix of member i, in the local coordinate system. Member stiffness matrix has twelve rows and twelve columns for 3-D space frames systems. Each row of this matrix can be obtained by assigning unit value to the each degree of freedom, while restraining the remaining degree of freedoms, respectively. When unit value is assigned to the degree of freedom, i, twelve end forces and end moments are obtained which constitutes the i^{th} column of the stiffness matrix. By assigning unit value to all the degree of freedoms as shown in Figure 2.3, the member stiffness matrix shown in (2.2) below is obtained.

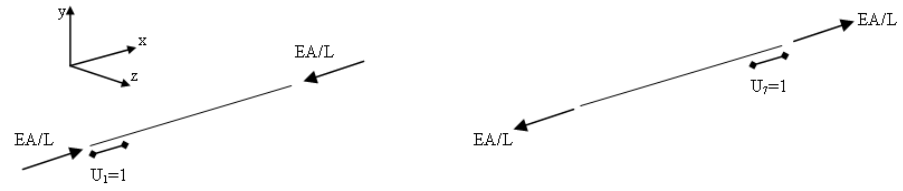

(a)

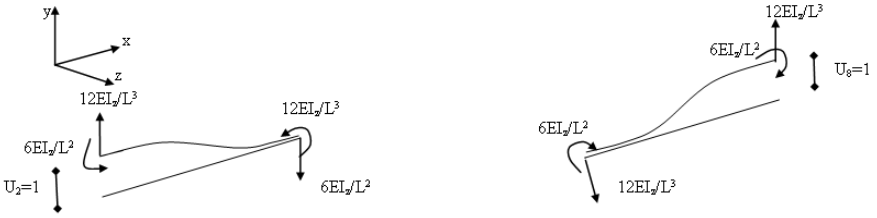

(b)

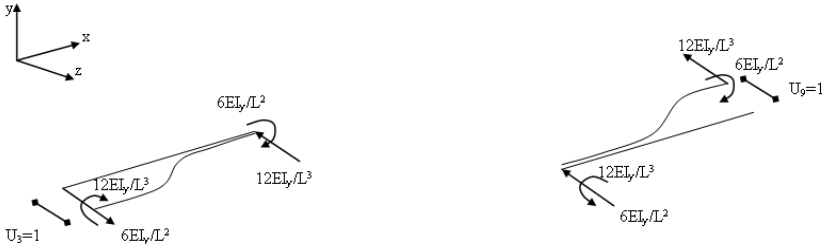

(c)

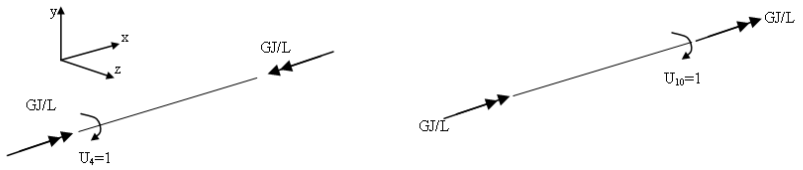

(d)

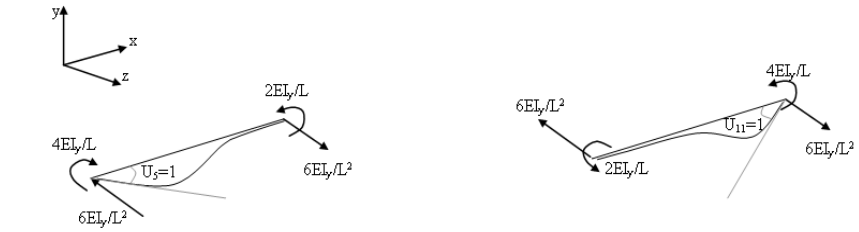

(e)

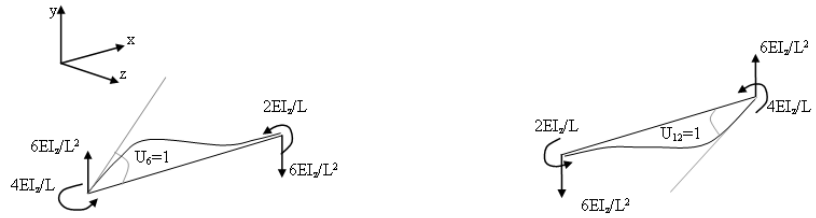

(f)

Figure 2.3 Member forces and moments for degree of freedoms; (a) $u_1=1$ and $u_7=1$, (b) $u_2=1$ and $u_8=1$, (c)) $u_3=1$ and $u_9=1$, (d) $u_4=1$ and $u_{10}=1$, (e) $u_5=1$ and $u_{11}=1$, (f) $u_6=1$ and $u_{12}=1$.

$$[k]=\begin{bmatrix}
\frac{EA}{\ell} & 0 & 0 & 0 & 0 & 0 & -\frac{EA}{\ell} & 0 & 0 & 0 & 0 & 0 \\
0 & \frac{12EI_z}{\ell^3} & 0 & 0 & 0 & \frac{6EI_z}{\ell^2} & 0 & -\frac{12EI_z}{\ell^3} & 0 & 0 & 0 & \frac{6EI_z}{\ell^2} \\
0 & 0 & \frac{12EI_y}{\ell^3} & 0 & -\frac{6EI_y}{\ell^2} & 0 & 0 & 0 & -\frac{12EI_y}{\ell^3} & 0 & -\frac{6EI_y}{\ell^2} & 0 \\
0 & 0 & 0 & \frac{GJ}{\ell} & 0 & 0 & 0 & 0 & 0 & -\frac{GJ}{\ell} & 0 & 0 \\
0 & 0 & -\frac{6EI_y}{\ell^2} & 0 & \frac{4EI_y}{\ell} & 0 & 0 & 0 & \frac{6EI_y}{\ell^2} & 0 & \frac{2EI_y}{\ell} & 0 \\
0 & \frac{6EI_z}{\ell^2} & 0 & 0 & 0 & \frac{4EI_z}{\ell} & 0 & -\frac{6EI_z}{\ell^2} & 0 & 0 & 0 & \frac{2EI_z}{\ell} \\
-\frac{EA}{\ell} & 0 & 0 & 0 & 0 & 0 & \frac{EA}{\ell} & 0 & 0 & 0 & 0 & 0 \\
0 & -\frac{12EI_z}{\ell^3} & 0 & 0 & 0 & -\frac{6EI_z}{\ell^2} & 0 & \frac{12EI_z}{\ell^3} & 0 & 0 & 0 & -\frac{6EI_z}{\ell^2} \\
0 & 0 & -\frac{12EI_y}{\ell^3} & 0 & \frac{6EI_y}{\ell^2} & 0 & 0 & 0 & \frac{12EI_y}{\ell^3} & 0 & \frac{6EI_y}{\ell^2} & 0 \\
0 & 0 & 0 & -\frac{GJ}{\ell} & 0 & 0 & 0 & 0 & 0 & \frac{GJ}{\ell} & 0 & 0 \\
0 & 0 & -\frac{6EI_y}{\ell^2} & 0 & \frac{2EI_y}{\ell} & 0 & 0 & 0 & \frac{6EI_y}{\ell^2} & 0 & \frac{4EI_y}{\ell} & 0 \\
0 & \frac{6EI_z}{\ell^2} & 0 & 0 & 0 & \frac{2EI_z}{\ell} & 0 & -\frac{6EI_z}{\ell^2} & 0 & 0 & 0 & \frac{4EI_z}{\ell}
\end{bmatrix} \tag{2.2}$$

2.2.2 Coordinate transformation

The joint displacements in the local axis and the joint displacements in the global axis are related to each other given below. This relation is obtained by carrying out coordinate transformations between the local and global axis.

$$\{U_i\} = [B_i]\{D_i\} \tag{2.3}$$

where, B_i is coordinate transformation matrix obtained from multiplication of the $[B]_x, [B]_y, [B]_z$ matrices. $[B]_x, [B]_y, [B]_z$ matrices are called the transformation matrices corresponding to the rotation about x, y, z local axis, respectively. These matrices are obtained as described in the following.

Rotation of γ about x axis

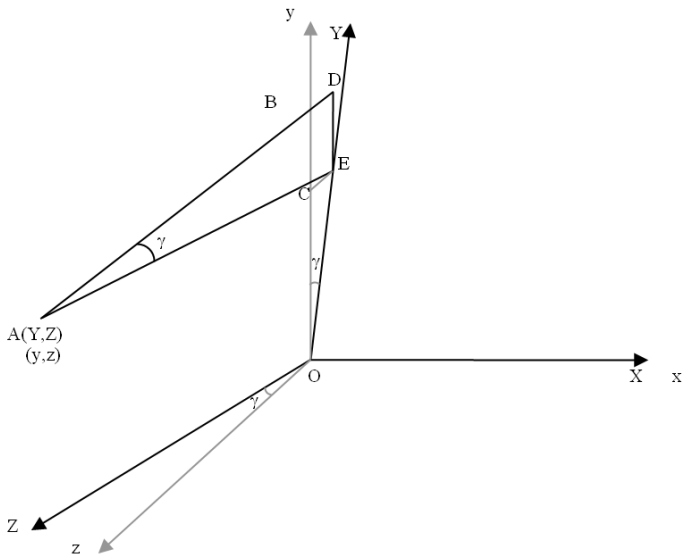

Figure 2.4 Rotation of γ about x axis

Consider that x axis is rotated amount of γ. In this case the coordinates of point A are related to each other as expressed in the following.

$$\begin{aligned} x &= X \\ y &= \bar{OB} = \bar{OC} + BC = Y\cos\gamma + Z\sin\gamma \\ z &= \bar{AB} = \bar{AD} - \bar{BD} = Z\cos\gamma - Y\sin\gamma \end{aligned} \tag{2.4}$$

by writing equations (2.4) in matrix form:

$$\begin{bmatrix} x \\ y \\ z \end{bmatrix} = \begin{bmatrix} 1 & 0 & 0 \\ 0 & \cos\gamma & \sin\gamma \\ 0 & -\sin\gamma & \cos\gamma \end{bmatrix} \begin{bmatrix} X \\ Y \\ Z \end{bmatrix} \tag{2.5}$$

Hence, transformation matrix corresponding to the rotation γ about x axis is obtained as;

$$[B]_x = \begin{bmatrix} 1 & 0 & 0 \\ 0 & \cos\gamma & \sin\gamma \\ 0 & -\sin\gamma & \cos\gamma \end{bmatrix} \tag{2.6}$$

Rotation of α about y axis

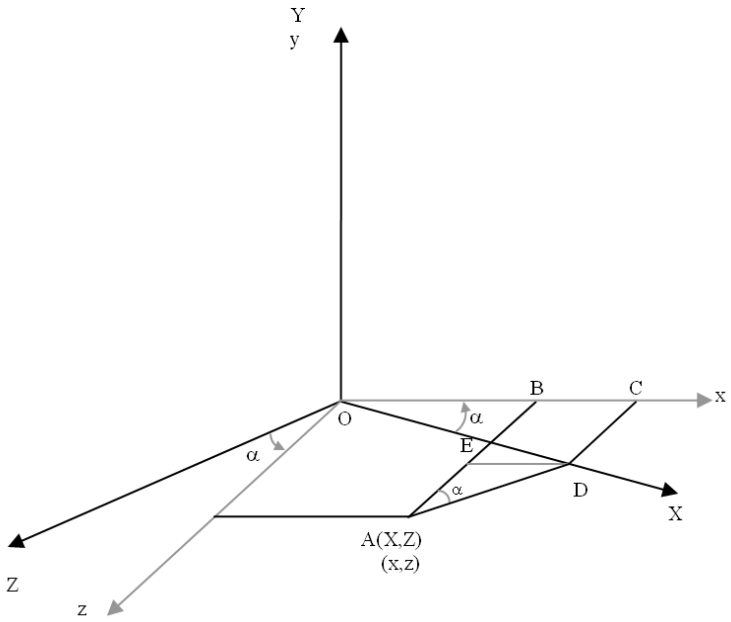

Figure 2.5 Rotation of α about y axis

For this case y axis is rotated by the amount of α the coordinates of point A in both x, z and X, Z axis are related as:

In $\overset{\Delta}{AED} \rightarrow \bar{BC} = \bar{ED} = \bar{AD}\,Sin\alpha = Z\sin\alpha$,

In $\overset{\Delta}{ODC} \rightarrow \bar{OC} = \bar{OD}\,Cos\alpha = X\,Cos\alpha$.

It follows that:

$$\begin{aligned} x &= \bar{OB} = \bar{OC} - BC = Y\,Cos\alpha - Z\,Sin\alpha \\ y &= Y \\ z &= \bar{AB} = \bar{AD} + \bar{BD} = Z\,Cos\alpha + Y\,Sin\alpha \end{aligned} \tag{2.7}$$

by writing equations (2.7) in matrix form;

$$\begin{bmatrix} x \\ y \\ z \end{bmatrix} = \begin{bmatrix} \cos\alpha & 0 & -\sin\alpha \\ 0 & 1 & 0 \\ \sin\alpha & 0 & \cos\alpha \end{bmatrix} \begin{bmatrix} X \\ Y \\ Z \end{bmatrix} \tag{2.8}$$

Hence, transformation matrix corresponding to the rotation α about y axis is obtained as;

$$[B]_y = \begin{bmatrix} \cos\alpha & 0 & -\sin\alpha \\ 0 & 1 & 0 \\ \sin\alpha & 0 & \cos\alpha \end{bmatrix} \tag{2.9}$$

Rotation of β about z axis

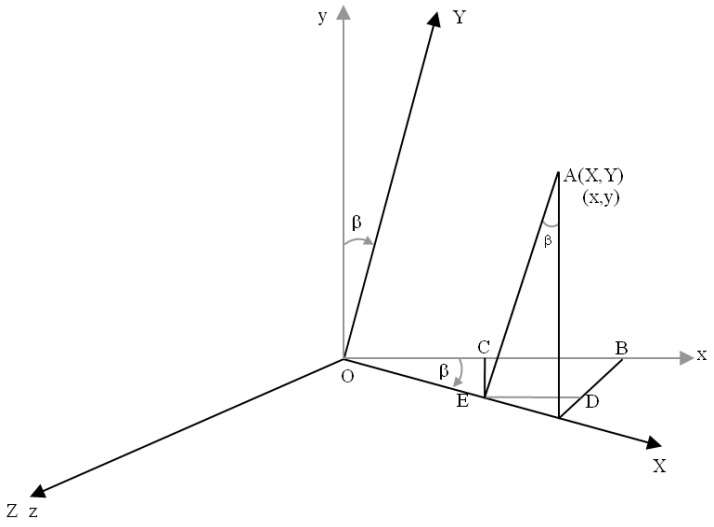

Figure 2.6 Rotation of β about z axis

In this case the coordinates of point A are related to each other as expressed in the following.

$$\text{In } \overset{\Delta}{AED} \rightarrow \bar{ED} = \bar{ED} = \bar{AE}\,Sin\beta = Y\,Sin\beta\,,\ \bar{AD} = Y\,Cos\beta$$

$$\text{In } \overset{\Delta}{ODE} \rightarrow \bar{OC} = \bar{OE}\,Cos\beta = X\,Cos\beta\,,\ \bar{BD} = \bar{CE} = \bar{OE}\cos\beta = X\,Cos\beta$$

It follows that:

$$\begin{aligned} x &= \bar{OB} = \bar{OC} + ED = X\cos\beta + Y\sin\beta \\ y &= \bar{AB} = \bar{AD} - \bar{BD} = -X\cos\beta + Y\sin\beta \\ z &= Z \end{aligned} \qquad (2.10)$$

by writing write equations (2.10) in matrix form;

$$\begin{bmatrix} x \\ y \\ z \end{bmatrix} = \begin{bmatrix} \cos\beta & \sin\beta & 0 \\ -\sin\beta & \cos\beta & 0 \\ 0 & 0 & 1 \end{bmatrix} \begin{bmatrix} X \\ Y \\ Z \end{bmatrix} \tag{2.11}$$

Hence, transformation matrix corresponding to the rotation β about z axis is obtained as;

$$[B]_y = \begin{bmatrix} \cos\beta & \sin\beta & 0 \\ -\sin\beta & \cos\beta & 0 \\ 0 & 0 & 1 \end{bmatrix} \tag{2.12}$$

When $[B]_x, [B]_y, [B]_z$ matrices are multiplied, coordinate transformation matrix shown in (2.13) is obtained.

$$[B] = \begin{bmatrix} 1 & 0 & 0 \\ 0 & \cos\gamma & \sin\gamma \\ 0 & -\sin\gamma & \cos\gamma \end{bmatrix} \begin{bmatrix} \cos\alpha & 0 & -\sin\alpha \\ 0 & 1 & 0 \\ \sin\alpha & 0 & \cos\alpha \end{bmatrix} \cdot \begin{bmatrix} \cos\beta & \sin\beta & 0 \\ -\sin\beta & \cos\beta & 0 \\ 0 & 0 & 1 \end{bmatrix}$$

$$[B] = \begin{bmatrix} \cos\beta\cdot\cos\alpha & \sin\beta & -\cos\beta\cdot\sin\alpha \\ \sin\alpha\cdot\sin\gamma - \cos\alpha\cdot\sin\beta\cdot\cos\gamma & \cos\beta\cdot\cos\gamma & \cos\alpha\cdot\sin\gamma + \sin\alpha\cdot\sin\beta\cdot\cos\gamma \\ \sin\alpha\cdot\cos\gamma + \cos\alpha\cdot\sin\beta\cdot\sin\gamma & -\cos\beta\cdot\sin\gamma & \cos\alpha\cdot\cos\gamma - \sin\alpha\cdot\sin\beta\cdot\sin\gamma \end{bmatrix} \tag{2.13}$$

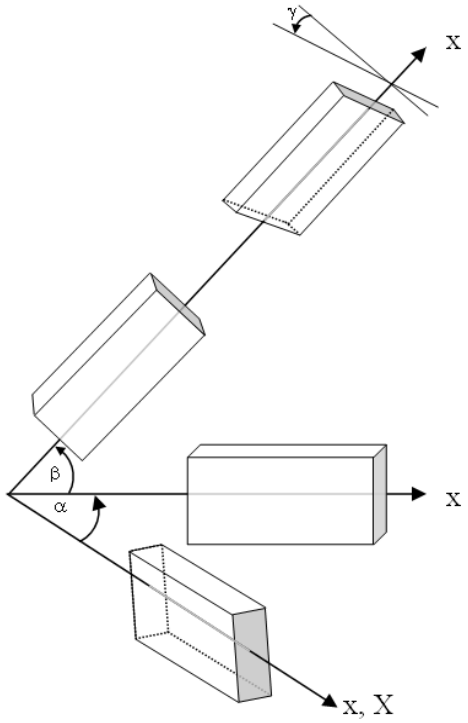

Figure 2.7 Coordinate transformation from local axis to global axis

It is apparent from Equation (2.13) that terms of the coordinate transformation matrix depend on angles α, β, and γ. γ angle is not related to the joint coordinates of a space frame member. Therefore, value of γ angle is entered manually in the program. Whereas, α and β angles are related to joint coordinates, so that joint coordinates of space frame member should be known in order to calculate the coordinate transformation matrix. It is possible to re-write the coordinate transformation matrix in terms of length of space frame members by using relationship between α, β angles and joint coordinates as explained in the following.

The length of a space frame member as shown Figure 2.8 is calculated as follows.

$$AB = l = \sqrt{(\Delta x)^2 + (\Delta y)^2 + (\Delta z)^2}$$
$$A_1B_1 = l_1 = \sqrt{(\Delta x)^2 + (\Delta z)^2} \tag{2.14}$$

When the terms $\cos\alpha, \cos\beta, \sin\alpha, \sin\beta$ are written in terms of the length of element.

$$Cos(-\alpha) = Cos\alpha = \frac{\Delta x}{l_1}, Sin(-\alpha) = -\sin\alpha = -\frac{\Delta z}{l_1}$$
$$Cos\beta = \frac{l_1}{l}, Sin\beta = \frac{\Delta z}{l_1} \tag{2.15}$$

Where, Δx, Δy and Δz terms are shown in Figure 2.8. When these terms are substituted in to the coordinate transformation matrix, following expression is obtained.

$$[B^*] = \begin{bmatrix} \frac{\Delta x}{l} & \frac{\Delta y}{l} & \frac{\Delta z}{l} \\ \frac{-l\cdot(\Delta z)\cdot\sin\gamma - (\Delta x)\cdot(\Delta y)\cdot\cos\gamma}{l\cdot l_1} & \frac{l_1\cdot\cos\gamma}{l} & \frac{l\cdot(\Delta x)\cdot\sin\gamma - (\Delta z)\cdot(\Delta y)\cdot\cos\gamma}{l\cdot l_1} \\ \frac{(\Delta x)\cdot(\Delta y)\cdot\sin\gamma - l\cdot(\Delta z)\cdot\cos\gamma}{l\cdot l_1} & -\frac{l_1\cdot\cos\gamma}{l} & \frac{l\cdot(\Delta x)\cdot\sin\gamma + (\Delta z)\cdot(\Delta y)\cdot\cos\gamma}{l\cdot l_1} \end{bmatrix} \tag{2.16}$$

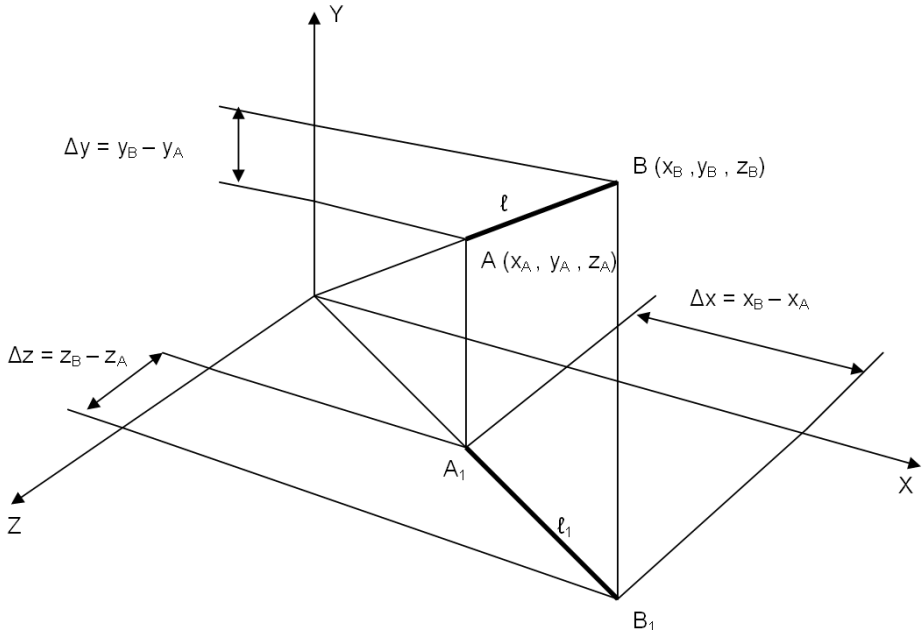

Figure 2.8 Calculation of the length of an element

The coordinate transformation matrix described in (2.16) represents transformations at one end of the space frame member. The complete displacement transformation matrix for the degree of freedom of both ends of the frame member has twelve columns and twelve rows as shown in (2.17).

$$[B] = \begin{bmatrix} b_{11} & b_{12} & b_{13} & 0 & 0 & 0 & 0 & 0 & 0 & 0 & 0 & 0 \\ b_{21} & b_{22} & b_{23} & 0 & 0 & 0 & 0 & 0 & 0 & 0 & 0 & 0 \\ b_{31} & b_{32} & b_{33} & 0 & 0 & 0 & 0 & 0 & 0 & 0 & 0 & 0 \\ 0 & 0 & 0 & b_{11} & b_{12} & b_{13} & 0 & 0 & 0 & 0 & 0 & 0 \\ 0 & 0 & 0 & b_{21} & b_{22} & b_{23} & 0 & 0 & 0 & 0 & 0 & 0 \\ 0 & 0 & 0 & b_{31} & b_{32} & b_{33} & 0 & 0 & 0 & 0 & 0 & 0 \\ 0 & 0 & 0 & 0 & 0 & 0 & b_{11} & b_{12} & b_{13} & 0 & 0 & 0 \\ 0 & 0 & 0 & 0 & 0 & 0 & b_{21} & b_{22} & b_{23} & 0 & 0 & 0 \\ 0 & 0 & 0 & 0 & 0 & 0 & b_{31} & b_{32} & b_{33} & 0 & 0 & 0 \\ 0 & 0 & 0 & 0 & 0 & 0 & 0 & 0 & 0 & b_{11} & b_{12} & b_{13} \\ 0 & 0 & 0 & 0 & 0 & 0 & 0 & 0 & 0 & b_{21} & b_{22} & b_{23} \\ 0 & 0 & 0 & 0 & 0 & 0 & 0 & 0 & 0 & b_{31} & b_{32} & b_{33} \end{bmatrix} \quad (2.17)$$

where; $b_{i,j}$ i=1, 2, 3 and j=1, 2, 3 are the terms of the coordinate transformation matrix described as follows.

$$b_{11}=\frac{\Delta x}{\ell}\ , \qquad b_{12}=\frac{\Delta y}{\ell}\ , \qquad b_{13}=\frac{\Delta z}{\ell}$$

$$b_{21}=\frac{-\ell\,(\Delta z)\sin\gamma-(\Delta x)(\Delta z)\cos\gamma}{\ell\,\ell_1}\ , \quad b_{22}=\frac{\ell_1\cos\gamma}{\ell}\ , \quad b_{23}=\frac{\ell\,(\Delta x)\sin\gamma-(\Delta z)(\Delta y)\cos\gamma}{\ell\,\ell_1} \tag{2.18}$$

$$b_{31}=\frac{(\Delta x)(\Delta y)\sin\gamma-\ell(\Delta z)\cos\gamma}{\ell\,\ell_1}\ , \quad b_{32}=-\frac{\ell_1\sin\gamma}{\ell}\ , \quad b_{33}=\frac{\ell\,(\Delta x)\cos\gamma-(\Delta z)(\Delta y)\sin\gamma}{\ell\,\ell_1}$$

Space frame members along the Y-Axis

It is apparent from relationship (2.14) that for a frame member along Y-axis, $\Delta x=\Delta y=0\,,\Delta z=l$ and $l_1=0.$ This causes division by zero in the expressions given (2.18) which makes them unstable as shown in (2.19). In order eliminate this discrepancy displacement transformation matrix is required to be re-constructed. These special matrices are given in (2.20) and (2.21). When x axis of space frame member is along to +Y axis, transformation matrix of (2.20) is used. when x axis of space frame member is along to -Y axis, transformation matrix of (2.21) is used. Directions of these members are shown in Figures 2.9 and 2.10. Detailed derivations of these cases are given in [115].

$$[B]=\begin{bmatrix} 0 & 1 & 0 \\ \frac{0}{0} & 0 & \frac{0}{0} \\ \frac{0}{0} & 0 & \frac{0}{0} \end{bmatrix} \tag{2.19}$$

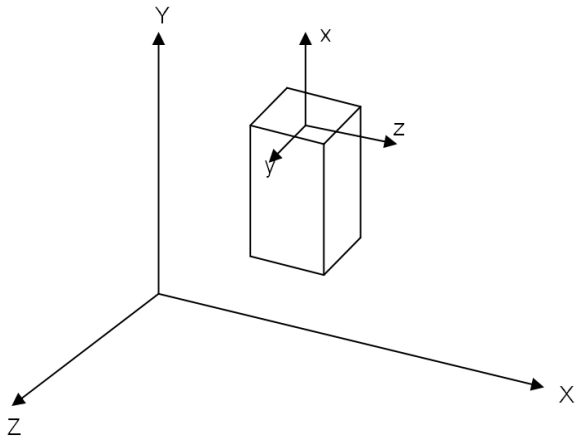

Figure 2.9 Local coordinates of vertical member in +Y direction

$$[B]=\begin{bmatrix}
0 & 1 & 0 & 0 & 0 & 0 & 0 & 0 & 0 & 0 & 0 & 0 \\
\sin\gamma & 0 & \cos\gamma & 0 & 0 & 0 & 0 & 0 & 0 & 0 & 0 & 0 \\
\cos\gamma & 0 & -\sin\gamma & 0 & 0 & 0 & 0 & 0 & 0 & 0 & 0 & 0 \\
0 & 0 & 0 & 0 & 1 & 0 & 0 & 0 & 0 & 0 & 0 & 0 \\
0 & 0 & 0 & \sin\gamma & 0 & \cos\gamma & 0 & 0 & 0 & 0 & 0 & 0 \\
0 & 0 & 0 & \cos\gamma & 0 & -\sin\gamma & 0 & 0 & 0 & 0 & 0 & 0 \\
0 & 0 & 0 & 0 & 0 & 0 & 0 & 1 & 0 & 0 & 0 & 0 \\
0 & 0 & 0 & 0 & 0 & 0 & \sin\gamma & 0 & \cos\gamma & 0 & 0 & 0 \\
0 & 0 & 0 & 0 & 0 & 0 & \cos\gamma & 0 & -\sin\gamma & 0 & 0 & 0 \\
0 & 0 & 0 & 0 & 0 & 0 & 0 & 0 & 0 & 0 & 1 & 0 \\
0 & 0 & 0 & 0 & 0 & 0 & 0 & 0 & 0 & \sin\gamma & 0 & \cos\gamma \\
0 & 0 & 0 & 0 & 0 & 0 & 0 & 0 & 0 & \cos\gamma & 0 & -\sin\gamma
\end{bmatrix} \tag{2.20}$$

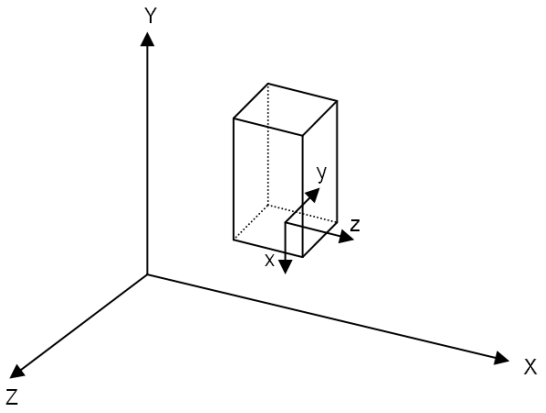

Figure 2.10 Local coordinates of vertical member in -Y direction

$$[B]=\begin{bmatrix}
0 & -1 & 0 & 0 & 0 & 0 & 0 & 0 & 0 & 0 & 0 & 0 \\
\sin\gamma & 0 & -\cos\gamma & 0 & 0 & 0 & 0 & 0 & 0 & 0 & 0 & 0 \\
\cos\gamma & 0 & \sin\gamma & 0 & 0 & 0 & 0 & 0 & 0 & 0 & 0 & 0 \\
0 & 0 & 0 & 0 & -1 & 0 & 0 & 0 & 0 & 0 & 0 & 0 \\
0 & 0 & 0 & \sin\gamma & 0 & -\cos\gamma & 0 & 0 & 0 & 0 & 0 & 0 \\
0 & 0 & 0 & \cos\gamma & 0 & \sin\gamma & 0 & 0 & 0 & 0 & 0 & 0 \\
0 & 0 & 0 & 0 & 0 & 0 & 0 & -1 & 0 & 0 & 0 & 0 \\
0 & 0 & 0 & 0 & 0 & 0 & \sin\gamma & 0 & -\cos\gamma & 0 & 0 & 0 \\
0 & 0 & 0 & 0 & 0 & 0 & \cos\gamma & 0 & \sin\gamma & 0 & 0 & 0 \\
0 & 0 & 0 & 0 & 0 & 0 & 0 & 0 & 0 & 0 & -1 & 0 \\
0 & 0 & 0 & 0 & 0 & 0 & 0 & 0 & 0 & \sin\gamma & 0 & -\cos\gamma \\
0 & 0 & 0 & 0 & 0 & 0 & 0 & 0 & 0 & \cos\gamma & 0 & \sin\gamma
\end{bmatrix} \tag{2.21}$$

2.2.3 Relationship between external loads and member end forces

The relationship between member end forces and member end deformations at joint i is given as $\{F_i\}=[k_i]\{U_i\}$. This equation can be generalized as $\{F\}=[k]\{U\}$ for the whole frame when all the members are included in the above expression. In this equation, dimension of vectors $\{F\}$ and $\{U\}$ is $6*m$ where, m is total number of joints in the space frame. Stiffness matrix $[k]$ in that equation is

obtained by collecting the local stiffness matrices of frame members. This matrix has dimension of ($6*m \times 6*m$). When this equation is expanded to include all the members in the frame, it follows that $\{U\} = [B]\{D\}$. In this expression, the dimension of matrix $[B]$ is ($6*m \times 6*m$) and the dimension of the displacement matrix $\{D\}$ is also ($6*m \times 1$).

When an elastic frame is subjected to external loads, frame joints are displaced and frame members are deflected. In this case, work done by the external loads acting on frame joints is equal to the strain energy stored in frame members on due to the law of conservation of energy. It follows that:

$$\frac{1}{2}\{P\}^T\{D\} = \frac{1}{2}\{F\}^T\{U\} \tag{2.22}$$

where; $\{P\}$ is the external load vector, $\{D\}$ is the joint displacements vector, $\{F\}$ is the vector of member end forces, and $\{U\}$ is the vector of member end displacement. Remembering from (2.22) that $\{U\} = [B]\{D\}$, it follows that

$$\frac{1}{2}\{P\}^T\{D\} = \frac{1}{2}\{F\}^T[B]\{D\} \quad \Rightarrow \quad \{P\}^T = \{F\}^T[B] \tag{2.23}$$

Transpose of equation (2.23) yields ;

$$\{P\} = [B]^T\{F\} \tag{2.24}$$

This equation represents the relationship between the external load vector and member end forces. $[B]^T$ in this equation is the transpose of the displacement transformation matrix $[B]$.

2.2.4 Overall stiffness matrix

The external load vector $\{P\}$ can be related to joint displacement vector $\{D\}$ using the relationships $\{U\}=[B]\{D\}$ and $\{F\}=[k]\{U\}$. When these expressions are substituted in (2.24);

$$\{P\}=[B]^T[k][B]\{D\}=[K]\{D\} \tag{2.25}$$

is obtained. Here, $[K]$ is called overall stiffness matrix of the structure in global coordinate system. This matrix is constructed by carrying out triple matrix multiplication shown in (2.25). It is apparent that the overall stiffness matrix can be obtained by collecting the contributions of each member to this matrix.

$$[K_S]=\sum_{i=1}^{m}[K_i]=\sum_{i=1}^{m}[B_i]^T[k_i][B_i] \tag{2.26}$$

where, m is the number of members in space frame. Overall stiffness matrix of a structure is diagonally symmetric. Therefore, it is sufficient to structure to the half of this matrix. In the coding of the computer program Compact Storage Scheme is used to store the overall stiffness matrix. In this scheme, only non-zero terms in the lower triangle part of the matrix are stored. 3-D frame shown in Figure 2.11 consist of four fixed support four joints and eight members. Since each joint has six degree of freedom, structure stiffness matrix has 24 columns and 24 rows. When the overall stiffness matrix is stored as two dimensional arrays, n the computer memory, 576 locations are required. However, if compact storage scheme is used, the total number of locations required is decreased to 264. Therefore, 54% of memory saving is achieved. In Figure 2.12, each box represents the contribution of matrices of members. Terms of stiffness matrix in global axis for each member are added to their place in structure stiffness matrix. For example, end joint numbers of member 5 are 1 and 3. If first end of this member is accepted as lower number, terms of member stiffness matrix in

global are added to boxes numbered (1,1) , (3,1) and (3,3) in the structure stiffness matrix. In the same way, terms of stiffness matrix for member 8 will be added to boxes numbered (2,2) , (4,2) and (4,4) in the overall stiffness matrix. It can be clearly seen from Figure 2.12 that, no terms are added in box numbered (4,1). Therefore, terms of this box are equal to zero and these terms are not required to be stored in computer memory. In addition, upper triangle terms of the structure stiffness matrix are not required to be stored. This small example clearly shows the advantage of using compact storage scheme for storing the overall stiffness matrix in the computer memory.

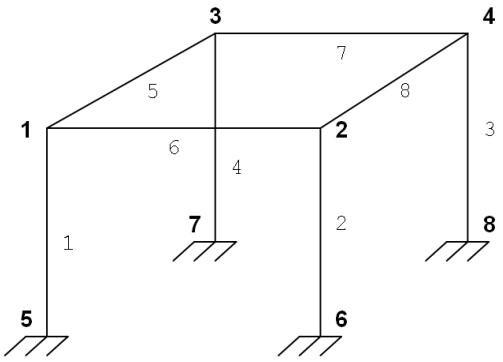

Figure 2.11 8 members 3-D frame

Joint1	Joint2	Joint3	Joint4
1 2 3 4 5 6 7 8 9 10 11 12 13 14 15 16 17 18 19 20 21			
22 23 24 25 26 27 29 30 31 32 33 34 37 38 39 40 41 42 46 47 48 49 50 51 56 57 58 59 60 61 67 68 69 70 71 72	28 35 36 43 44 45 52 53 54 55 62 63 64 65 66 73 74 75 76 77 78		
79 80 81 82 83 84 92 93 94 95 96 97 106 107 108 109 110 111 121 122 123 124 125 126 137 138 139 140 141 142 154 155 156 157 158 159	85 86 87 88 89 90 98 99 100 101 102 103 112 113 114 115 116 117 127 128 129 130 131 132 143 144 145 146 147 148 160 161 162 163 164 165	91 104 105 118 119 120 133 134 135 136 149 150 151 152 153 166 167 168 169 170 171	
	172 173 174 175 176 177 185 186 187 188 189 190 199 200 201 202 203 204 214 215 216 217 218 219 230 231 232 233 234 235 247 248 249 250 251 252	178 179 180 181 182 183 191 192 193 194 195 196 205 206 207 208 209 210 220 221 222 223 224 225 236 237 238 239 240 241 253 254 255 256 257 258	184 197 198 211 212 213 226 227 228 229 242 243 244 245 246 259 260 261 262 263 264

Figure 2.12 Position of stiffness matrix terms for 8 members 3-D frame

2.2.5 Member end conditions

In some cases, beams of steel frames are connected to columns with hinge connections where bending moment transfer is not possible. In such a case, value of the bending moment is equal to zero at that joint. Therefore end displacements and end forces should be recalculated by equating bending moment to the zero at the hinged joint. Consequently, member stiffness matrix for a member having a hinge connection at one end is not same as the one which is rigidly connected to columns. In general, there can be 4 types of members in a steel frame. These members depending on the end conditions are tabulated in Table 2.1 and described in the following.

Table 2.1 Type of hinge conditions

Member Type	Type of Ends
Type 1	Both ends are moment resisting
Type 2	First end is hinged
Type 3	Far end is hinged
Type 4	Both ends are hinged

Type 1: Frame member both ends are moment resisting

Stiffness and transformation matrices for that condition were given in (2.2) and (2.17)

Type 2: Frame member having a hinge connection at its first end

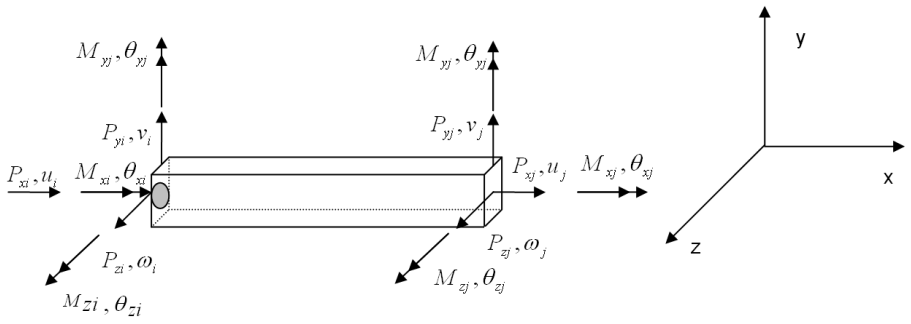

Figure 2.13 3-D frame member having a hinge connection at its first end

It is clear from Figure 2.13 that when first the end of a frame member is hinged the bending moment about z axis becomes zero at that joint ($M_{zi} = 0$**)**. This condition yields the following Equation (2.27).

$$\frac{6EI_z}{L^2}v_i+\frac{4EI_z}{L}\theta_{zi}-\frac{6EI_z}{L^2}v_j+\frac{2EI_z}{L}\theta_{zj}=0\rightarrow\quad\theta_{zi}=-\frac{3}{2L}v_i+\frac{3}{2L}v_j-\frac{\theta_{zj}}{2}\tag{2.27}$$

In Equation (2.27), if θ_{zi} equality is substituted in to stiffness equations following equations are obtained.

$$P_{xi}=\frac{EA}{L}u_i-\frac{EA}{L}u_j$$

$$P_{yi}=\frac{12EI_z}{L^3}v_i+\frac{6EI_z}{L^2}\left(-\frac{3}{2L}v_i+\frac{3}{2L}v_j-\frac{\theta_{zj}}{2}\right)-\frac{12EI_z}{L^3}v_j+\frac{6EI_z}{L^2}\theta_{zj}$$

$$P_{yi}=\frac{3EI_z}{L^3}v_i-\frac{3EI_z}{L^3}v_j+\frac{3EI_z}{L^2}\theta_{zj}$$

$$P_{zi}=\frac{12EI_y}{L^3}\omega_i-\frac{6EI_y}{L^2}\theta_{yi}-\frac{12EI_y}{L^3}\omega_j-\frac{6EI_y}{L^2}\theta_{yj}$$

$$M_{xi}=\frac{GJ}{L}\theta_{xi}-\frac{GJ}{L}\theta_{ji}\tag{2.28}$$

$$M_{yi}=-\frac{6EI_y}{L^2}\omega_i+\frac{4EI_y}{L}\theta_{yi}+\frac{6EI_y}{L^2}\omega_j+\frac{2EI_y}{L}\theta_{yj}$$

$$P_{xj}=-\frac{EA}{L}u_i+\frac{EA}{L}u_j$$

$$P_{yj}=-\frac{12EI_z}{L^3}v_i-\frac{6EI_z}{L^2}\left(-\frac{3}{2L}v_i+\frac{3}{2L}v_j-\frac{\theta_{zj}}{2}\right)+\frac{12EI_z}{L^3}v_j-\frac{6EI_z}{L^2}\theta_{zj}$$

After simplification, the relationships between end forces and displacements are obtained as follows.

$$
\begin{aligned}
P_{yj} &= -\frac{3EI_z}{L^3}v_i + \frac{3EI_z}{L^3}v_j - \frac{3EI_z}{L^2}\theta_{zj} \\
P_{zj} &= -\frac{12EI_y}{L^3}\omega_i + \frac{6EI_y}{L^2}\theta_{yi} + \frac{12EI_y}{L^3}\omega_j + \frac{6EI_y}{L^2}\theta_{yj} \\
M_{xj} &= -\frac{GJ}{L}\theta_{xi} + \frac{GJ}{L}\theta_{xj} \\
M_{yj} &= -\frac{6EI_y}{L^2}\omega_i + \frac{2EI_y}{L}\theta_{yi} + \frac{6EI_y}{L^2}\omega_j + \frac{4EI_y}{L}\theta_{yj} \\
M_{zj} &= \frac{6EI_z}{L^2}v_i + \frac{2EI_z}{L}\left(-\frac{3}{2L}v_i + \frac{3}{2L}v_j - \frac{\theta_{zj}}{2}\right) - \frac{6EI_z}{L^2}v_j + \frac{4EI_z}{L}\theta_{zj} \\
M_{zj} &= \frac{3EI_z}{L^2}v_i - \frac{3EI_z}{L^2}v_j + \frac{3EI_z}{L}\theta_{zj}
\end{aligned}
\tag{2.29}
$$

When these are expressed in a matrix form, following stiffness matrix is obtained for a frame member having a hinge at its first end.

$$[k]=\begin{bmatrix}
\frac{EA}{L} & 0 & 0 & 0 & 0 & 0 & -\frac{EA}{L} & 0 & 0 & 0 & 0 & 0 \\
0 & \frac{12EI_z}{L^3} & 0 & 0 & 0 & \frac{6EI_z}{L^2} & 0 & \frac{-12EI_z}{L^3} & 0 & 0 & 0 & \frac{6EI_z}{L^2} \\
0 & 0 & \frac{12EI_y}{L^3} & 0 & -\frac{6EI_y}{L^2} & 0 & 0 & 0 & -\frac{12EI_y}{L^3} & 0 & -\frac{6EI_y}{L^2} & 0 \\
0 & 0 & 0 & \frac{GJ}{L} & 0 & 0 & 0 & 0 & 0 & -\frac{GJ}{L} & 0 & 0 \\
0 & 0 & -\frac{6EI_y}{L^2} & 0 & \frac{4EI_y}{L} & 0 & 0 & 0 & \frac{6EI_y}{L^2} & 0 & \frac{2EI_y}{L} & 0 \\
0 & 0 & 0 & 0 & 0 & 0 & 0 & 0 & 0 & 0 & 0 & 0 \\
-\frac{EA}{L} & 0 & 0 & 0 & 0 & 0 & \frac{EA}{L} & 0 & 0 & 0 & 0 & 0 \\
0 & \frac{-12EI_z}{L^3} & 0 & 0 & 0 & -\frac{6EI_z}{L^2} & 0 & \frac{12EI_z}{L^3} & 0 & 0 & 0 & -\frac{6EI_z}{L^2} \\
0 & 0 & -\frac{12EI_y}{L^3} & 0 & \frac{6EI_y}{L^2} & 0 & 0 & 0 & \frac{12EI_y}{L^3} & 0 & \frac{6EI_y}{L^2} & 0 \\
0 & 0 & 0 & -\frac{GJ}{L} & 0 & 0 & 0 & 0 & 0 & \frac{GJ}{L} & 0 & 0 \\
0 & 0 & -\frac{6EI_y}{L^2} & 0 & \frac{2EI_y}{L} & 0 & 0 & 0 & \frac{6EI_y}{L^2} & 0 & \frac{4EI_y}{L} & 0 \\
0 & \frac{3EI_z}{L^2} & 0 & 0 & 0 & 0 & 0 & -\frac{3EI_z}{L^2} & 0 & 0 & 0 & \frac{3EI_z}{L}
\end{bmatrix} \tag{2.30}$$

Displacement transformation matrix of a frame member having a hinge at its first end is given in the following (2.31). Only difference between this matrix and displacement transformation matrix for type 1 given in (2.17) is that all terms in line parallel to θ_{zi} be equal to zero. Since θ_{zi} term, representing rotation on hinged joint is eliminated from stiffness equations. Transformation matrix for that case becomes in the following.

$$[B]=\begin{bmatrix}
b_{11} & b_{12} & b_{13} & 0 & 0 & 0 & 0 & 0 & 0 & 0 & 0 & 0 \\
b_{21} & b_{22} & b_{23} & 0 & 0 & 0 & 0 & 0 & 0 & 0 & 0 & 0 \\
b_{31} & b_{32} & b_{33} & 0 & 0 & 0 & 0 & 0 & 0 & 0 & 0 & 0 \\
0 & 0 & 0 & b_{11} & b_{12} & b_{13} & 0 & 0 & 0 & 0 & 0 & 0 \\
0 & 0 & 0 & b_{21} & b_{22} & b_{23} & 0 & 0 & 0 & 0 & 0 & 0 \\
0 & 0 & 0 & 0 & 0 & 0 & 0 & 0 & 0 & 0 & 0 & 0 \\
0 & 0 & 0 & 0 & 0 & 0 & b_{11} & b_{12} & b_{13} & 0 & 0 & 0 \\
0 & 0 & 0 & 0 & 0 & 0 & b_{21} & b_{22} & b_{23} & 0 & 0 & 0 \\
0 & 0 & 0 & 0 & 0 & 0 & b_{31} & b_{32} & b_{33} & 0 & 0 & 0 \\
0 & 0 & 0 & 0 & 0 & 0 & 0 & 0 & 0 & b_{11} & b_{12} & b_{13} \\
0 & 0 & 0 & 0 & 0 & 0 & 0 & 0 & 0 & b_{21} & b_{22} & b_{23} \\
0 & 0 & 0 & 0 & 0 & 0 & 0 & 0 & 0 & b_{31} & b_{32} & b_{33}
\end{bmatrix} \tag{2.31}$$

where, $b_{i,j}$ $i=1,2,3$ $j=1,2,3$ terms are given in (2.18). Transformation matrix of vertical member in +Y direction is given in the following.

$$[B]=\begin{bmatrix} 0 & 1 & 0 & 0 & 0 & 0 & 0 & 0 & 0 & 0 & 0 & 0 \\ \sin\gamma & 0 & \cos\gamma & 0 & 0 & 0 & 0 & 0 & 0 & 0 & 0 & 0 \\ \cos\gamma & 0 & -\sin\gamma & 0 & 0 & 0 & 0 & 0 & 0 & 0 & 0 & 0 \\ 0 & 0 & 0 & 0 & 1 & 0 & 0 & 0 & 0 & 0 & 0 & 0 \\ 0 & 0 & 0 & \sin\gamma & 0 & \cos\gamma & 0 & 0 & 0 & 0 & 0 & 0 \\ 0 & 0 & 0 & 0 & 0 & 0 & 0 & 0 & 0 & 0 & 0 & 0 \\ 0 & 0 & 0 & 0 & 0 & 0 & 0 & 1 & 0 & 0 & 0 & 0 \\ 0 & 0 & 0 & 0 & 0 & 0 & \sin\gamma & 0 & \cos\gamma & 0 & 0 & 0 \\ 0 & 0 & 0 & 0 & 0 & 0 & \cos\gamma & 0 & -\sin\gamma & 0 & 0 & 0 \\ 0 & 0 & 0 & 0 & 0 & 0 & 0 & 0 & 0 & 0 & 1 & 0 \\ 0 & 0 & 0 & 0 & 0 & 0 & 0 & 0 & 0 & \sin\gamma & 0 & \cos\gamma \\ 0 & 0 & 0 & 0 & 0 & 0 & 0 & 0 & 0 & \cos\gamma & 0 & -\sin\gamma \end{bmatrix} \quad (2.32)$$

Similarly, transformation matrix of vertical member in -Y direction is given in the following.

$$[B]=\begin{bmatrix} 0 & -1 & 0 & 0 & 0 & 0 & 0 & 0 & 0 & 0 & 0 & 0 \\ \sin\gamma & 0 & -\cos\gamma & 0 & 0 & 0 & 0 & 0 & 0 & 0 & 0 & 0 \\ \cos\gamma & 0 & \sin\gamma & 0 & 0 & 0 & 0 & 0 & 0 & 0 & 0 & 0 \\ 0 & 0 & 0 & 0 & -1 & 0 & 0 & 0 & 0 & 0 & 0 & 0 \\ 0 & 0 & 0 & \sin\gamma & 0 & -\cos\gamma & 0 & 0 & 0 & 0 & 0 & 0 \\ 0 & 0 & 0 & 0 & 0 & 0 & 0 & 0 & 0 & 0 & 0 & 0 \\ 0 & 0 & 0 & 0 & 0 & 0 & 0 & -1 & 0 & 0 & 0 & 0 \\ 0 & 0 & 0 & 0 & 0 & 0 & \sin\gamma & 0 & -\cos\gamma & 0 & 0 & 0 \\ 0 & 0 & 0 & 0 & 0 & 0 & \cos\gamma & 0 & \sin\gamma & 0 & 0 & 0 \\ 0 & 0 & 0 & 0 & 0 & 0 & 0 & 0 & 0 & 0 & -1 & 0 \\ 0 & 0 & 0 & 0 & 0 & 0 & 0 & 0 & 0 & \sin\gamma & 0 & -\cos\gamma \\ 0 & 0 & 0 & 0 & 0 & 0 & 0 & 0 & 0 & \cos\gamma & 0 & \sin\gamma \end{bmatrix} \quad (2.33)$$

Type 3: Frame member having a hinge connection at its second end

When second end of a frame member is hinged, as shown in Figure 2.13, bending moment about z axis will be zero at that joint ($M_{zj}=0$). From this equation rotation about z axis of that end of frame member (θ_{zj}) is obtained as follows.

$$\frac{6EI_z}{L^2}v_i+\frac{2EI_z}{L}\theta_{zi}-\frac{6EI_z}{L^2}v_j+\frac{4EI_z}{L}\theta_{zj}=0\rightarrow\theta_{zj}=-\frac{3}{2L}v_i-\frac{\theta_{zi}}{2}+\frac{3}{2L}v_j \quad (2.34)$$

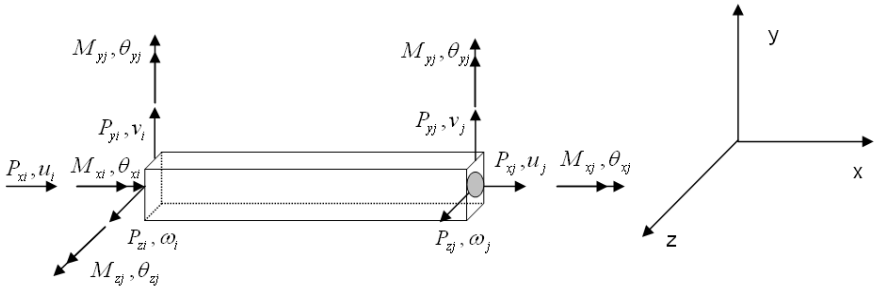

Figure 2.14 3-D frame member having a hinge connection at its second end

Substituting θ_{zj} in (2.1), following equations are obtained

$$
\begin{aligned}
&. P_{xi} = \frac{EA}{L} u_i - \frac{EA}{L} u_j \\
&P_{yi} = \frac{12EI_z}{L^3} v_i + \frac{6EI_z}{L^2} \theta_{zi} - \frac{12EI_z}{L^3} v_j + \frac{6EI_z}{L^2} \left(-\frac{3}{2L} v_i + \frac{3}{2L} v_j - \frac{\theta_{zj}}{2} \right) \\
&P_{yi} = \frac{3EI_z}{L^3} v_i + \frac{3EI_z}{L^2} \theta_{zi} - \frac{3EI_z}{L^3} v_j \\
&P_{zi} = \frac{12EI_y}{L^3} \omega_i - \frac{6EI_y}{L^2} \theta_{yi} - \frac{12EI_y}{L^3} \omega_j - \frac{6EI_y}{L^2} \theta_{yj} \\
&M_{xi} = \frac{GJ}{L} \theta_{xi} - \frac{GJ}{L} \theta_{xj} \\
&M_{yi} = -\frac{6EI_y}{L^2} \omega_i + \frac{4EI_y}{L} \theta_{yi} + \frac{6EI_y}{L^2} \omega_j + \frac{2EI_y}{L} \theta_{yj} \\
&M_{zi} = \frac{6EI_z}{L^2} v_i + \frac{4EI_z}{L} \theta_{zi} - \frac{6EI_z}{L^2} v_j + \frac{2EI_z}{L} \left(-\frac{3}{2L} v_i + \frac{3}{2L} v_j - \frac{\theta_{zj}}{2} \right) \\
&M_{zi} = \frac{3EI_z}{L^2} v_i + \frac{3EI_z}{L} \theta_{zi} - \frac{3EI_z}{L^2} v_j
\end{aligned}
\tag{2.35}
$$

After simplification, the relationships between end forces and displacements are obtained.

$$
\begin{aligned}
P_{xj} &= -\frac{EA}{L}u_i + \frac{EA}{L}u_j \\
P_{yj} &= -\frac{12EI_z}{L^3}v_i - \frac{6EI_z}{L^2}\theta_{zj} + \frac{12EI_z}{L^3}v_j - \frac{6EI_z}{L^2}\left(-\frac{3}{2L}v_i + \frac{3}{2L}v_j - \frac{\theta_{zj}}{2}\right) \\
P_{yj} &= -\frac{3EI_z}{L^3}v_i - \frac{3EI_z}{L^2}\theta_{zj} + \frac{3EI_z}{L^3}v_j \\
P_{zj} &= -\frac{12EI_y}{L^3}\omega_i + \frac{6EI_y}{L^2}\theta_{yi} + \frac{12EI_y}{L^3}\omega_j + \frac{6EI_y}{L^2}\theta_{yj} \\
M_{xj} &= -\frac{GJ}{L}\theta_{xi} + \frac{GJ}{L}\theta_{xj} \\
M_{yj} &= -\frac{6EI_y}{L^2}\omega_i + \frac{2EI_y}{L}\theta_{yi} + \frac{6EI_y}{L^2}\omega_j + \frac{4EI_y}{L}\theta_{yj}
\end{aligned}
\tag{2.36}
$$

When they are written in matrix form, following equation system is obtained.

$$
[k] = \begin{bmatrix}
\frac{EA}{L} & 0 & 0 & 0 & 0 & 0 & -\frac{EA}{L} & 0 & 0 & 0 & 0 & 0 \\
0 & \frac{12EI_z}{L^3} & 0 & 0 & 0 & \frac{6EI_z}{L^2} & 0 & \frac{-12EI_z}{L^3} & 0 & 0 & 0 & \frac{6EI_z}{L^2} \\
0 & 0 & \frac{12EI_y}{L^3} & 0 & -\frac{6EI_y}{L^2} & 0 & 0 & 0 & -\frac{12EI_y}{L^3} & 0 & -\frac{6EI_y}{L^2} & 0 \\
0 & 0 & 0 & \frac{GJ}{L} & 0 & 0 & 0 & 0 & 0 & -\frac{GJ}{L} & 0 & 0 \\
0 & 0 & -\frac{6EI_y}{L^2} & 0 & \frac{4EI_y}{L} & 0 & 0 & 0 & \frac{6EI_y}{L^2} & 0 & \frac{2EI_y}{L} & 0 \\
0 & \frac{3EI_z}{L^2} & 0 & 0 & 0 & \frac{3EI_z}{L} & 0 & \frac{-3EI_z}{L^2} & 0 & 0 & 0 & 0 \\
-\frac{EA}{L} & 0 & 0 & 0 & 0 & 0 & \frac{EA}{L} & 0 & 0 & 0 & 0 & 0 \\
0 & \frac{-12EI_z}{L^3} & 0 & 0 & 0 & -\frac{6EI_z}{L^2} & 0 & \frac{12EI_z}{L^3} & 0 & 0 & 0 & -\frac{6EI_z}{L^2} \\
0 & 0 & -\frac{12EI_y}{L^3} & 0 & \frac{6EI_y}{L^2} & 0 & 0 & 0 & \frac{12EI_y}{L^3} & 0 & \frac{6EI_y}{L^2} & 0 \\
0 & 0 & 0 & -\frac{GJ}{L} & 0 & 0 & 0 & 0 & 0 & \frac{GJ}{L} & 0 & 0 \\
0 & 0 & -\frac{6EI_y}{L^2} & 0 & \frac{2EI_y}{L} & 0 & 0 & 0 & \frac{6EI_y}{L^2} & 0 & \frac{4EI_y}{L} & 0 \\
0 & 0 & 0 & 0 & 0 & 0 & 0 & 0 & 0 & 0 & 0 & 0
\end{bmatrix}
\tag{2.37}
$$

Displacement transformation matrix for a frame member having a hinge connection at its second end is given in (2.38). Difference between this matrix and

transformation matrix given in (2.17) is that all terms, corresponding to θ_{zj}, term is equal to zero. Because, θ_{zj} is eliminated from the equation system given in (2.36). Therefore, displacement transformation matrix changes to the following form.

$$[B]=\begin{bmatrix} b_{11} & b_{12} & b_{13} & 0 & 0 & 0 & 0 & 0 & 0 & 0 & 0 & 0 \\ b_{21} & b_{22} & b_{23} & 0 & 0 & 0 & 0 & 0 & 0 & 0 & 0 & 0 \\ b_{31} & b_{32} & b_{33} & 0 & 0 & 0 & 0 & 0 & 0 & 0 & 0 & 0 \\ 0 & 0 & 0 & b_{11} & b_{12} & b_{13} & 0 & 0 & 0 & 0 & 0 & 0 \\ 0 & 0 & 0 & b_{21} & b_{22} & b_{23} & 0 & 0 & 0 & 0 & 0 & 0 \\ 0 & 0 & 0 & b_{31} & b_{32} & b_{33} & 0 & 0 & 0 & 0 & 0 & 0 \\ 0 & 0 & 0 & 0 & 0 & 0 & b_{11} & b_{12} & b_{13} & 0 & 0 & 0 \\ 0 & 0 & 0 & 0 & 0 & 0 & b_{21} & b_{22} & b_{23} & 0 & 0 & 0 \\ 0 & 0 & 0 & 0 & 0 & 0 & b_{31} & b_{32} & b_{33} & 0 & 0 & 0 \\ 0 & 0 & 0 & 0 & 0 & 0 & 0 & 0 & 0 & b_{11} & b_{12} & b_{13} \\ 0 & 0 & 0 & 0 & 0 & 0 & 0 & 0 & 0 & b_{21} & b_{22} & b_{23} \\ 0 & 0 & 0 & 0 & 0 & 0 & 0 & 0 & 0 & 0 & 0 & 0 \end{bmatrix} \quad (2.38)$$

For a frame member along the +Y axis displacement transformation matrix has the following form.

$$[B]=\begin{bmatrix} 0 & 1 & 0 & 0 & 0 & 0 & 0 & 0 & 0 & 0 & 0 & 0 \\ \sin\gamma & 0 & \cos\gamma & 0 & 0 & 0 & 0 & 0 & 0 & 0 & 0 & 0 \\ \cos\gamma & 0 & -\sin\gamma & 0 & 0 & 0 & 0 & 0 & 0 & 0 & 0 & 0 \\ 0 & 0 & 0 & 0 & 1 & 0 & 0 & 0 & 0 & 0 & 0 & 0 \\ 0 & 0 & 0 & \sin\gamma & 0 & \cos\gamma & 0 & 0 & 0 & 0 & 0 & 0 \\ 0 & 0 & 0 & \cos\gamma & 0 & -\sin\gamma & 0 & 0 & 0 & 0 & 0 & 0 \\ 0 & 0 & 0 & 0 & 0 & 0 & 0 & 1 & 0 & 0 & 0 & 0 \\ 0 & 0 & 0 & 0 & 0 & 0 & \sin\gamma & 0 & \cos\gamma & 0 & 0 & 0 \\ 0 & 0 & 0 & 0 & 0 & 0 & \cos\gamma & 0 & -\sin\gamma & 0 & 0 & 0 \\ 0 & 0 & 0 & 0 & 0 & 0 & 0 & 0 & 0 & 0 & 1 & 0 \\ 0 & 0 & 0 & 0 & 0 & 0 & 0 & 0 & 0 & \sin\gamma & 0 & \cos\gamma \\ 0 & 0 & 0 & 0 & 0 & 0 & 0 & 0 & 0 & 0 & 0 & 0 \end{bmatrix} \quad (2.39)$$

If the frame member is along the -Y axis displacement transformation becomes.

$$[B]=\begin{bmatrix} 0 & -1 & 0 & 0 & 0 & 0 & 0 & 0 & 0 & 0 & 0 & 0 \\ \sin\gamma & 0 & -\cos\gamma & 0 & 0 & 0 & 0 & 0 & 0 & 0 & 0 & 0 \\ \cos\gamma & 0 & \sin\gamma & 0 & 0 & 0 & 0 & 0 & 0 & 0 & 0 & 0 \\ 0 & 0 & 0 & 0 & -1 & 0 & 0 & 0 & 0 & 0 & 0 & 0 \\ 0 & 0 & 0 & \sin\gamma & 0 & -\cos\gamma & 0 & 0 & 0 & 0 & 0 & 0 \\ 0 & 0 & 0 & \cos\gamma & 0 & \sin\gamma & 0 & 0 & 0 & 0 & 0 & 0 \\ 0 & 0 & 0 & 0 & 0 & 0 & 0 & -1 & 0 & 0 & 0 & 0 \\ 0 & 0 & 0 & 0 & 0 & 0 & \sin\gamma & 0 & -\cos\gamma & 0 & 0 & 0 \\ 0 & 0 & 0 & 0 & 0 & 0 & \cos\gamma & 0 & \sin\gamma & 0 & 0 & 0 \\ 0 & 0 & 0 & 0 & 0 & 0 & 0 & 0 & 0 & 0 & -1 & 0 \\ 0 & 0 & 0 & 0 & 0 & 0 & 0 & 0 & 0 & \sin\gamma & 0 & -\cos\gamma \\ 0 & 0 & 0 & 0 & 0 & 0 & 0 & 0 & 0 & 0 & 0 & 0 \end{bmatrix} \quad (2.40)$$

Type 4: Frame member having a hinge connections at both ends

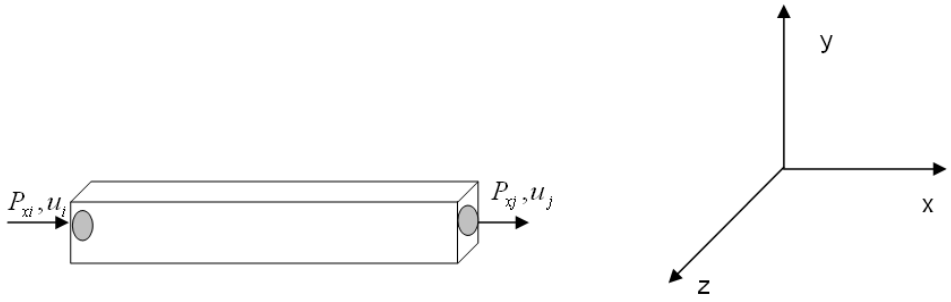

Figure 2.15 3-D frame member having a hinge connections at both ends

When both ends of a frame member are hinged, member becomes an axial member. It only transfer axial forces. In this case, $v_i, v_j, \omega_i, \omega_j, M_{xi}, M_{xj}, M_{yi}, M_{yj}, M_{zi}$ and M_{zj} terms become equal to zero. Thus, relationships between end forces and joint displacements are reduced to those given in the following (2.41).

$$P_{xi} = \frac{EA}{L}u_i - \frac{EA}{L}u_j \qquad \text{and} \qquad P_{xj} = -\frac{EA}{L}u_i + \frac{EA}{L}u_j \tag{2.41}$$

when these equations are written in matrix form, the following stiffness matrix is obtained.

$$[k]=\begin{bmatrix} \frac{EA}{L} & 0 & 0 & 0 & 0 & 0 & -\frac{EA}{L} & 0 & 0 & 0 & 0 & 0 \\ 0 & 0 & 0 & 0 & 0 & 0 & 0 & 0 & 0 & 0 & 0 & 0 \\ 0 & 0 & 0 & 0 & 0 & 0 & 0 & 0 & 0 & 0 & 0 & 0 \\ 0 & 0 & 0 & 0 & 0 & 0 & 0 & 0 & 0 & 0 & 0 & 0 \\ 0 & 0 & 0 & 0 & 0 & 0 & 0 & 0 & 0 & 0 & 0 & 0 \\ 0 & 0 & 0 & 0 & 0 & 0 & 0 & 0 & 0 & 0 & 0 & 0 \\ -\frac{EA}{L} & 0 & 0 & 0 & 0 & 0 & \frac{EA}{L} & 0 & 0 & 0 & 0 & 0 \\ 0 & 0 & 0 & 0 & 0 & 0 & 0 & 0 & 0 & 0 & 0 & 0 \\ 0 & 0 & 0 & 0 & 0 & 0 & 0 & 0 & 0 & 0 & 0 & 0 \\ 0 & 0 & 0 & 0 & 0 & 0 & 0 & 0 & 0 & 0 & 0 & 0 \\ 0 & 0 & 0 & 0 & 0 & 0 & 0 & 0 & 0 & 0 & 0 & 0 \\ 0 & 0 & 0 & 0 & 0 & 0 & 0 & 0 & 0 & 0 & 0 & 0 \end{bmatrix} \tag{2.42}$$

The displacement transformation matrix for this case is given in (2.43). In this displacement transformation matrix all terms corresponding to v_i, v_j, ω_i , $\omega_j, \theta_{xi}, \theta_{xj}, \theta_{yi}, \theta_{yj,} \theta_{zi}$ and θ_{zj} are equal to zero. Consequently the displacement transformation takes the following form.

$$[B]=\begin{bmatrix} b_{11} & b_{12} & b_{13} & 0 & 0 & 0 & 0 & 0 & 0 & 0 & 0 & 0 \\ 0 & 0 & 0 & 0 & 0 & 0 & 0 & 0 & 0 & 0 & 0 & 0 \\ 0 & 0 & 0 & 0 & 0 & 0 & 0 & 0 & 0 & 0 & 0 & 0 \\ 0 & 0 & 0 & 0 & 0 & 0 & 0 & 0 & 0 & 0 & 0 & 0 \\ 0 & 0 & 0 & 0 & 0 & 0 & 0 & 0 & 0 & 0 & 0 & 0 \\ 0 & 0 & 0 & 0 & 0 & 0 & 0 & 0 & 0 & 0 & 0 & 0 \\ 0 & 0 & 0 & 0 & 0 & 0 & b_{11} & b_{12} & b_{13} & 0 & 0 & 0 \\ 0 & 0 & 0 & 0 & 0 & 0 & 0 & 0 & 0 & 0 & 0 & 0 \\ 0 & 0 & 0 & 0 & 0 & 0 & 0 & 0 & 0 & 0 & 0 & 0 \\ 0 & 0 & 0 & 0 & 0 & 0 & 0 & 0 & 0 & 0 & 0 & 0 \\ 0 & 0 & 0 & 0 & 0 & 0 & 0 & 0 & 0 & 0 & 0 & 0 \\ 0 & 0 & 0 & 0 & 0 & 0 & 0 & 0 & 0 & 0 & 0 & 0 \end{bmatrix} \tag{2.43}$$

When the member along the +Y axis displacement transformation matrix becomes.

$$[B]=\begin{bmatrix} 0 & 1 & 0 & 0 & 0 & 0 & 0 & 0 & 0 & 0 & 0 & 0 \\ 0 & 0 & 0 & 0 & 0 & 0 & 0 & 0 & 0 & 0 & 0 & 0 \\ 0 & 0 & 0 & 0 & 0 & 0 & 0 & 0 & 0 & 0 & 0 & 0 \\ 0 & 0 & 0 & 0 & 0 & 0 & 0 & 0 & 0 & 0 & 0 & 0 \\ 0 & 0 & 0 & 0 & 0 & 0 & 0 & 0 & 0 & 0 & 0 & 0 \\ 0 & 0 & 0 & 0 & 0 & 0 & 0 & 0 & 0 & 0 & 0 & 0 \\ 0 & 0 & 0 & 0 & 0 & 0 & 0 & 1 & 0 & 0 & 0 & 0 \\ 0 & 0 & 0 & 0 & 0 & 0 & 0 & 0 & 0 & 0 & 0 & 0 \\ 0 & 0 & 0 & 0 & 0 & 0 & 0 & 0 & 0 & 0 & 0 & 0 \\ 0 & 0 & 0 & 0 & 0 & 0 & 0 & 0 & 0 & 0 & 0 & 0 \\ 0 & 0 & 0 & 0 & 0 & 0 & 0 & 0 & 0 & 0 & 0 & 0 \\ 0 & 0 & 0 & 0 & 0 & 0 & 0 & 0 & 0 & 0 & 0 & 0 \end{bmatrix} \tag{2.44}$$

For a frame member along –Y axis displacement transformation matrix has following form.

$$[B]=\begin{bmatrix} 0 & -1 & 0 & 0 & 0 & 0 & 0 & 0 & 0 & 0 & 0 & 0 \\ 0 & 0 & 0 & 0 & 0 & 0 & 0 & 0 & 0 & 0 & 0 & 0 \\ 0 & 0 & 0 & 0 & 0 & 0 & 0 & 0 & 0 & 0 & 0 & 0 \\ 0 & 0 & 0 & 0 & 0 & 0 & 0 & 0 & 0 & 0 & 0 & 0 \\ 0 & 0 & 0 & 0 & 0 & 0 & 0 & 0 & 0 & 0 & 0 & 0 \\ 0 & 0 & 0 & 0 & 0 & 0 & 0 & 0 & 0 & 0 & 0 & 0 \\ 0 & 0 & 0 & 0 & 0 & 0 & 0 & -1 & 0 & 0 & 0 & 0 \\ 0 & 0 & 0 & 0 & 0 & 0 & 0 & 0 & 0 & 0 & 0 & 0 \\ 0 & 0 & 0 & 0 & 0 & 0 & 0 & 0 & 0 & 0 & 0 & 0 \\ 0 & 0 & 0 & 0 & 0 & 0 & 0 & 0 & 0 & 0 & 0 & 0 \\ 0 & 0 & 0 & 0 & 0 & 0 & 0 & 0 & 0 & 0 & 0 & 0 \\ 0 & 0 & 0 & 0 & 0 & 0 & 0 & 0 & 0 & 0 & 0 & 0 \end{bmatrix} \tag{2.45}$$

2.2.6 General steps for 3-D frame analysis

Frame analysis steps in this program are described as follows:

Firstly input data is read from program. These data consists of modulus of elasticity, shear module, section properties, member end joint numbers, member group numbers, joint coordinates and frame forces. The structure stiffness matrix $[K_s]$ and the load vector $[P]$ are calculated in Equation (2.25) by using these values. Then, Equation system, given in (2.25) ($\{P\} = [K]\{D\}$), is solved and joint displacements in global coordinates ($\{D\} = [K]^{-1}\{P\}$) are obtained. By then, the vector member end forces and moments are calculated by using $\{F\} = [k][B]\{D\}$ equality. Consequently, in addition to joint displacements and joint rotations in global X, Y, Z coordinates, axial forces, shear forces in local y, z axis and moments x, y, z coordinates are obtained by using the frame analysis program.

Computer Program written in FORTRAN for analyzing 3-D frames is tested and results are compared to package program STRAND 7 in numerical example that are shown in section 2.4.1.

2.3 The effect of warping in thin walled members

Warping effect occurs due to a twisting moment. When a twisting moment acts on thin walled beam as shown in Figure 2.16, the horizontal fibers of the beam along x axis, which are located on top and bottom surface on the beam, rotate. As a result of this rotation, particles located top and bottom surfaces of the beam move along z axis from their initial position in space. Therefore, the top and bottom surfaces of the beam do not remain plane and become warped. If the far

end of the beam is rigidly fixed, warping of beam is restrained. This restraint causes same longitudinal strains and stresses. The presence of the longitudinal stresses occur by applying part of the work done by twisting moment. The twisting moment develops shear and normal stresses associated with the *St. Venant Twist* and flexural twist. The twisting moment acting on the section consist of two parts.

$$T = T_{SV} + T_w \tag{2.46}$$

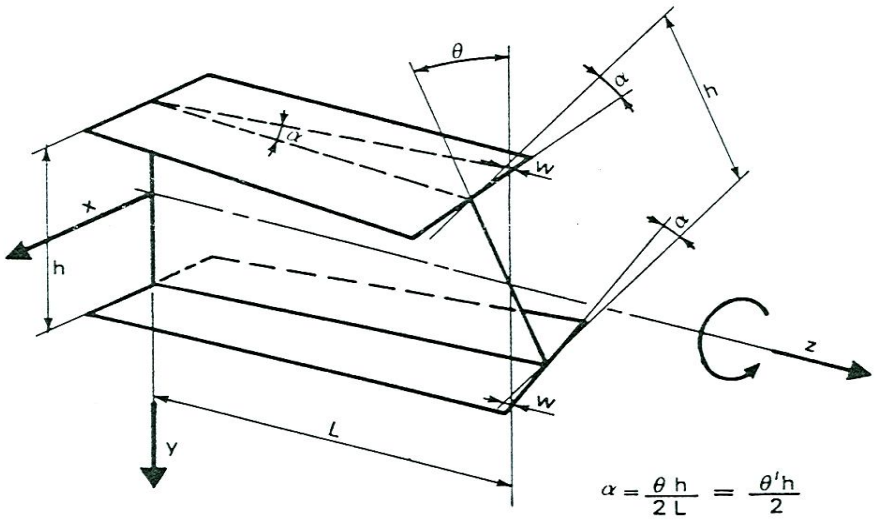

Figure 2.16 Warping effect of thin walled beam

where, T_{SV} is the *St. Venant* torsional moment and T_w is the *flexural* twist. These torsional moment components can be expressed in terms of twisting as follows:

$$T_{sv} = GJ\frac{d\theta}{dz} \quad , \qquad T_w = EI_w\frac{d^2\theta}{dz^2} \tag{2.47}$$

Substituting these equations into (2.46), following differential equation is obtained (2.48).

$$T = GJ\frac{d\theta}{dz} - EI_w\frac{d^2\theta}{dz^2} \tag{2.48}$$

In case of distributed torque along the beam:

$$t = \frac{dT}{dz} = GJ\frac{d^2\theta}{dz^2} - EI_w\frac{d^3\theta}{dz^3} \tag{2.49}$$

Dividing both sides by EI_w the following equation is obtained.

$$\theta_z^{III} - \alpha^2\theta_z^{II} = 0 \tag{2.50}$$

where, $\alpha^2 = \dfrac{GJ}{EI_w}$

The general solution of this equation is:

$$\theta_z = A\sinh(\alpha z) + B\cosh(\alpha z) + Cz + D \tag{2.51}$$

Where A, B, C, D are constants which are obtained from homogeneous solution of the differential equation (2.50). Consequently, relationship between the torsional moment and the twisting angle is demonstrated with equation (2.51). In order to use this relationship in matrix displacement method, torsional stiffness matrix needs to be constructed.

Torsional stiffness matrix

The total torque acting on a member is a vector that acts longitudinal direction of a member [115]. In Figure 2.17, M_{xi} and M_{xj} are the *St. Venant* tornional moments, and θ_{xi} and θ_{xj} are the resulting displacement parameters. The *St Venant* torque is a vector that acts in the same direction as these end-torsional moments. However, warping torque T_w vector does not act in the same direction. For thin walled members the warping torque can be represented in terms of the pair of bending moments, and these moments can be represented as a vector that acts in the direction of Y axis (see Figure 2.18). These moments (M_{wi} and M_{wj}) are called as bi moment. General definition of a bi moment is a pair equal but opposite bending moments acting in two parallel planes. The resulting displacement parameters of the warping torque (θ_{wi} and θ_{wj}) can be represented as vector which are the first derivative of the resulting displacement parameters of the *St Venant* torque (θ_{xi} and θ_{xj}). Relationship between the resulting displacement parameters ($\theta_{xi}, \theta_{xj}, \theta_{wi}$ and θ_{wj}) and torsional moments (M_{xi}, M_{xj}, M_{wi} and M_{wj}) can be represented as equilibrium given as follows.

$$\begin{bmatrix} [TS_{1,1}] & \vdots & [TS_{1,2}] \\ \cdots \quad \cdots & \vdots & \cdots \quad \cdots \\ [TS_{2,1}] & \vdots & [TS_{2,2}] \end{bmatrix} \begin{bmatrix} \theta_{xi} \\ \theta_{wi} \\ \cdots \\ \theta_{xj} \\ \theta_{wj} \end{bmatrix} = \begin{bmatrix} M_{xi} \\ M_{wi} \\ \cdots \\ M_{xj} \\ M_{wj} \end{bmatrix} \tag{2.52}$$

where, $[TS_{ij}]$ is the torsional stiffness matrix. Terms of this matrix are calculated in the following

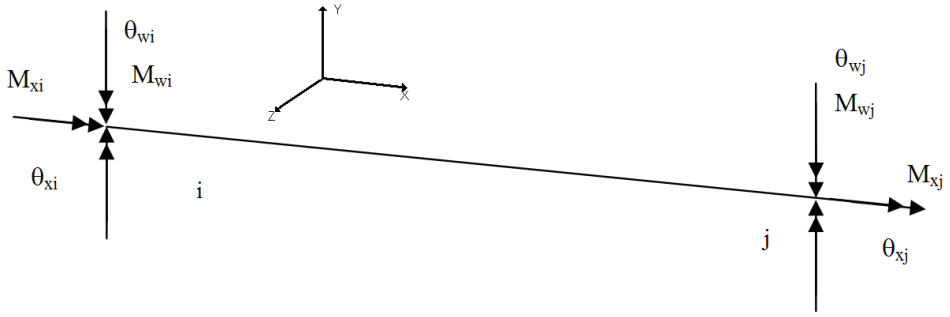

Figure 2.17 Beam element subjected to the torsion

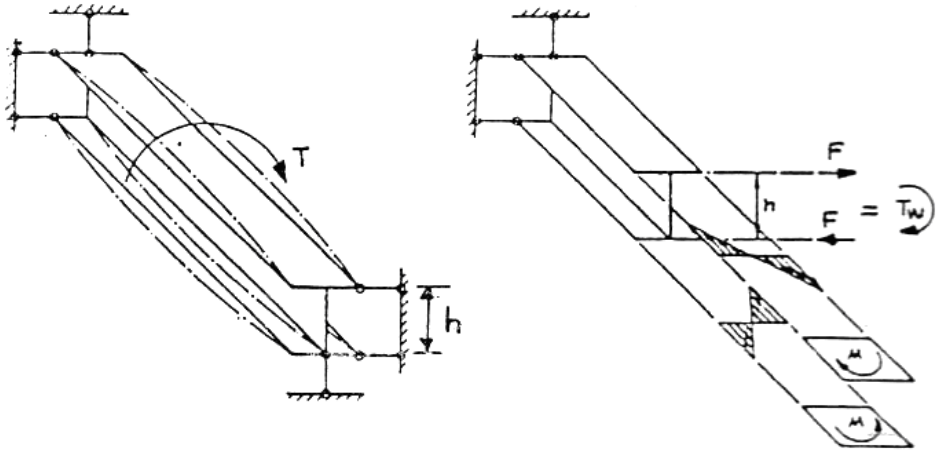

Figure 2.18 Twisting torque acting on beam element

Let consider a beam which is subjected to the torsion given in the Figure 2.17. Following boundary conditions is applied to Equation (2.49) in order to obtain the terms of torsional stiffness matrix of the beam.

First boundary condition ($\theta_{xi}=1 \quad \theta_{xj}=0 \quad \theta_{wi}=0 \quad \theta_{wj}=0$): After applying these boundary conditions, end moments are obtained as in the following:

$$M_{xi}=-M_{xj}=-GJ\cdot\sqrt{\frac{GJ}{EI_w}}\,\frac{\sinh(\alpha l)}{2\cosh(\alpha l)-\alpha l\cosh(\alpha l)-2} \tag{2.50}$$

and

$$M_{wi}=-M_{wj}=-GJ\cdot\frac{\cosh(\alpha l)-1}{2\cosh(\alpha l)-\alpha l\cosh(\alpha l)-2} \tag{2.51}$$

Second boundary condition ($\theta_{xi}=0 \quad \theta_{xj}=0 \quad \theta_{wi}=1 \quad \theta_{wj}=0$): If these boundary conditions are applied, following end moments are obtained:

$$M_{xi}=-M_{xj}=-GJ\cdot\frac{\cosh(\alpha l)-1}{2\cosh(\alpha l)-\alpha l\cosh(\alpha l)-2} \tag{2.52}$$

$$M_{wi}=\frac{GJ}{\alpha}\cdot\frac{\sinh(\alpha l)-\alpha l\cosh(\alpha l)}{2\cosh(\alpha l)-\alpha l\cosh(\alpha l)-2} \tag{2.53}$$

$$M_{wj}=\frac{GJ}{\alpha}\cdot\frac{\alpha l-\sinh(\alpha l)}{2\cosh(\alpha l)-\alpha l\cosh(\alpha l)-2} \tag{2.54}$$

If Equations (2.50), (2.51), (2.52), (2.53) and (2.54) are written in matrix form, following equation system is obtained.

$$\begin{bmatrix} -T_1 & -T_2 & T_1 & -T_2 \\ -T_2 & T_3 & T_2 & T_4 \\ T_1 & T_2 & -T_1 & T_2 \\ -T_2 & T_4 & T_2 & T_3 \end{bmatrix}\cdot\begin{bmatrix} \theta_{xi} \\ \theta_{wi} \\ \theta_{xj} \\ \theta_{wj} \end{bmatrix}=\begin{bmatrix} M_{xi} \\ M_{wi} \\ M_{xj} \\ M_{wj} \end{bmatrix} \tag{2.55}$$

where;

$$T_1 = GJ\frac{\alpha\sinh(\alpha l)}{2\cosh(\alpha l)-\alpha l\cosh(\alpha l)-2} \tag{2.56}$$

$$T_2 = GJ\frac{\cosh(\alpha l)-1}{2\cosh(\alpha l)-\alpha l\cosh(\alpha l)-2} \tag{2.57}$$

$$T_3 = \frac{GJ}{\alpha}\cdot\frac{\sinh(\alpha l)-\alpha l\cosh(\alpha l)}{2\cosh(\alpha l)-\alpha l\cosh(\alpha l)-2} \tag{2.58}$$

$$T_4 = \frac{GJ}{\alpha}\cdot\frac{\alpha l-\sinh(\alpha l)}{2\cosh(\alpha l)-\alpha l\cosh(\alpha l)-2} \tag{2.59}$$

By then, these terms are added to the local stiffness matrix which has twelve rows and twelve columns as shown in (2.2). This brings the total number of degrees of freedom to seven at a joint of space frame. These degrees of freedoms are the usual three translations along X, Y, and Z axes, three rotations about the global axes and additional warping deformation. Consequently, the member stiffness matrix in local coordinate system has fourteen rows and fourteen columns which is shown in (2.60). Three dimensional frames are analyzed takes into account warping effect by using this stiffness matrix. At the end of the analysis, in addition to the member end forces and end moments, which are obtained from without warping case, bi-moments are obtained.

$$[k]=\begin{bmatrix}
\frac{EA}{L} & 0 & 0 & 0 & 0 & 0 & 0 & -\frac{EA}{L} & 0 & 0 & 0 & 0 & 0 & 0 \\
0 & \frac{12EI_z}{L^3} & 0 & 0 & 0 & 0 & \frac{6EI_z}{L^2} & 0 & -\frac{12EI_z}{L^3} & 0 & 0 & 0 & 0 & \frac{6EI_z}{L^2} \\
0 & 0 & \frac{12EI_y}{L^3} & 0 & 0 & -\frac{6EI_y}{L^2} & 0 & 0 & 0 & -\frac{12EI_y}{L^3} & 0 & 0 & -\frac{6EI_y}{L^2} & 0 \\
0 & 0 & 0 & -T_1 & -T_2 & 0 & 0 & 0 & 0 & 0 & T_1 & -T_2 & 0 & 0 \\
0 & 0 & 0 & -T_2 & T_3 & 0 & 0 & 0 & 0 & 0 & T_2 & T_4 & 0 & 0 \\
0 & 0 & -\frac{6EI_y}{L^2} & 0 & 0 & \frac{4EI_y}{L} & 0 & 0 & 0 & \frac{6EI_y}{L^2} & 0 & 0 & \frac{2EI_y}{L} & 0 \\
0 & \frac{6EI_z}{L^2} & 0 & 0 & 0 & 0 & \frac{4EI_z}{L} & 0 & -\frac{6EI_z}{L^2} & 0 & 0 & 0 & 0 & \frac{2EI_z}{L} \\
-\frac{EA}{L} & 0 & 0 & 0 & 0 & 0 & 0 & \frac{EA}{L} & 0 & 0 & 0 & 0 & 0 & 0 \\
0 & -\frac{12EI_z}{L^3} & 0 & 0 & 0 & 0 & -\frac{6EI_z}{L^2} & 0 & \frac{12EI_z}{L^3} & 0 & 0 & 0 & 0 & -\frac{6EI_z}{L^2} \\
0 & 0 & -\frac{12EI_y}{L^3} & 0 & 0 & \frac{6EI_y}{L^2} & 0 & 0 & 0 & \frac{12EI_y}{L^3} & 0 & 0 & \frac{6EI_y}{L^2} & 0 \\
0 & 0 & 0 & T_1 & T_2 & 0 & 0 & 0 & 0 & 0 & -T_1 & T_2 & 0 & 0 \\
0 & 0 & 0 & -T_2 & T_4 & 0 & 0 & 0 & 0 & 0 & T_2 & T_3 & 0 & 0 \\
0 & 0 & -\frac{6EI_y}{L^2} & 0 & 0 & \frac{2EI_y}{L} & 0 & 0 & 0 & \frac{6EI_y}{L^2} & 0 & 0 & \frac{4EI_y}{L} & 0 \\
0 & \frac{6EI_z}{L^2} & 0 & 0 & 0 & 0 & \frac{2EI_z}{L} & 0 & -\frac{6EI_z}{L^2} & 0 & 0 & 0 & 0 & \frac{4EI_z}{L}
\end{bmatrix} \tag{2.60}$$

2.4 Numerical examples

2.4.1 Numerical example eight member 3-D frame

Eight member 3-D frame is selected as an example problem. This frame, whose load conditions and geometry are shown in Figure 2.19, is firstly analyzed by using developed algorithm. Input data of this algorithm for this frame is demonstrated at Table 2.2

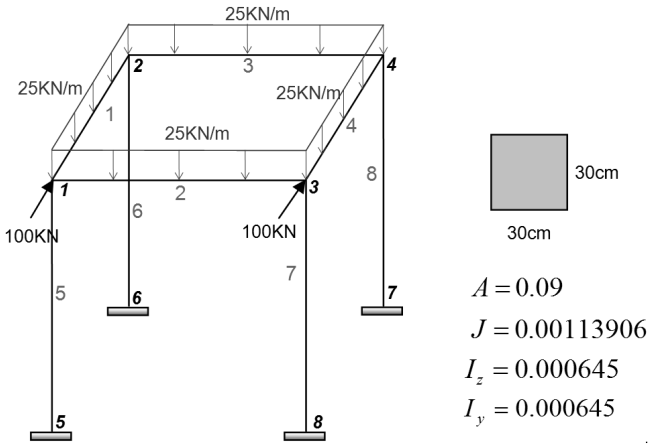

Figure 2.19 Eight member 3-D frame

Table 2.2 Input data of eight member 3-D frame

4	8	1	4	5	1	2.08e8	0.7885e8																	
1	2	2	4	3	4	1	3	1	5	2	6	3	7	4	8									
1	1	1	1	1	1	1	1	1																
0	0	0	0	0	0	0	0																	
1	1	1	1	1	1	1	1																	
0.09	6.75e-4	6.75e-4	1.14e-2																					
0	4	4	0	4	0	4	4	4	4	4	0	0	0	4	0	0	0	4	0	4	4	0	0	
1	1																							
2																								
1	0	0	-100	0	0	0																		
3	0	0	-100	0	0	0																		
4																								
1	0	1	0	0																				
-25	-25	0	4																					
2	0	1	0	0																				
-25	-25	0	4																					
3	0	1	0	0																				
-25	-25	0	4																					
4	0	1	0	0																				
-25	-25	0	4																					

Joint displacements and rotations obtained from thesis program are tabulated in Table 2.3 and members end forces and end moments are shown in Table 2.4.

Table 2.3 Joint displacements of eight member 3-D frame

DISPLACEMENTS OF JOINTS						
JOINT NO	X-DISP (m)	Y-DISP (m)	Z-DISP (m)	THETA-X (Radian)	THETA-Y (Radian)	THETA-Z (Radian)
1	0.90319E-06	-0.12404E-04	-0.27672E-02	-0.57910E-03	0.79385E-09	-0.16082E-03
2	0.90088E-06	-0.30957E-04	-0.27546E-02	-0.25475E-03	0.84763E-09	-0.16082E-03
3	-0.90095E-06	-0.12404E-04	-0.27673E-02	-0.57910E-03	0.83961E-09	0.16082E-03
4	-0.90327E-06	-0.30957E-04	-0.27546E-02	-0.25475E-03	0.82861E-09	0.16082E-03

Table 2.4 Member end forces of eight member 3-D frame

MEMBER FORCES							
MEM. NO.	END NO.	FX (kN)	FY (kN)	FZ (kN)	MX (kN-m)	MY (kN-m)	MZ (kN-m)
1	1	0.5825E02	0.7213E01	-0.2502E-04	0.3290E-04	0.4818E-04	-0.6346E02
1	2	-0.5825E02	0.9279E02	0.2502E-04	-0.3290E-04	0.5190E-04	-0.1077E03
2	1	0.8322E01	0.5000E02	0.1133E-03	0.1172E-03	-0.2247E-03	0.2221E02
2	2	-0.8322E01	0.5000E02	-0.1133E-03	-0.1172E-03	-0.2284E-03	-0.2221E02
3	1	0.5825E02	0.7213E01	-0.2639E-04	0.4064E-04	0.5317E-04	-0.6346E02
3	2	-0.5825E02	0.9279E02	0.2639E-04	-0.4064E-04	0.5241E-04	-0.1077E03
4	1	0.8322E01	0.5000E02	0.1217E-03	0.1067E-03	-0.2418E-03	0.2221E02
4	2	-0.8322E01	0.5000E02	-0.1217E-03	-0.1067E-03	-0.2295E-03	-0.2221E02
5	1	0.5721E02	0.4175E02	-0.8322E01	-0.1782E-03	0.2221E02	0.6346E02
5	2	-0.5721E02	-0.4175E02	0.8322E01	0.1782E-03	0.1108E02	0.1035E03
6	1	0.1428E03	0.5825E02	-0.8322E01	-0.1903E-03	0.2221E02	0.1077E03
6	2	-0.1428E03	-0.5825E02	0.8322E01	0.1903E-03	0.1108E02	0.1253E03
7	1	0.5721E02	0.4175E02	0.8322E01	-0.1885E-03	-0.2221E02	0.6346E02
7	2	-0.5721E02	-0.4175E02	-0.8322E01	0.1885E-03	-0.1108E02	0.1035E03
8	1	0.1428E03	0.5825E02	0.8322E01	-0.1860E-03	-0.2221E02	0.1077E03
8	2	-0.1428E03	-0.5825E02	-0.8322E01	0.1860E-03	-0.1108E02	0.1253E03

This frame also is analyzed by using package program STAND7. Displacements and rotations of joints obtained from STRAND7 are tabulated in Table 2.5 and end forces and end moments of frame members are shown in Table 2.6. It is apparent from the tables that there is no considerable difference between results obtained by the program developed and these found by STAND7 program results. There are small differences observed between these results, since STRAND7 program consider the shear effect for analyzing frames. However, this effect is not important in example problems. Therefore, absolute difference between results is around 10^{-3}-10^{-5}. In addition, sign differences are seen between values because of the difference in sign convention.

Table 2.5 Joint displacements of eight member 3-D frame obtained by STRAND7

	DX (m)	DY (m)	DZ (m)	RX (Radian)	RY (Radian)	RZ (Radian)
Node1	0	0	-0.0028	-0.5794E-03	0	-0.16057E-03
Node2	0	0	-0.0028	-0.2548E-03	0	-0.16057E-03
Node3	0	0	-0.0028	-0.5794E-03	0	0.16057E-03
Node4	0	0	-0.0028	-0.2548E-03	0	0.16057E-03
Node5	0	0	0	0	0	0
Node6	0	0	0	0	0	0
Node7	0	0	0	0	0	0
Node8	0	0	0	0	0	0

Table 2.6 Member end forces of eight member 3-D frame obtained by STRAND7

	FX (kN)	FY (kN)	FZ (kN)	MX (kN-m)	MY (kN-m)	MZ (kN-m)
Beam1:End1	-58.2514	7.2116	0	0	0	63.4638
Beam1:End2	-58.2514	-92.7884	0	0	0	-107.69
Beam2:End1	-8.3216	50	0	0	0	-22.2066
Beam2:End2	-8.3216	-50	0	0	0	-22.2066
Beam3:End1	-8.3216	50	0	0	0	-22.2066
Beam3:End2	-8.3216	-50	0	0	0	-22.2066
Beam4:End1	-58.2514	7.2116	0	0	0	63.4638
Beam4:End2	-58.2514	-92.7884	0	0	0	-107.69
Beam5:End1	-57.2116	-8.3216	41.7486	0	22.2066	-63.4638
Beam5:End2	-57.2116	-8.3216	41.7486	0	-11.0799	103.5306
Beam6:End1	-142.788	-8.3216	58.2514	0	22.2066	-107.69
Beam6:End2	-142.788	-8.3216	58.2514	0	-11.0799	125.3159
Beam7:End1	-57.2116	8.3216	41.7486	0	-22.2066	-63.4638
Beam7:End2	-57.2116	8.3216	41.7486	0	11.0799	103.5306
Beam8:End1	-142.788	8.3216	58.2514	0	-22.2066	-107.69
Beam8:End2	-142.788	8.3216	58.2514	0	11.0799	125.3159

A computer program is coded in FORTRAN based on the matrix displacement method above. The program reads the input data which is includes the geometrical information of the frame as well as cross sectional properties of the W sections adopted for the beams and columns of the frame. Furthermore, the loading of the frame is also read. Two numerical examples are considered to demonstrate the effect of warping in behavior of frame. First example is two-bay, two-storey three dimensional, irregular frame shown in Figure 2.20, second example is a 468 member twenty storey three dimensional, irregular frame shown in Figures 2.21 and 2.22

2.4.2 Two-bay two-storey three dimensional irregular frame

Two-bay, two-storey three dimensional, irregular frame shown in Figure 2.20 is considered to demonstrate the effect of warping. The dimensions of the frame are shown in same figure. The frame consists of 21 members that are collected in 2 independent groups. In this frame the W310x86 section is assigned to columns and the W250x67 section is selected for beams. The frame is subjected to wind loading -50 KN at Z direction.

At the end of the analysis joint displacements are demonstrated in tables 2.7 and 2.8; member end forces are demonstrated in table 2.9 and 2.10.

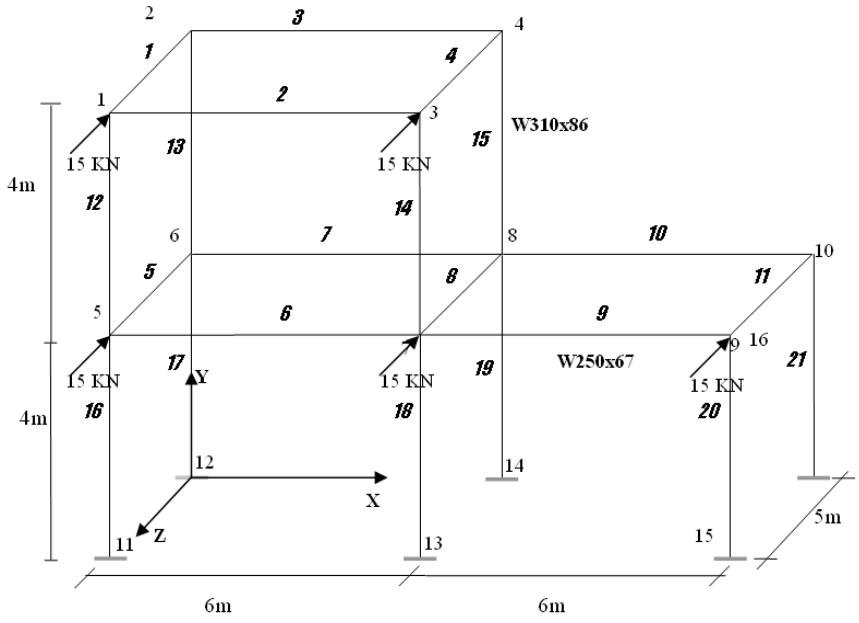

Figure 2.20 Beam Element subjected to the torsion

Table 2.7 Displacements (excluding warping effect)

JOINT NO	X-DISP	Y-DISP	Z-DISP	THETA-X	THETA-Y	THETA-Z
1	-0.5786E-2	0.1579E-3	-0.6043E-1	-0.2055E-2	-0.3322E-2	0.1144E-2
2	0.2783E-2	-0.1416E-3	-0.6036E-1	-0.2058E-2	-0.3320E-2	-0.3032E-3
3	-0.5779E-2	0.7129E-2	-0.2894E-1	-0.3517E-2	-0.3318E-2	0.1325E-2
4	0.2781E-2	-0.1166E-3	-0.2887E-1	-0.3735E-2	-0.3316E-2	-0.3420E-3
5	-0.1473E-2	0.1226E-3	-0.3401E-1	-0.4537E-2	-0.3380E-2	0.9015E-3
6	0.1050E-2	-0.1094E-3	-0.3394E-1	-0.4527E-2	-0.3151E-2	-0.3574E-3
7	-0.1437E-2	0.7088E-2	0.1094E-2	-0.3515E-2	-0.6750E-3	0.4993E-3
8	0.1028E-2	-0.7301E-4	0.9532E-3	-0.2506E-2	-0.1309E-2	-0.2823E-3
9	-0.1380E-2	0.4530E-4	-0.1581E-1	-0.1577E-2	0.1286E-2	-0.1356E-3
10	0.1000E-2	-0.3158E-4	-0.1574E-1	-0.1562E-2	0.1450E-2	-0.2389E-3

Table 2.8 Displacements (including warping effect)

JOINT NO	X-DISP	Y-DISP	Z-DISP	THETA-X	THETA-W	THETA-Y	THETA-Z
1	-0.5779E-2	0.1579E-3	-0.6041E-1	-0.2054E-2	0.1319E-3	-0.3324E-2	0.1143E-2
2	0.2774E-2	-0.1416E-3	-0.6034E-1	-0.2057E-2	0.5547E-4	-0.3319E-2	-0.3025E-3
3	-0.5773E-2	0.7125E-2	-0.2894E-1	-0.3516E-2	-0.4820E-3	-0.3301E-2	0.1323E-2
4	0.2774E-2	-0.1166E-3	-0.2887E-1	-0.3734E-2	-0.3127E-3	-0.3310E-2	-0.3406E-3
5	-0.1471E-2	0.1226E-3	-0.3400E-1	-0.4536E-2	-0.3722E-3	-0.3363E-2	0.9003E-3
6	0.1048E-2	-0.1094E-3	-0.3393E-1	-0.4526E-2	-0.3304E-3	-0.3136E-2	-0.3562E-3
7	-0.1436E-2	0.7085E-2	0.1094E-2	-0.3514E-2	-0.1043E-3	-0.6761E-3	0.4985E-3
8	0.1025E-2	-0.7301E-4	0.9524E-3	-0.2506E-2	-0.2532E-3	-0.1309E-2	-0.2815E-3
9	-0.1379E-2	0.4528E-4	-0.1581E-1	-0.1577E-2	0.3357E-3	0.1284E-2	-0.1355E-3
10	0.9975E-3	-0.3157E-4	-0.1574E-1	-0.1562E-2	0.3370E-3	0.1446E-2	-0.2386E-3

Table 2.9 Member end forces (excluding warping effect)

Member End	FX (kN)	FY (kN)	FZ (kN)	MX (kN-m)	MY (kN-m)	MZ (kN-m)	σ (kPa)
7	1.37E2	1.72E-3	1.45	-8.24E–3	-9.85	4.41	6.235E3
13	-1.37E2	-1.72E-3	-1.45	8.24E–3	2.45	-4.40	4.124E3

Table 2.10 Member end forces (including warping effect)

Member End	FX (kN)	FY (kN)	FZ (kN)	MX (kN-m)	MW (kN-m^2)	MY (kN-m)	MZ (kN-m)	σ (kPa)
7	1.37E2	1.91E–2	1.45	-2.59E–2	-5.16E–2	-9.85	4.46	7.276E3
13	-1.37E2	-1.91E–2	-1.45	2.59E–2	-3.85E–2	2.45	-4.36	4.839E3

It is clearly seen from table 2.9 and table 2.10 that there is a 16% increases in the normal stress value for member 7 when the effect of warping is included in the analysis of the frame.

2.4.3 468 Member twenty storey three dimensional irregular frame

The three dimensional view and plan view of 20-story irregular steel frame shown in Figures 2.21 and 2.22 is taken from previous studies given in reference [114 - 116]. The frame consists of 210 joints and 460 members that are grouped into 13 independent design groups. Frame sections assigned these groups are tabulated in Table 2.11 The frame is subjected to a uniformly distributed vertical load of 4.79kN/m^2 on each floor and wind load of 0.958kN/m^2 along the Z axis.

At the end of the analysis displacements and rotations are demonstrated in Figures 2.23 and 2.24. Values of the stresses for critical members are tabulated in Table 2.12.

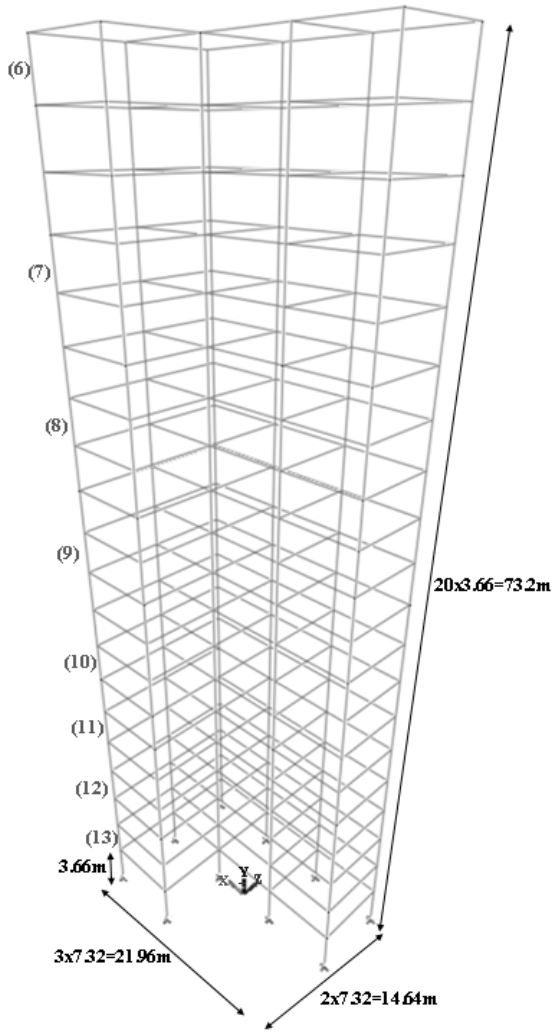

Figure 2.21 3-D view of twenty-story, three-bay irregular frame

Table 2.11 Assigned sections for each group

Group Number	Assigned Section
1	W310X97
2	W310X38.7
3	W610X101
4	W530X85
5	W530X92
6	W310X38.7
7	W250X101
8	W310X129
9	W310X158
10	W360X196
11	W360X216
12	W360X237
13	W360X262

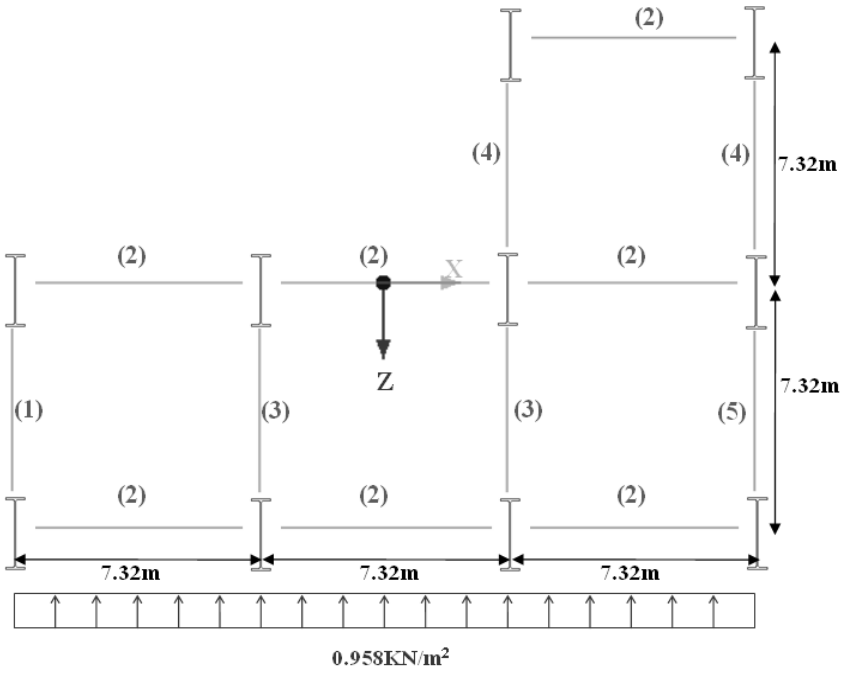

Figure 2.22 Plan view of twenty-story, three-bay irregular frame

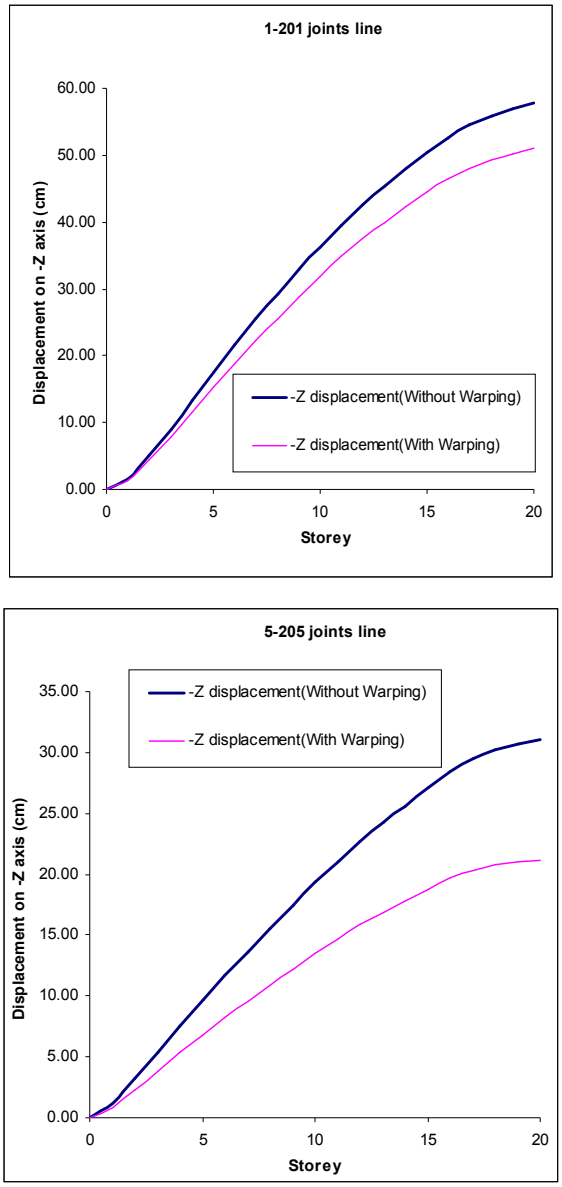

Figure 2.23 Displacements of twenty-story, three-bay irregular frame

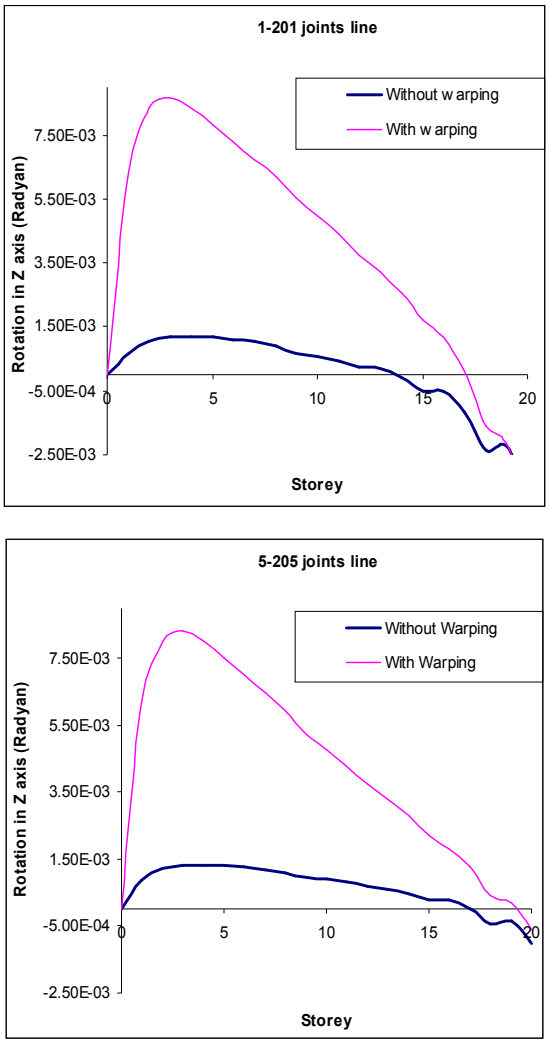

Figure 2.24 Rotations of twenty-story, three-bay irregular frame

Table 2.12 Stresses for twenty-story, three-bay irregular frame

		Without Warping				With Warping					Diff. %	Diff. MPa
Mem	End	σ_P (MPa)	σ_Z (MPa)	σ_Y (MPa)	Total (MPa)	σ_P (MPa)	σ_Z (MPa)	σ_Y (MPa)	σ_W (MPa)	Total (MPa)		
258	1	1.17	49.1	2.61	52.8	1.16	105	.418	1.46	108	104.24	55.07
258	2	1.17	124	0.364	126	1.16	68.9	1.95	1.59	73.6	-41.53	-52.28
206	1	0.131	23.7	15.5	39.3	0.149	116	9.46	1.74	128	224.76	88.24
206	2	0.131	150	12.3	162	0.149	57.7	11.6	1.73	71.2	-56.08	-90.91
141	1	0.151	33.1	24.6	57.7	0.028	106	19.5	1.22	127	119.61	69.06
141	2	0.151	135	20.9	156	0.028	62.9	21.4	1.21	85.5	-45.28	-70.72
76	1	0.126	47.9	33.6	81.6	0.145	89.1	19	0.527	109	33.23	27.11
76	2	0.126	108	29.2	137	0.145	67.3	21.2	0.458	89.1	-35.03	-48.03
11	1	2.46	40.9	33.1	76.5	2.44	45.4	22.4	0.391	70.7	-7.52	-5.75
11	2	2.46	47.1	29.1	78.6	2.44	42.7	24.1	0.722	70.0	-10.95	-8.60

It is apparent from to Table 2.12 that effect of warping is significant in the computation of normal stresses. In addition, Figures 2.23 and 2.24 show that the effect of warping causes considerable changes in joint displacements and rotations. Hence it can be concluded that warping has a considerable effect in the behavior of the irregular frames.

CHAPTER 3

DESIGN OF STEEL BEAM-COLUMN MEMBER ACCORDING TO LRFD-AISC INCLUDING EFFECT OF WARPING

3.1 Introduction

Steel members that are subject to axial force as well as bending moments are called beam columns. In this chapter, the design of beam-column members according to according to LRFD-AISC [30] the design code is explained. At the beginning, information about how to design frame members according to design specifications will be given. The design constraints that are required to be satisfied for a steel beam column so that the member can be considered safe are explained.

3.2 Design of steel beam-column members

3.2.1 Design of steel beam-column members without considering the effect of warping

Strength limitations of beam-column members for without considering the effect of warping specified in Chapter H in the LRFD-AISC design code. These limitations are described in the below [30].

3.2.1.1 Members under combined forces and torsion

Doubly and singly symmetric member in flexure and tension

The interaction of flexure and tension in symmetric shapes is limited by Equations (H1-1a) and (H1-1b) in the LRFD-AISC design code [30], given in Equations (3.1) and (3.2).

$$\text{For}\ \frac{P_u}{\phi P_n} \geq 0.2\ ;\ \frac{P_u}{\phi P_n} + \frac{8}{9}\left(\frac{M_u}{\phi_b M_{nx}} + \frac{M_u}{\phi_b M_{ny}}\right) \leq 1.0 \tag{3.1}$$

$$\text{For}\ \frac{P_u}{\phi P_n} \geq 0.2\ ;\ \frac{P_u}{2\phi P_n} + \left(\frac{M_u}{\phi_b M_{nx}} + \frac{M_u}{\phi_b M_{ny}}\right) \leq 1.0 \tag{3.2}$$

where;

P_u = required tensile strength, N

P_n = nominal tensile strength established in accordance with Chapter D in the LRFD-AISC, N

M_u = required flexural strength established in accordance with Chapter C in the LRFD-AISC, N-mm.

M_n = nominal flexural strength established in accordance with Chapter F in the LRFD-AISC, N-mm.

x = subscript of strong axis bending symbol

y = subscript of weak axis bending symbol.

$\phi = \phi_t$ = resistance factor for tension (see section D1 in LRFD-AISC)

ϕ_b = resistance factor for flexure = 0.90.

A more detailed analysis of the interaction of flexure and tension is permitted in lie of Equations (H1-1a) and (H1-1b) in the LRFD-AISC design code [30].

Doubly and singly symmetric members in flexure and compression

Similarly, the interaction of flexure and compression in symmetric shapes shall be limited by Equations (3.1) and (3.2).

where;

P_u = required compressive strength, N

P_n = nominal compressive strength established in accordance with Chapter E in the LRFD-AISC, N

M_u = required flexural strength established in accordance with Chapter C in the LRFD-AISC, N-mm

M_n = nominal flexural strength established in accordance with Chapter F in the LRFD-AISC, N-mm

x = subscript of strong axis bending symbol.

y = subscript of weak axis bending symbol.

$\phi = \phi_c$ = resistance factor for compression, = 0.85

ϕ_b = resistance factor for flexure = 0.90.

3.2.1.2 Calculation of required flexural strength

Second order effects

LRFD-AISC clause C1 imposes that second order $(P-\Delta)$ effects should be considered in the design of steel frames. "*In structures designed on the basis of plastic analysis, the required flexural strength (M_u) shall be determined from a second-order plastic analysis that satisfies the requirements of Section C2 in the LRFD-AISC. In structures designed on the basis of elastic analysis, M_u for beam-columns, connections, and connected members shall be determined from a second-order elastic analysis or from the following approximate second-order analysis procedure*" [30]:

$$M_u = B_1 M_{nt} + B_2 M_{nt} \tag{3.3}$$

where;

M_{nt} = required flexural strength in member without considering lateral translation of the frame, N-mm

M_{lt} = required flexural strength in member considering only lateral translation of the frame, N-mm

$$B_1 = \frac{C_m}{\left(1 - \frac{P_u}{P_{e1}}\right)} \geq 1 \tag{3.4}$$

$P_{e1} = A_g \frac{F_y}{\lambda_c^2}$ where, λ_c is the slenderness parameter, in which the effective K in the plane of bending shall be determined in accordance with Section C2.1 in the LRFD-AISC [30], for the braced frame.

$$\lambda_c = \frac{Kl}{r\pi}\sqrt{\frac{F_y}{E}}$$

P_u = required axial compressive strength for the member under consideration, N

C_m = a coefficient based on elastic first-order analysis assuming no lateral translation of the frame whose value shall be taken as follows:

(a) For compression members not subject to transverse loading between their supports in the plane of bending, the value of C_m is calculated as:

$$C_m = 0.6 - 0.4\left(\frac{M_1}{M_2}\right) \tag{3.5}$$

where; $\frac{M_1}{M_2}$ is the ratio of the smaller to larger moments at the ends of that portion of the member un-braced in the plane of bending under consideration.

M_1 / M_2 is positive when the member is bent in reverse curvature, negative when bent in single curvature.

(b) For compression members subjected to transverse loading between their supports, the value of C_m shall be determined either by rational analysis or by the use of the following values:

For members whose ends are restrained. . . . . C_m=0.85

For members whose ends are unrestrained. . . . . C_m=1.00

$$B_2 = \frac{1}{1 - \sum P_u \left(\frac{\Delta_{oh}}{\sum HL} \right)}$$

or (3.6)

$$B_2 = \frac{1}{1 - \frac{\sum P_u}{\sum P_{e2}}}$$

where;

$\sum P_u$ = required axial strength of all columns in a story, N

Δ_{oh} = lateral inter-story deflection, mm

$\sum H$ = sum of all story horizontal forces producing Δ_{oh}, N

L = story height, mm

$P_{e1} = A_g \frac{F_y}{\lambda_c^2}$, N

where λ_c is the slenderness parameter, in which the effective length factor K in the plane of bending shall be determined in accordance with Section C2.2 in the LRFD-AISC [30], for the un-braced frame.

3.2.1.3 Calculation of nominal tensile strength

Design tensile strength

The design strength of tension members $\phi_t P_n$ shall be the lower value obtained according to the limit states of yielding in the gross section and fracture in the net section [30].

For yielding in the gross section:

$$\phi_t = 0.90$$
$$P_n = F_y A_g \tag{3.7}$$

For fracture in the net section:

$$\phi_t = 0.75$$
$$P_n = F_u A_e \tag{3.8}$$

where;

A_e = effective net area, mm^2

A_g = gross area of member, mm^2

F_y = specified minimum yield stress, MPa

F_u = specified minimum tensile strength, MPa

P_n = nominal axial strength, N.

3.2.1.4 Calculations of nominal compressive strength

Effective length and slenderness limitations

Effective length

The effective length factor K shall be determined in accordance with Section C2 in LRFD-AISC [30].

Design by Plastic Analysis

If the column slenderness parameter λ_c does not exceed $1.5K$, design by plastic analysis is permitted [30].

Design Compressive Strength for Flexural Buckling

The design strength for flexural buckling of compression is $\phi_c P_n$ [30]:

$$\phi_c = 0.85$$
$$P_n = A_g F_{cr} \tag{3.9}$$

For $\lambda_c \leq 1.5$;

$$F_{cr} = (0.658^{\lambda_c^2})F_y \tag{3.10}$$

For $\lambda_c > 1.5$;

$$F_{cr} = \left[\frac{0.877}{\lambda_c^2}\right]F_y \tag{3.11}$$

where;

$$\lambda_c = \frac{Kl}{r\pi}\sqrt{\frac{F_y}{E}} \tag{3.12}$$

A_g = gross area of member, mm^2

F_y = specified yield stress, MPa

E = modulus of elasticity, MPa

K = effective length factor

l = laterally unbraced length of member, mm

r = governing radius of gyration about the axis of buckling, mm.

3.2.1.5 Calculations of Nominal Flexural Strength

Design for Flexure

"*The nominal flexural strength is the lowest value obtained according to the limit stress of: (a) yielding; (b) lateral-torsional buckling; (c) flange local buckling; and (d) web local buckling*" [30]. In order to calculate nominal strength of weak axis, only the limit state of yielding is required. Calculation of these limit states are described in the following.

Yielding

The flexural design strength of beams, determined by the limit state of yielding, is $\phi_b M_n$ [30]:

$$\begin{aligned} \phi_b &= 0.90 \\ M_n &= M_p \end{aligned} \tag{3.13}$$

where;

M_p = plastic moment (= $F_y Z_x \leq 1.5 M_{yx}$ for homogeneous sections), N-mm

M_y = moment corresponding to onset of yielding at the extreme fiber from an elastic stress distribution (= $F_y S$ for homogeneous section), N-mm.

Lateral-Torsional Buckling

This limit state is only applicable to members subject to major axis bending. The flexural design strength, determined by the limit state of lateral-torsional buckling, is $\phi_b M_n$ [30]:

$\phi_b = 0.90$

M_n = nominal strength determined as follows:

Doubly Symmetric Shapes and Channels with $L_b \leq L_r$

The nominal flexural strength is [30]:

$$M_n = C_b \left[M_p - \left(M_p - M_r \right) \left(\frac{L_b - L_r}{L_r - L_p} \right) \right] \leq M_p \tag{3.14}$$

where;

L_b = distance between points braced against lateral displacement of the compression flange, or between points braced to prevent twist of the cross section, mm.

In the Equation (3.14), C_b is a modification factor for non-uniform moment diagrams where, when both ends of the beam segment are braced:

$$C_b = \frac{12.5 M_{max}}{2.5 M_{max} + 3 M_A + 4 M_B + 3 M_C} \tag{3.15}$$

where;

$M_{\max}$ = absolute value of maximum moment in the un-braced segment, N-mm

M_A = absolute value of moment at quarter point of the un-braced segment, N-mm

M_B = absolute value of moment at centerline of the un-braced beam segment, N-mm

M_C = absolute value of moment at three-quarter point of the un-braced beam segment, N-mm

"*C_b is permitted to be conservatively taken as 1.0 for all cases. For cantilevers or overhangs where the free end is un-braced, C_b = 1.0*" [23].

The limiting un-braced length for full plastic bending capacity, L_p, shall be determined as follows [30]:

$$L_p = 1.76 r_y \sqrt{\frac{E}{F_{yf}}} \tag{3.16}$$

The limiting laterally un-braced length L_r and the corresponding buckling moment M_r shall be determined as follows [30]:

$$L_r = \frac{r_y X_1}{F_L}\sqrt{1+\sqrt{1+X_2 F_L^2}} \tag{3.17}$$

$$M_r = F_L S_x \tag{3.18}$$

$$X_1 = \frac{\pi}{S_x}\sqrt{\frac{EGJA}{2}} \tag{3.19}$$

$$X_2 = 4\frac{C_w}{I_y}\left(\frac{S_x}{GJ}\right)^2 \tag{3.20}$$

where,

S_x = section modulus about major axis, mm^2

E = modulus of elasticity of steel (205 000 MPa)

G = shear modulus of elasticity of steel (77 200 MPa)

F_L = smaller of ($F_{yf} - F_r$) or F_{yw}

F_r = compressive residual stress in flange; 69 MPa

F_{yf} = yield stress of flange, MPa

F_{yw} = yield stress of web, MPa

I_y = moment of inertia about y-axis, mm^4

C_w = warping constant, mm^6

Equations (3.16) and (3.17) are conservatively based on $C_b = 1.0$.

Doubly Symmetric Shapes and Channels with $L_b > L_r$

The nominal flexural strength is:

$$M_n = M_{cr} \leq M_p \tag{3.21}$$

where, M_{cr} is the critical elastic moment, determined as follows [30]:

$$M_{cr} = C_b \frac{\pi}{L_b} \sqrt{EI_y GJ + \left(\frac{\pi E}{L_b}\right)^2 I_y C_w}$$

$$= \frac{C_b S_x X_1 \sqrt{2}}{L_b / r_y} \sqrt{1 + \frac{X_1^2 X_2}{2\left(L_b / r_y\right)^2}} \,. \tag{3.22}$$

Flange Local Buckling

The flexural design strength, determined by the limit state of flange local buckling, is $\phi_b M_n$ [30] :

$\phi_b = 0.90$

$M_n =$ nominal strength determined as follows [30]:

Doubly Symmetric Shapes and Channels with $\lambda \le \lambda_p$

$$M_n = M_p$$

Doubly Symmetric Shapes and Channels with $\lambda_p < \lambda \le \lambda_r$

$$M_n = C_b \left[M_p - \left(M_p - M_r\right)\left(\frac{\lambda - \lambda_r}{\lambda_r - \lambda_p}\right)\right]$$

where,

$\lambda =$ with-thickness ratio, is equal to $\dfrac{b}{2t_f}$

$\lambda_p =$ limiting with-thickness ratio for compact sections, calculated from (Table B5-1) in the LRFD-AISC [30], described as follows:

$$\lambda_p = 0.38\sqrt{\frac{E}{F_y}} \tag{3.23}$$

λ_r = limiting with-thickness ratio for non-compact sections, calculated from (Table B5-1) in the LRFD-AISC [30], described as follows:

$$\lambda_r = 0.83\sqrt{\frac{E}{(F_y - 69)}} \tag{3.24}$$

Doubly Symmetric Shapes and Channels with $\lambda_r < \lambda$

$$M_n = M_{cr} = F_{cr}\, S$$

where, F_{cr} = critical stress, MPa.

Web local buckling

The flexural design strength, determined by the limit state of web local buckling, is $\phi_b M_n$ [30] :

$\phi_b = 0.90$

M_n = nominal strength determined as follows:

Doubly symmetric shapes and channels with $\lambda \le \lambda_p$

$$M_n = M_p$$

Doubly symmetric shapes and channels with $\lambda_p < \lambda \le \lambda_r$

$$M_n = C_b\left[M_p - (M_p - M_r)\left(\frac{\lambda - \lambda_r}{\lambda_r - \lambda_p}\right)\right]$$

where;

$\lambda =$ with-thickness ratio, is equal to $\frac{h}{t_w}$

$\lambda_p =$ limiting with-thickness ratio for compact sections, calculated from (Table B5-1) in the LRFD-AISC [30], described as follows:

For $\frac{P_u}{\phi_b P_y} \leq 0.125$;

$$\lambda_p = 3.76\sqrt{\frac{E}{F_y}}\left(1-\frac{2.75P_u}{\phi_b\ P_y}\right) \tag{3.25}$$

For $\frac{P_u}{\phi_b P_y} > 0.125$;

$$\lambda_p = 1.12\sqrt{\frac{E}{F_y}}\left(2.33-\frac{P_u}{\phi_b\ P_y}\right) \geq 1.49\sqrt{\frac{E}{F_y}}$$

$\lambda_r =$ limiting with-thickness ratio for non-compact sections, calculated from (Table B5-1) in the LRFD-AISC [30], described as follows

$$\lambda_r = 5.70\sqrt{\frac{E}{F_y}}\left(1-\frac{0.74P_u}{\phi_b\ P_y}\right) \tag{3.26}$$

Doubly symmetric shapes and channels with $\lambda_r < \lambda$

For this case member is slender member and nominal strength is not calculated.

3.2.2 Strength constraints with considering the effect of warping

Stress limitations of beam-column members with warping case are specified in AISC Design Guide Series number 9 (Torsional Analysis of Structural Steel Members) Equation (4.16a) [118]. It has the following form.

$$\frac{\sigma_a}{0.85F_{cr1}} \pm \frac{\sigma_{bx}}{\phi_b F_{cr2}} \pm \frac{\sigma_{by}}{\phi_b F_y} \pm \frac{\sigma_w}{0.9F_y} \leq 1.0 \tag{3.27}$$

where;

$F_{cr1} =$ compressive critical stress for flexural or flexural-torsional member buckling from LRFD-AISC Chapter E ($F_{cr1} = \frac{P_n}{A_g}$), MPa

$F_{cr2} =$ critical flexural stress controlled by yielding, lateral torsional buckling (LTB), web local buckling (WLB), or flange local buckling (FLB) from LRFD-AISC specification Chapter F ($F_{cr2} = \frac{M_{nx}}{I_x} y$), MPa

$\sigma_a =$ normal stress due to axial load ($\sigma_a = \frac{P_u}{A_g}$), MPa

σ_{bx} is normal stress due to bending about x axis ($\sigma_{bx} = \frac{M_{ux}}{I_x} y$), MPa

$\sigma_{by} =$ normal stress due to bending about y axis ($\sigma_{by} = \frac{M_{uy}}{I_y} x$), MPa

$\sigma_w =$ normal stress due to warping ($\sigma_w = M_w \frac{\omega(s)}{I_\omega}$) where, M_w is bi-moment N-mm^2, I_w is warping moment of inertia or warping constant mm^6, $\omega(s)$ sectorial coordinate of section or normalized warping constant mm^2, F_y is yield stress 250 MPa.

Detailed calculations of P_u, M_{ux}, M_{uy}, M_{nx} and M_w terms were mentioned in section 3.2.1. Values of I_x, I_y, I_w and $w(s)$ terms for W shapes are determined from LRFD-AISC (Part 1 dimension and properties) [30].

CHAPTER 4

ANT COLONY OPTIMIZATION AND HARMONY SEARCH METHODS

4.1 Introduction

Ant colony optimization and harmony search methods are two of stochastic search techniques that are proved to be robust and efficient in finding the solution of structural optimization problems [33]. Ant colony optimization method was inspired from natural behavior of ants while they are spreading around in search of food. Once they find the food source the colony carries the food to their nest through the shortest distance between the food and their nest. Harmony search method was developed simulating music improvisation. Musician tries to carry out the perfect state of harmony during composition of a melody. Similarly, an optimizer also tries to find the optimum solution of the optimization problem under consideration. Both of these methods are robust techniques and widely used in large scale optimization problems [29, 86, 94, 114, 119 and 120].

In this chapter, two metaheuristic optimization techniques among others; ant colony optimization method and harmony search algorithm are introduced. These optimization techniques are tested and compared with other optimization techniques in finding the solution of optimization problems in order to demonstrate their comparative performance.

4.2 Ant colony optimization

The ant colony optimization algorithm (ACO), introduced by Marco Dorigo [87, 90, 121 and 122], is one of the stochastic methods for solving optimization problems.

4.2.1 Natural behavior of ants

Ant colony optimization technique is inspired from the way that ant colonies find the shortest route between the food source and their nest. Ethnologists have discovered that ants are able to find the shortest path between the food source and their nest, despite the fact that they are completely blind [78, 82, and 83]. They achieve this by depositing a chemical substance called pheromone which is secreted from ants. This behavior of ants in finding the shortest path between food source and their nest can be described as follows. First an ant will move randomly by itself. As the ant moves the pheromone is secreted from this ants along a path. Following ants will sense the pheromone and will be inclined to follow it. When the leading ant takes the shorter path, it will return to its nest quicker. Therefore; the ant will be able to return to the food source to collect more food and make more tour and secrete more amount of pheromone along its path. If the ant continues to take the shortest path, higher concentrations of pheromone will remain on the path and more ants will be inclined to follow the shorter path. Hence, all ants take the shorter path and the shortest path is found as shown in Figure 4.1.

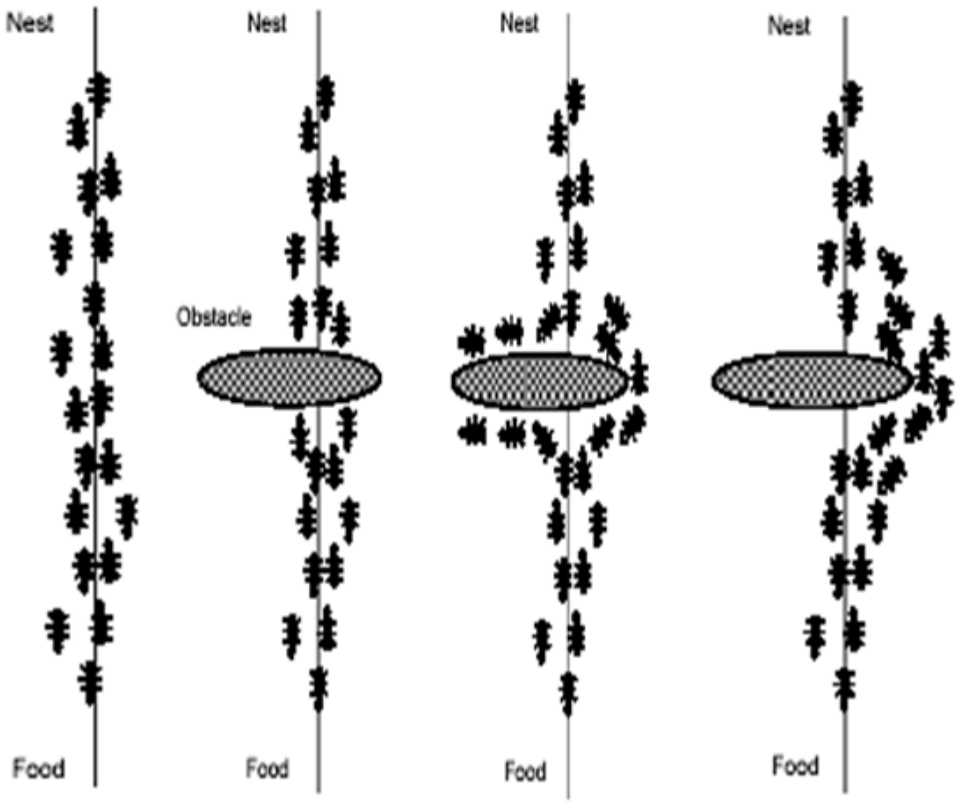

Figure 4.1 Natural behavior of ants.

4.2.2 Method

The ant colony optimization algorithm is first proposed by Gambardella and Dorigo [121 and 122]. In this study, ant colony optimization algorithm is applied to the travelling salesman problem defined as follows. In this problem, it is required to find the shortest route for a salesman when he/she needs to visit among number of cities. Consider that a salesman has to visit city j from another city i and the distance between these two cities is known as d_{ij}. Distances between for all possible cities form the distance matrix $\bar{d}$, whose dimensions are $n \times n$, where n is the number of cities to be visited in the travelling salesman problem.

By using these distances the amount of the visibility is v_{ij} calculated between the cities i and j is defined with the following formula:

$$v_{ij} = \frac{1}{d_{ij}} \tag{4.2}$$

After calculation visibility and distance values, the initial pheromone amount is calculated. The initial pheromone amount, represented by the $\tau_{ij}(0)$ or τ_0 notations, is calculated in the equation below (4.3):

$$\tau_0 = \frac{1}{n\, L_{nn}} \tag{4.3}$$

where, n is number of cities the salesman must visit and L_{nn} is the length of the tour created by the nearest-neighbor heuristic

After calculation of the initial pheromone amount, m number of ants are placed their initial cities randomly. Then each ant chooses the next city which has the best probability. The probability $p_{ij}^{k}(t)$ that ant k will choose to travel from city i to city j at cycle t is formulated in the equation below (4.4):

$$p_{ij}^{k}(t) = \frac{a_{ij}(t)}{\sum_{l \in allowed}^{n} a_{ij}(t)} \tag{4.4}$$

where $a_{ij}(t)$ called the ant decision table, is described in the following equation:

$$a_{ij}(t) = \frac{\left[\tau_{ij}(t)\right]^{\alpha} \cdot \left[v_{ij}\right]^{\beta}}{\sum_{l \in allowed}^{n} \left[\tau_{ij}(t)\right]^{\alpha} \cdot \left[v_{ij}\right]^{\beta}} \tag{4.5}$$

where $\tau_{ij}(t)$ represents the pheromone amount on the path that connects city i to city j at cycle t. α and β are the parameters used to adjust of pheromone amount and visibility respectively. After all ants have selected their next cities, one iteration is completed. At the end of the each iteration, local update rule is applied. In the local update rule, the amount of pheromone on the path connecting these two cities is adjusted. This rule is represented by the following formula:

$$\tau_{ij}(t) = \xi \tau_{ij}(t) \tag{4.6}$$

where, ξ is the parameter between 0 and 1 representing evaporation rate of the pheromone amount. After completing local update rule, the ant starts to select the next cities by using the aforementioned decision process. This procedure continues until all ants visit all the cities meaning one cycle is completed. After each cycle m path is obtained (where m is the number of ants). Length of each path is calculated and global update scheme is applied. This rule is described in Equation below (4.7):

$$\tau_{ij}(t+1) = \rho\ \tau_{ij}(t) + \Delta\tau_{ij} \tag{4.7}$$

where ρ is constant between 0 and 1 chosen so that $(1-\rho)$ represents the evaporation of pheromone amount between cycle t and $t+1$ (the amount of time required to complete a cycle). $\Delta\tau_{ij}$ is the change in pheromone amount on the path connecting city i to city j. Value of $\Delta\tau_{ij}$ is represented by the following formula:

$$\Delta\tau_{ij} = \sum_{k=1}^{m} \Delta\tau_{ij}^{k} \tag{4.8}$$

where k represents any ant from 1 to m (where m is the number of ants) and $\Delta\tau_{ij}^{k}$ is the change in pheromone amount added by ant k. Calculation of $\Delta\tau_{ij}^{k}$ term is described in Equation below (4.9):

$$\Delta\tau_{ij}^{k} = \frac{1}{L_k} \tag{4.9}$$

where, L_k is the length of the path chosen by ant k.

After the global update, a new cycle is started. All ants return to their initial city and start to select their next path by using the foregoing decision process. This process continues until the termination a criterion which is generally taken as the maximum number of cycles is satisfied.

4.3 Harmony search algorithm

Harmony search algorithm is developed by using simulation of the improvisation process of a skilled musician. Musican has three alternatives in order to improve musical harmony. First one is that musician play any melody from his or her memory. Second one is that musician play something similar to aforementioned melody by just adjusting pitch slightly. Third one is that musician play a melody completely new. These chocies are simulated in three main parts in harmony search algorithm. These are consideration of harmony memory matrix (HMCR),

pitch adjusting (PAR) and randomly selection. The steps of the algorithm are outlined in the following as given in [119]:

4.3.1 Initialization of harmony memory matrix:

Firstly harmony memory matrix **H** is generated. Then it is filled with specified number of solutions which is equal to harmony memory size(HMS). This process is similar to a design population in genetic algorithm or evolutionary strategies. Each solution (harmony vector, $\mathbf{I}^i$) consists of ng member groups, and is represented in a separate row of the matrix; consequently the size of **H** is $HMS \times ng$. General form of harmony memory matrix are shown in 4.10

$$[\mathbf{H}] = \begin{bmatrix} x_1^1 & x_2^1 & \cdots & x_{ng-1}^1 & x_{ng}^1 \\ x_1^2 & x_2^2 & \cdots & x_{ng-1}^2 & x_{ng}^2 \\ \vdots & \cdots & \cdots & \cdots & \cdots \\ x_1^{HMS-1} & x_2^{HMS-1} & \cdots & x_{ng-1}^{HMS-1} & x_{ng}^{HMS-1} \\ x_1^{HMS} & x_2^{HMS} & \cdots & x_{ng-1}^{HMS} & x_{ng}^{HMS} \end{bmatrix} \tag{4.10}$$

where, x_i^j is the ith design variable of the jth solution vector and μ is the harmony memory size.

4.3.2 Evaluation of harmony memory matrix:

HMS solutions are then evaluated, and their objective function values are calculated. If there are unfeasible solutions in harmony memory matrix, these solutions are discarded out of harmony memory matrix and new solutions generated randomly instead of these solutions. This process continues by the time that harmony memory matrix filled with feasible solutions. The solutions evaluated are sorted in the matrix in the increasing order of objective function values, that is $\phi(\mathbf{I}^1) \leq \phi(\mathbf{I}^2) \leq \ldots \leq \phi(\mathbf{I}^{HMS})$.

4.3.3 Improvising a new harmony:

A new solution $\mathbf{I}' = \left[I'_1, I'_2, .., I'_{ng}\right]$ is generated by selecting each design variable from either harmony memory or the entire discrete set. The probability that a design variable is selected from the harmony memory is controlled by a parameter called harmony memory considering rate ($HMCR$). To execute this probability, a random number r_i is generated between 0 and 1 for each variable I_i. If r_i is smaller than or equal to $HMCR$, the variable is chosen from harmony memory. Otherwise, a random value is assigned to the variable from the entire discrete set Equation (4.11).

$$I'_i = \begin{cases} I'_i \in \left\{I_i^1, I_i^2, ..., I_i^{\mu}\right\} & if\ r_i \leq HMCR \\ I'_i \in \{1, .., N_s\} & if\ r_i > HMCR \end{cases} \tag{4.11}$$

If a design variable attains its value from harmony memory, it is checked whether this value should be pitch-adjusted or not. In pitch adjustment, the value of a design variable is altered to its very upper or lower neighboring value obtained by adding ± bw to its current value where, bw is arbitrary distance bandwidth. In

thesis algorithm value of *bw* is taken as 1. Similar to *HMCR* parameter, it is operated with a probability known as pitch adjustment rate (*PAR*). If not activated by *PAR* , the value of the variable does not change Equation (4.12).

$$I_i'' = \begin{cases} I_i' \pm 1 & if\ r_i \le PAR \\ I_i' & if\ r_i > PAR \end{cases} \tag{4.12}$$

Improvising new Harmony memory process is illustrated in the Figure 4.2

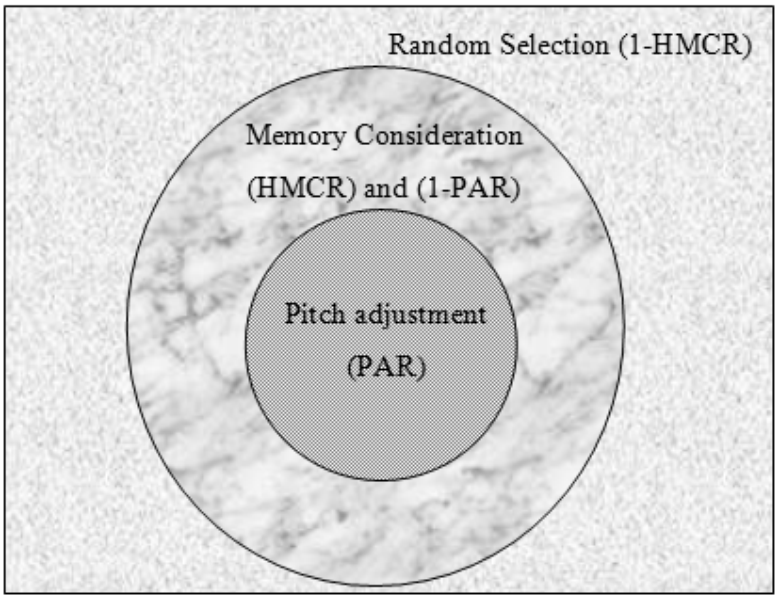

Figure 4.2 Improvising new harmony memory process.

4.3.4 Update of harmony matrix:

After generating the new solution vector, it is evaluated and its objective function value is calculated. If this value is better than that of the worst harmony vector in the harmony memory, it is replaced with the worst one in the harmony memory

matrix. The updated harmony memory matrix is then sorted in ascending order of the objective function value.

4.3.5 Check stopping criteria:

Steps 4.3.3 and 4.3.4 are repeated until the maximum number of iterations is reached.

Aforementioned steps of the harmony search algorithm is illustrated as a flowchart given in Figure 4.3

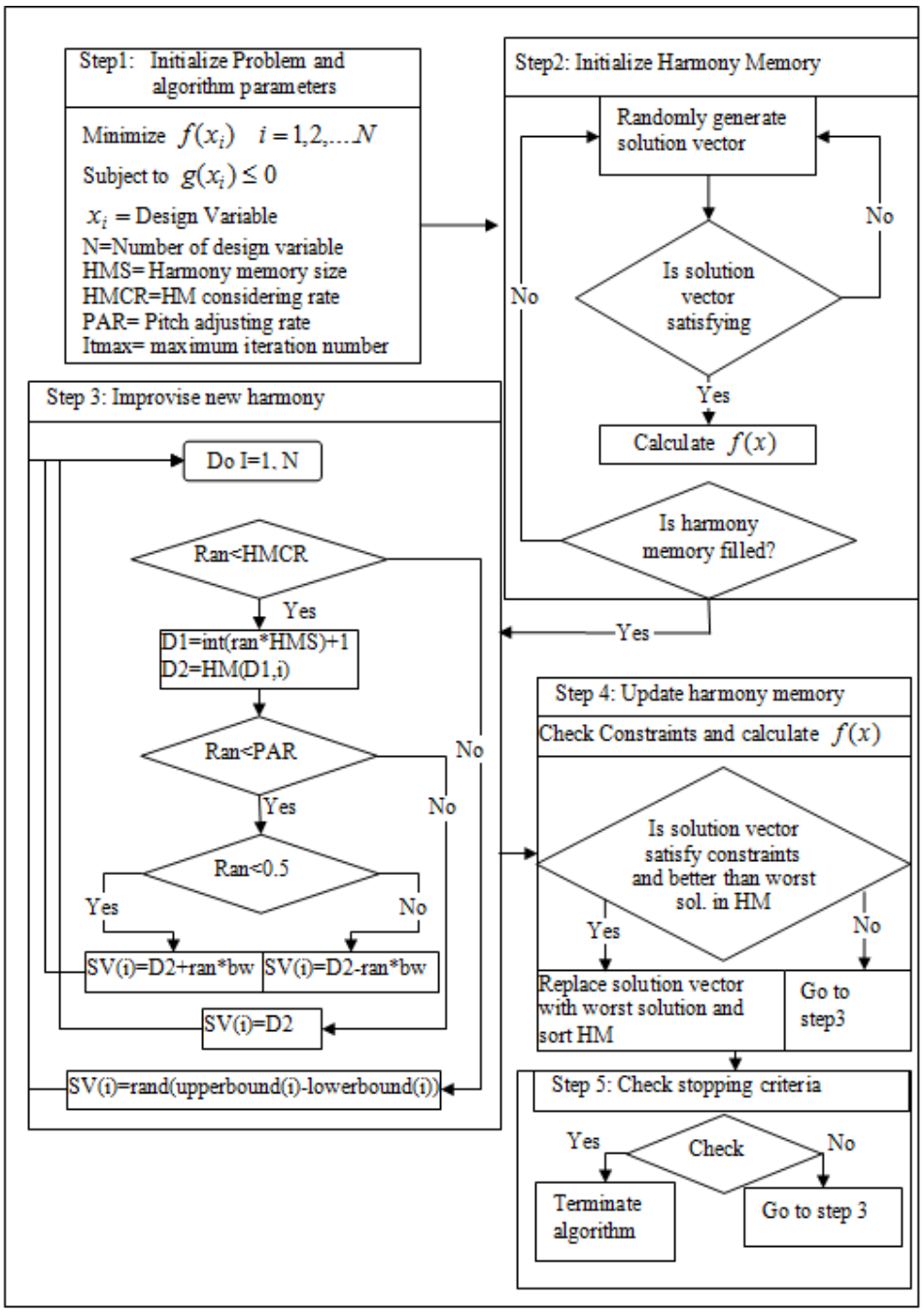

Figure 4.3 Flowchart of harmony search algorithm.

4.4 Numerical Applications

Firstly ant colony optimization method applied on travelling salesman problem. Then, three optimization problems are solved in order to compare the performance of ant colony optimization and harmony serach techniques in the following section.

4.4.1 Travelling Salesman Problem

In this example, a salesman has to visit all cities which are demonstrated in Figure 4.4 and the salesman has to visit each city once. The ant colony optimization method is used in order to the find the shortest path between these cities. Distances between cities are known and these values are tabulated in Table 4.1.

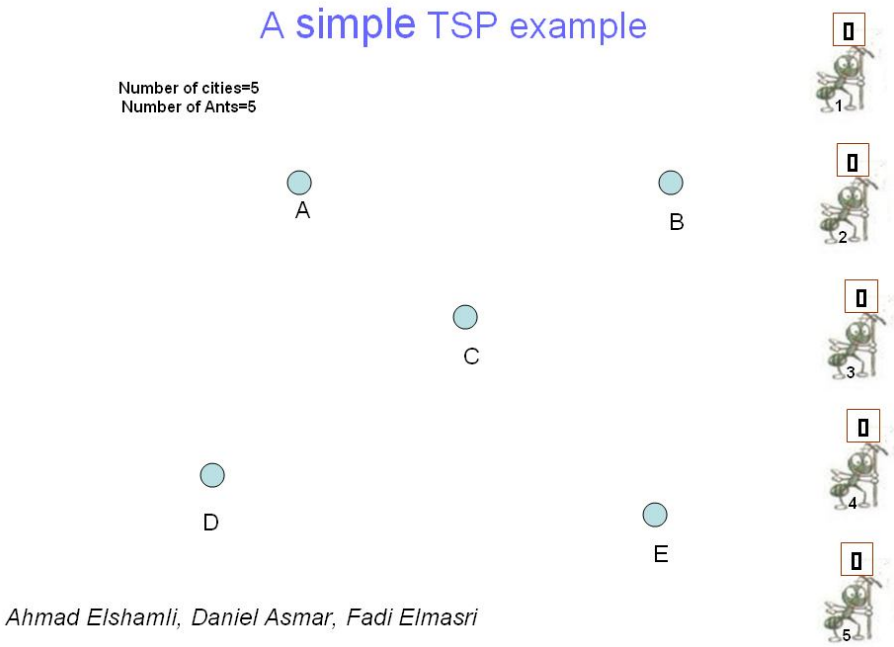

Figure 4.4 A simple travelling Salesman Problem [116]

By using Equation (4.2) visibility matrix v_{ij} between the cities is calculated and demonstrated in Table 4.2. For this problem, number of ants is defined as 5. The initial pheromone amount is calculated by using Equation (4.3) as:

$$\tau_0 = \frac{1}{n\, L_{nn}} = \frac{1}{5 \cdot 60} = 0.00333$$

Table 4.1 Distances between cities

	A	B	C	D	E
A		110	60	90	140
B	110		70	160	100
C	60	70		90	80
D	90	160	90		130
E	140	100	80	130	

Table 4.2 Visibility Matrix

	A	B	C	D	E
A		0.0091	0.0167	0.0111	0.0071
B	0.0091		0.0143	0.0063	0.0100
C	0.0167	0.0143		0.0111	0.0125
D	0.0111	0.0063	0.0111		0.0077
E	0.0071	0.0100	0.0125	0.0077	

At the beginning of the problem, five ants are placed in their initial cities as demonstrated in Figure 4.5. By then, probabilities are calculated for all possible

cities by using Equation (4.4). Then each ant selects their next city which has the best probability. For instance Ant 1 is placed in city A. Probabilities of B, C and D cities, where Ant 1 can possibly move to, are calculated for this ant. At the beginning of the problem, pheromone amount is equal to τ_0 which is the constant value for all paths. Therefore; the city, which has the best probability for Ant 1, is city C since city C is the closest city to the city A. Hence, Ant 1 selects city C as its second city move to as demonstrated in Figure 4.6.

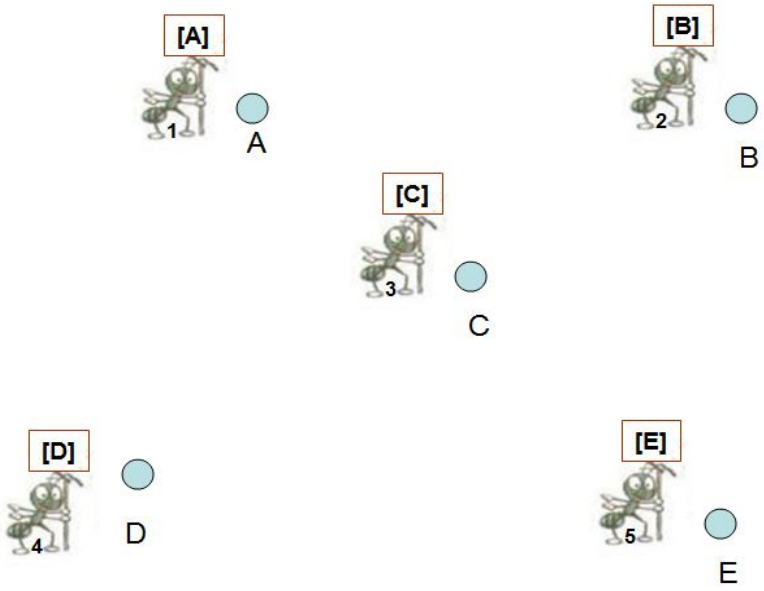

Figure 4.5 Initial cities of ants at the beginning of the problem [123]

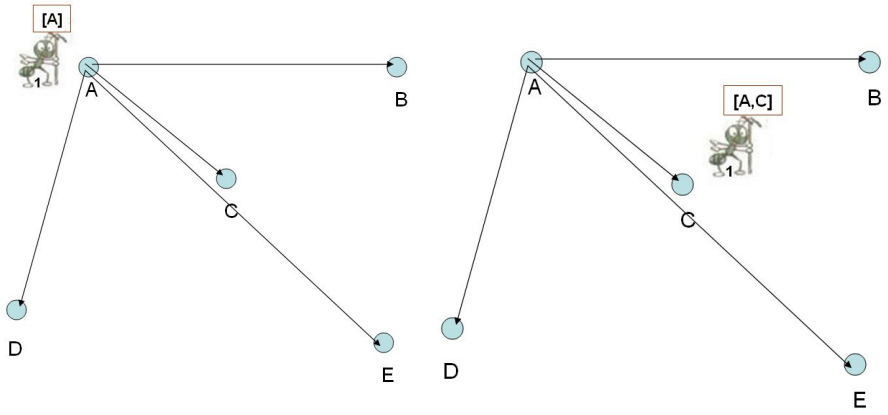

Figure 4.6 Selection of second city for Ant 1 [123]

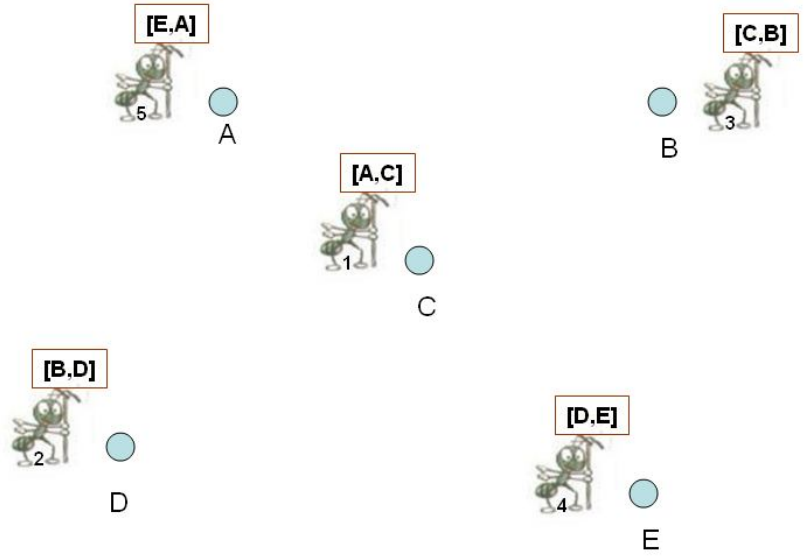

Figure 4.7 Position of ants at the end of first iteration [116]

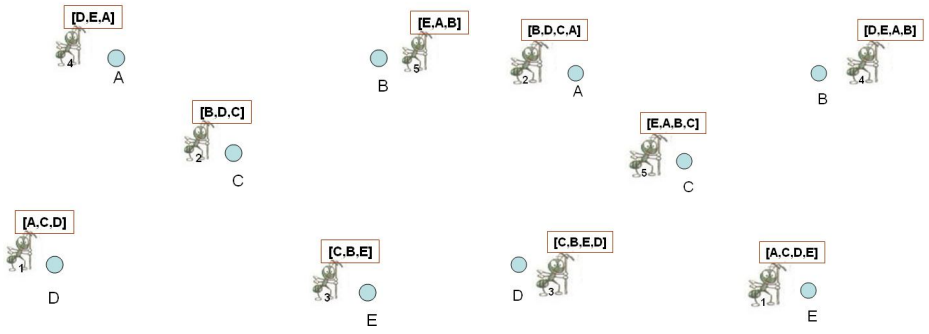

(a) Second iteration (b) Third iteration

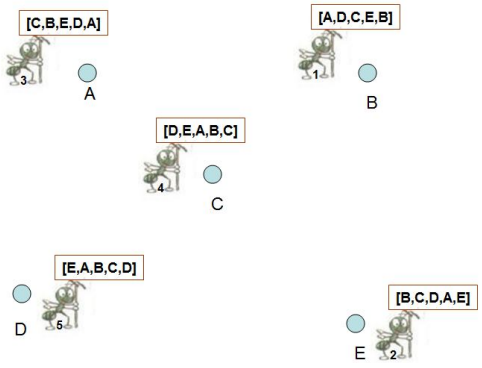

(b) Fourth iteration

Figure 4.8 Position of ants at the end of (a) second, (b) third and (c) fourth iterations [123]

This selection process is carried out for the other four ants and when all finished one cycle of the method comes to an end. As previously described, at the end of the each iteration, the local update rule is applied. In that rule, pheromone values are lowered by using Equation (4.6). By then, all ants select the next cities. This procedure continues until all ants visit all the cities. After that length of each path is calculated and global update rule is applied by using Equation (4.7). All these calculations are tabulated in Table 4.3.

After global update rule, ants return to the initial cities and a new cycle is started. This process continues until one of the foregoing termination criteria, which is mentioned above, is satisfied.

Table 4.3 Calculation of global updates

Ant No: Path	1 A.C.D.E.B	2 B.D.C.A.E	3 C.B.E.D.A	4 D.E.A.B.C	5 E.A.B.C.D	
Length (m)	380	450	390	450	410	Total
$\Delta\tau_{A,B}$	-	-	-	0.002222	0.002439	0.004661
$\Delta\tau_{A,C}$	0.002632	-	-	-	-	0.002632
$\Delta\tau_{A,E}$	-	0.002222	-	-	-	0.002222
$\Delta\tau_{B,C}$	-	-	-	0.002222	0.002439	0.004661
$\Delta\tau_{B,D}$	-	0.002222	-	-	-	0.002222
$\Delta\tau_{B,E}$	-	-	0.002564	-	-	0.002564
$\Delta\tau_{C,A}$	-	0.002222	-	-	-	0.002222
$\Delta\tau_{C,B}$	-	-	0.002564	-	-	0.002564
$\Delta\tau_{C,D}$	0.002632	-	-	-	0.002439	0.005071
$\Delta\tau_{C,E}$	-	-	-	-	-	0.002702
$\Delta\tau_{D,A}$	-	-	0.002564	-	-	0.004603
$\Delta\tau_{D,C}$	-	0.002222	-	-	-	0.002222
$\Delta\tau_{D,E}$	0.002632	-	-	0.002222	-	0.004854
$\Delta\tau_{E,A}$	-	-	-	0.002222	0.002439	0.004661
$\Delta\tau_{E,B}$	0.002632	-	-	-	-	0.002632
$\Delta\tau_{E,D}$	-	-	0.002564	-	-	0.002564

4.4.2 Continuous Optimization Problem 1

The first mathematical optimization problem is a minimization problem with two design variables and two inequality constraints, solved by Deb[124] and Geem [96]. Objective function and constraint functions of this problem are shown as follows.

Minimize, $f(x) = (x_1^2 + x_2 - 11)^2 + (x_1 + x_2^2 - 7)^2$

Subject to,

$g_1(x) = 4.84 - (x_1 - 0.05)^2 - (x_2 - 2.5)^2 \geq 0$

$g_2(x) = x_1^{\,2} + (x_2 - 2.5)^2 - 4.84 \geq 0$

where, $0 \leq x_1 \leq 6, \quad 0 \leq x_2 \leq 6,$

This problem is solved by using ant colony optimization (ACO) algorithm and obtained results are compared results in the literature. All results are tabulated in Table 4.4. The minimum solution vector is obtained as x = [2.246826, 2.381865] with an objective function value equal to f(x) = 13.59085 by using Harmony Search algorithm [96]. Deb [124], who recently solved this problem using an efficient constraint handling method for the GA, found the best solution of function value f(x)=13.58958, however solution vector is not given. Minimum objective function value is founded f(x) = 13.5928 with a solution vector x = (2.2464, 2.3742) by using ACO approximately 10.000 iteration.

Table 4.4 Optimum solutions of continuous optimization problem 1

Methods	Optimal Design variables		Objective Function value
	x_1	x_2	
Deb	Unavailable	Unavailable	13.58958
GA with PS (R=0.01)	Unavailable	Unavailable	13.59108
GA with PS (R=1)	Unavailable	Unavailable	13.59085
GA with TS=R	Unavailable	Unavailable	13.590845
HS	2.24684	2.381865	13.59085
ACO	2.2464	2.3742	13.5928

4.4.3 Continuous Optimization Problem 2

Continuous optimization problem given above has five design variables and six inequality constraints, and has been solved by many researchers [57, 89, 124–126]. Objective function and constraint functions of this problem are illustrated as follows.

Maximize $f(x) = 5.357847x_3^2 + 0.8356891x_1x_5 + 37.293239x_1 - 40792141$

Subject to,

$g_1(x) = 85.334407 + 0.0056858x_2x_5 + 0.0006262x_1x_4 - 0.002205x_3x_5 \geq 0$

$g_2(x) = 85.334407 + 0.0056858x_2x_5 + 0.0006262x_1x_4 - 0.002205x_3x_5 \leq 92$

$g_3(x) = 80.5149 + 0.0071317x_2x_5 + 0.0029955x_1x_2 + 0.0021813x_3^2 \geq 90$

$g_4(x) = 80.5149 + 0.0071317x_2x_5 + 0.0029955x_1x_2 + 0.0021813x_3^2 \leq 110$

$g_5(x) = 9.300961 + 0.0047026x_3x_5 + 0.0029955x_1x_3 + 0.0021813x_3x_4 \geq 20$

$g_6(x) = 9.300961 + 0.0047026x_3x_5 + 0.0029955x_1x_3 + 0.0021813x_3x_4 \leq 25$

where, $78 \leq x_1 \leq 102, 33 \leq x_2 \leq 45, 27 \leq x_i \leq 45 \qquad (i = 3,4,5).$

This problem is solved by using ant colony optimization (ACO) algorithm and obtained results are compared results in the literature. The best known objective function is obtained as f(x) =-31025.561 with a the optimum solution vector x = [78.0, 33.0, 27.0799, 45.0, 44.969] by using a modified particle swarm optimization algorithm as reported by Kennedy, Shi and Eberhart [24]. Geem [96] and Deb [124] also solved this problem using harmony search(HS) algorithm and genetic algorithm(GA) respectively and obtained the best solution with the objective function value of f(x) =- 30665.5. Homaifar et al.[125] and Coello [126] and obtained the best solution with f(x) = -30005.7 and f(x) = -31020.859, respectively, using the genetic algorithm based methods. Table 4.5 lists the optimum solution of this problem obtained by the ant colony optimization algorithm, and compares them with earlier results reported by Homaifar et al.

[125], Coello [126], Deb [124], Kennedy, Shi and Eberhart [24] and Geem[96]. The ant colony optimization algorithm found solution vector of x = [78.02, 33.07, 30.14, 44.92, 36.44] with a function value of f(x) = -30639.443 after 10.000 searches.

Table 4.5 Optimum solutions of continuous optimization problem 1

Methods	Optimum Design Variables					Objective Function
	x_1	x_2	x_3	x_4	x_5	
Homifar et al.	80.39	35.07	37.05	40.33	34.33	-30005.70
Coello	78.0495	33.007	27.081	45.00	44.94	-31020.86
Shi berhart	78.0	33.0	27.0799	45	44.969	-31025.56
HS [124]	Un available	Un available	Un available	Un available	Un available	-30665.50
HS [96]	78.0	33.0	29.995	45	36.776	-30665.50
ACO	78.02	33.07	30.14	44.92	36.44	-30639.44

4.4.4 Welded cantilever beam design

The welded rectangular cantilever beam shown in Figure 4.9 has been considered by many researchers [96, 127] to evaluate the performance of their algorithms. The design problem requires finding the cross sectional dimensions of the beam such that the total fabrication cost is the minimum under the given load (P). The design variables are the dimensions of the cross section as well as the required thicknesses and length of welds used in connecting the beam to the gusset plate. Accordingly the design variables are; $h = x_1$ represents the weld thickness, $I = x_2$ is weld length, $t = x_3$ is the depth of the beam and $b = x_4$ is the width of the beam. x_1 and x_2 are the discrete design variables. These variables are represented as discrete set of terms whose started from lower boundary of the variable and ascended with times of 0.0064 to the upper boundary of the variable. The lower and the upper boundaries of each variable are given in mathematical model of problem written as follows. In this problem 7 constraints are defined. These are: constraints about shear stress in beam(τ) and normal stress due to

bending; critical buckling load (P_c); deflection of beam and upper and lower bound limitations for beam and weld dimensions.

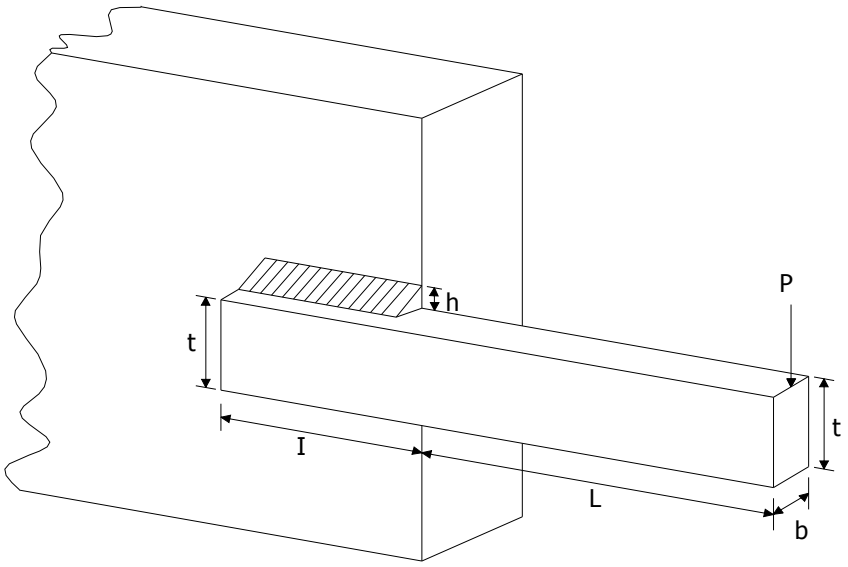

Figure 4.9 Welded cantilever beam

Mathematical model of this problem can be defined as follows:

Minimize,

$$f(x) = 1.10471 x_1^{\,2} x_2 + 0.04811 x_3 x_4 (14.0 + x_2)$$

Subject to

$g_1(x) = \tau(x) - \tau_{\max} \le 0$ → Shear stress

$g_2(x) = \sigma(x) - \sigma_{\max} \le 0$ → Normal stress due to bending

$g_3(x) = x_1 - x_4 \le 0$ → Side constraint

$g_4(x) = 0.10471 x_1^{\,2} + 0.04811 x_3 x_4 (14.0 + x_2) - 5 \le 0$ → Side constraint

$g_5(x) = 0.125 - x_1 \le 0$ → Side constraint

$g_6(x) = \delta(x) - \delta_{\max} \le 0$ → Displacement at the end node of the beam

$g_7(x) = P - P_c(x) \le 0$ → Lateral torsional buckling constraint

Where,

$$\tau(x) = \sqrt{(\tau')^2 + 2\,\tau'\tau''\,\frac{x_2}{2R} + (\tau'')^2}$$

$$\tau' = \frac{P}{\sqrt{2}x_1 x_2} \qquad \tau'' = \frac{MR}{J}$$

$$M = P\left(L + \frac{x_2}{2}\right) \qquad R = \sqrt{\frac{{x_2}^2}{4} + \left(\frac{x_1 + x_3}{2}\right)^2}$$

$$J = 2\left\{x_1 x_2 \sqrt{2}\left[\frac{{x_2}^2}{4} + \left(\frac{x_1 + x_3}{2}\right)^2\right]\right\} \qquad \delta(x) = \frac{6PL^3}{E{x_3}^3 x_4}$$

$$\sigma(x) = \frac{6PL}{x_4 {x_3}^2} \qquad P_c(x) = \frac{4.013E\sqrt{\frac{(x_3^2 x_4^6)}{36}}}{L^2}\left(1 - \frac{x_3}{2L}\sqrt{\frac{E}{4G}}\right)$$

$P = 6000\ lb, \quad L = 14\ in., \quad E = 30\times10^6\ psi, \quad G = 12\times10^6\ psi$

$\tau_{\max} = 13{,}600\ psi, \quad \sigma_{\max} = 30{,}000\ psi, \quad \delta_{\max} = 0.25\ in.$

Upper bound and lower bounds of the design variables:

$0.1 \le x_1 \le 2.0, \quad 0.1 \le x_2 \le 10$
$0.1 \le x_3 \le 10, \quad 0.1 \le x_4 \le 2.0$

Aforementioned design problem is solved by using simulating annealing, genetic algorithm, and ant colony optimization and harmony search methods. Solutions obtained from these methods are tabulated in Table 4.6. Solution obtained from particle swarm optimization method [127] is added in Table 4.6.

Table 4.6 Optimum solutions for example 3

Design variables Constraints Objective function	Genetic Algorithm	Simulating Annealing Algorithm	Particle Swarm Optimization Method	Ant Colony Optimization Algorithm	Harmony Search Method
x_1	0.2489	0.2389	0.244369	0.2320	0.2220
x_2	6.1730	2.4802	6.217519	3.608	3.0510
x_3	8.1789	9.2299	8.291471	8.4416	9.5450
x_4	0.2533	0.2389	0.244369	0.2384	0.2630
$g_1(x)$	-5758.60	-0.2881	-5741.1769	-274.01	-3240.01
$g_2(x)$	-255.58	-5341.32	-0.0000007	-332.9	-8965.95
$g_3(x)$	-0.0044	-0.001033	0.000000	-0.0064	-0.0410
$g_4(x)$	-2.9829	-3.2383	-3.022954	-3.3425	-2.9356
$g_5(x)$	-0.12390	-0.1139	-0.119369	-0.107	-0.0970
$g_6(x)$	-0.2342	-0.2384	-0.234241	-0.234	0.1584
$g_7(x)$	-618.82	-102.32	-0.000309	-2491.84	-2212.053
$f(x)$	2.433116	1.9046	2.380956	1.834	2.2290

It is apparent from the Table 4.6 that best solution is obtained by ant colony optimization method. Objective function value for this solution is 1.834 which is obtained after 5000 iterations. Objective function of the third best solution is obtained as 2.2290 by using harmony search method with 1000 iterations. Iteration number is an important parameter for optimization problems. Therefore, it cannot be said definitely that ant colony optimization method is the best method for this problem as the iteration number of this method is five times higher than the iteration number of the harmony search method. As a result, it can be stated

that both harmony search and ant colony optimization algorithms show performance in this example.

CHAPTER 5

OPTIMUM DESIGN OF STEEL SPACE FRAMES

5.1 Introduction

Optimum design of steel frames problems is a challenging problem in structural engineering due to fact that structural designer has to assign sections from a discrete set of available sections list. In traditional methods, the designer assigns any one of these sections to any one of the member groups in the frame by using his/her experience or arbitrarily. After such an assignment it becomes important to analyze and design the frame to figure out whether the frame satisfies the constraints set by design codes or not. It is apparent that quite large number of combinations is possible for the member groups of a frame depending upon the total number of practically available sections [26]. "*For example, for a frame where the members are collected in eight groups and assuming that the total number of available sections is 272, there are 2.996065x1019 possible combinations that require to be considered*" [60]. Although the designer's practical experience makes some reductions in these possible combinations, still an exhaustive search will need huge amount of computation time and effort to obtain the optimum solution. In some cases traditional methods may not even be practically possible. Therefore, optimization methods especially recent stochastic search methods are the efficient tools for the frame design problems.

In this chapter, firstly, a mathematical formulation of the optimum design problem of steel space frame according to LRFD-AISC is described. The solution of the

optimum design problem is obtained by using both ant colony optimization and harmony search algorithms.

5.2 Discrete optimum design of space steel frames to LRFD-AISC

The design of space steel frames necessitates the selection of steel sections for its columns and beams from a standard steel section tables such that the frame satisfies the serviceability and strength requirements specified by the code of practice while the economy is observed in the overall or material cost of the frame. When the design constraints are implemented from LRFD-AISC [30] the following discrete programming problem is obtained.

5.2.1 The objective function

The objective function is taken as the minimum weight of the frame which is expressed as follows.

$$Minimize \quad W = \sum_{r=1}^{ng} m_r \sum_{s=1}^{t_r} \ell_s \tag{5.1}$$

where, W is the weight of the frame, m_r is the unit weight of the steel section selected from the standard steel sections table that is to be adopted for group r, t_r is the total number of members in group r, ng is the total number of groups in the frame, and l_s is the length of member s.

5.2.2 Constraints functions

The design of steel frames according to LRFD-AISC necessitates aforementioned constraints to be met described as follows:

1. Strength Constraints: It is required that each frame member has sufficient strength to resist the internal forces developed due to factored external loading.

2. Serviceability Constraints: Deflection of beams and lateral displacement of the frame should be less than the limits specified in the code.

3. Geometric Constraints: Steel sections that are selected for columns and beams at each beam-to-column connection and column-to-column connection should be compatible so that they can be connected to each other.

These constraints are explained in detail in the following sections.

5.2.2.1 Strength Constraints

Without considering the effect of warping

For the case where the effect of warping is not included in the computation of the strength capacity of W-sections that are selected for beam-column members of the frame the following inequalities given in Chapter H of LRFD-AISC is required to be satisfied.

$$g_{s,i} = \left(\frac{P_u}{\phi P_n}\right)_{il} + \frac{8}{9}\left(\frac{M_{ux}}{\phi_b M_{nx}} + \frac{M_{uy}}{\phi_b M_{ny}}\right)_{il} - 1.0 \le 0 \qquad for \frac{P_u}{\phi P_n} \ge 0.2 \qquad (5.2)$$

or

$$g_{s,i} = \left(\frac{P_u}{2\phi P_n} \right)_{il} + \left(\frac{M_{ux}}{\phi_b M_{nx}} + \frac{M_{uy}}{\phi_b M_{ny}} \right)_{il} - 1.0 \le 0 \qquad for \frac{P_u}{\phi P_n} < 0.2 \tag{5.3}$$

where, M_{nx} is the nominal flexural strength at strong axis (x axis), M_{ny} is the nominal flexural strength at weak axis (y axis), M_{ux} is the required flexural strength at strong axis (x axis) , M_{uy} is the required flexural strength at weak axis (y axis), P_n is the nominal axial strength (tension or compression) and P_u is the required axial strength (tension or compression) for member i. ℓ represents the loading case. Detailed information about calculation of these terms were given in Chapter 3.

Considering the effect of warping

In the case where the effect of warping is included in the computation of strength capacity of W-sections that are selected for beam-column members of the frame, the following inequality which is suggested in AISC Torsional Analysis of Structural Steel Members Design Guide [118] (Equation 4.16.a) is required to be satisfied. This constraint has the following form.

$$g_{s,i} = \frac{\sigma_{ai}}{0.85\, F_{cr,i}} \pm \frac{\sigma_{b\,x,i}}{\phi_b\ F_{cr,i}} \pm \frac{\sigma_{b\,y,i}}{0.9\, F_y} \pm \frac{\sigma_{w,i}}{0.9\, F_y} - 1.0 \le 0 \tag{5.4}$$

where $g_{s,i}$ is the strength constraint for member i, σ_{ai} is the largest stress occurring in the section due to the axial force, $\sigma_{bx,i}$ is the maximum stress occurring in the section due to bending about the major axis, $\sigma_{by,i}$ is the maximum stress occurring in the section due to bending about the minor axis, F_y is the yield stress and $F_{cr,i}$ is the critical stress which is computed as described in Chapter E of LRFD-AISC. Detailed information about calculations of these terms were given in Chapter 3.

5.2.2.2 Serviceability Constraints

The lateral displacements and deflection of beams in steel frames are limited by the ASCE Ad Hoc Committee report [128], the accepted range of drift limits by first-order analysis is 1/750 to 1/250 times the building height H with a recommended value of H/400. The typical limits on the inter-story drift are 1/500 to 1/200 times the story height. Based on this report the deflection limits recommended are proposed in [62 and 63] for general use which is repeated in Table 1.

Table 5.1 Displacement limitations for steel frames

	Item	Deflection limit
1	Floor girder deflection for service live load	L/360
2	Roof girder deflection	L/240
3	Lateral drift for service wind load	H/400
4	Inter-story drift for service wind load	h/300

Deflection Constraints

It is necessary to limit the mid-span deflections of beams not to cause cracks in brittle finishes that they may support due to excessive displacements. Deflection constraints are expressed by the following inequality.

$$g_{dj} = \frac{\delta_{jl}}{\delta_j^u} - 1 \le 0 \qquad j = 1,....,n_{sm}\ , \quad l = 1,.....n_{lc} \tag{5.5}$$

where, δ_{jl} is the maximum deflection of j^{th} member under the l^{th} load case, δ_j^u is the upper bound on this deflection which is defined in the code as span/360 for beams carrying brittle finishers, n_{sm} is the total number of members where deflections limitations are to be imposed and n_{lc} is the number of load cases.

Drift Constraints

These constraints are of two types. One is the restriction applied to the top story sway and the other is the limitation applied on the inter-story drift.

Top Storey Drift Constraints

Top story drift limitation is expressed as in the

$$g_{td\ j} = \frac{\left(\Delta_{top}\right)_{jl}}{DriftLimit} - 1 \le 0 \qquad j = 1,\ldots,n_{jtop}\ , \quad l = 1,\ldots,n_k \tag{5.6}$$

where is the height of the frame, n_{jtop} is the number of joints on the top story, n_{lc} is the number of load cases, $\left(\Delta_{top}\right)_{jl}$ is the top story drift of the jth joint under l^{th} load case. Drift limit value is generally taken as H/400 where H is height of structure.

Inter-Storey Drift Constraints

In multi-story steel frames the relative lateral displacements of each floor is required to be limited. This limit is generally defined as that maximum inter-story drift which is generally specified as $h_{sx}/300$ where h_{sx} is the story height.

$$g_{idj} = \frac{\left(\Delta_{oh}\right)_{jl}}{h_{sx}/300} - 1 \le 0 \qquad j = 1,....,n_{st}\ , \quad l = 1,.....n_{lc} \tag{5.7}$$

where n_{st} is the number of story, n_{lc} is the number of load cases and $\left(\Delta_{oh}\right)_{jl}$ is the story drift of the jth story under l^{th} load case.

5.2.2.3 Geometric Constraints

These constraints are needed to satisfy the practical requirements. It is apparent that column sections in a steel frame should have larger sections from top story to lower stories. It is not desired to have a bigger W-section for the upper column section. Such case requires special joint arrangements which is neither preferred in practice nor is economical. The same applies to the beam-column connections. The W-section selected for any beam should have flange width smaller or equal to the flange width of the W-section selected for the column to which the beam is to be connected. These are named as geometric constraints and they are included in the design optimization model to satisfy practical requirements. Two types of geometric constraints are considered in the mathematical model. These are column-to-column geometric constraints and beam-to-column geometric limitations.

Column-to-Column Geometric Constraints

The depths and the unit weight of W sections selected for the columns of two consecutive stories should be either equal to each other or the one in the above story should be smaller than the one in the below story. These limitations are included in the design problem as in the following.

$$g_{cdi} = \frac{d_{ic(upper)}}{d_{ic(lower)}} - 1 \le 0 \quad ic = 1.....n_{cc} \tag{5.8}$$

$$g_{cmi} = \frac{W_{i(upper)}}{W_{i(lower)}} - 1 \le 0 \quad i = 1.....n_{cc} \tag{5.9}$$

where; n_{cc} is the number of column to column geometric constraints defined in frame design problem, $W_{ic(upper)}$ is the unit weight of W section selected for of column upper storey, $W_{ic(lower)}$ is the unit weight of W section selected for of column lower storey, $d_{ic(upper)}$ is the depth of W section selected for of column

upper storey and $d_{ic(lower)}$ is the depth of W section selected for of column lower storey.

Beam-to-Column Geometric Constraints

If a beam is connected to flange of a column, the flange width of the beam should be less than or equal to the flange width of the column in the connection. If a beam is connected to the web of a column, the flange width of the beam should be less than or equal to $(d - 2t_b)$ of the column web dimensions in the connection where d is the depth of W section and t_b is the flange thickness of W section. These limitations are described as constraint functions in the Equations (5.10) and (5.11).

$$g_{bci} = \frac{(b'_{fb})_{ib}}{(d_{cl})_{ib} - 2(t_{fl})_{ib}} - 1 \le 0 \tag{5.10}$$

or

$$g_{bbi} = \frac{(b_{fbk})_{ib}}{(b_{fc})_{ib}} - 1 \le 0 \tag{5.11}$$

$ib = 1,2.....n_{cb}$

where; nb is number of beam to column constraints defined in frame design problem, b_{fbk}, b'_{fbk} and b_{fc} are the flange width of the beam B1, the beam B2 and the column, respectively, d_{cl} is the depth of the column and t_{fl} is the flange width of the column in Figure 5.1.

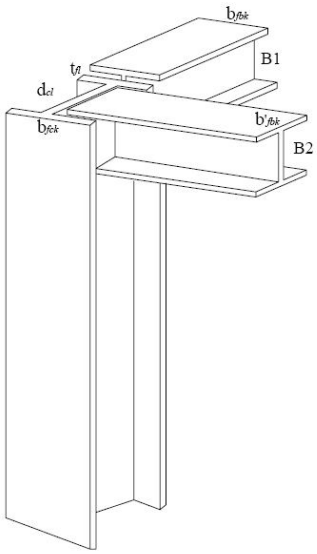

Figure 5.1 Beam-Columns Geometric Constraints

5.3 Optimum Structural Design Algorithms

5.3.1 Ant colony optimization based optimum design algorithm

Ant colony optimization method is applied by Camp and Bichon for frame design problem in 2005 [94]. This method's algorithm for frame design problem is described in the following steps.

Step1: In first step, initial pheromone amount (τ_0) is calculated by using following equation.

$$\tau_0 = \frac{1}{W_{min}} \tag{5.12}$$

where; W_{min} is the minimum weight of the frame regardless of whether it satisfies the constraints or not. The minimum weight of the frame is calculated by assigning the smallest unit weight of the section to each member groups from section table list in LRFD-AISC [30].

Step2: After choosing initial parameters and initial pheromone amount, each ant in the colony is assigned to its first member groups of the frame. Then ants select a section from section table list for their groups. This selection is determined through a decision process. In that decision process, probabilities of all possible sections are calculated for each ant and each ant selects the section which has the best probability. Probabilities of sections are described as follows.

$$P_{ij}(t) = \frac{\left[\tau_{ij}(t)\right] \cdot \left[v_{ij}\right]^{\beta}}{\sum_{j \in allowed}^{NofSec} \left[\tau_{ij}(t)\right] \cdot \left[v_{ij}\right]^{\beta}} \tag{5.13}$$

where, $P_{i,j}$ is the probability of section j for the group i at cycle t, τ_{ij} is the amount of pheromone, v_{ij} is called the value of visibility of section j for the group i calculated from the Equation (5.14), and β is the parameter which is used to arrange to the influence of pheromone amount and visibility.

$$v_{ij} = \frac{1}{w_{ij}} \tag{5.14}$$

where, w_j is the unit weight of section j for the group i. This process continues until all ants select sections for their first assigned group. After this process first tour is completed.

Step3: At the end of the each tour the local update rule is applied. In the local update rule, pheromone amount of sections selected by ants is lowered in order to promote exploration in the search. This rule is shown as follows.

$$\tau_{ij}(t) = \xi \tau_{ij}(t) \tag{5.15}$$

where, ξ is a parameter, called local update coefficient, whose value changes between from 0 to 1.

Step4: After completing local update rule, ant starts to select new sections for next assigned group (i+1) by using decision process mentioned in step2. Then local update rule reapplied at the end of the tour. This procedure continues by the time that all ants select selections for their all assigned member groups. After this procedure one cycle is completed. At the end of the each cycle each ant has one design. In other words, as much as number of ant, designs of frame are obtained. All designs of frame are analyzed using the matrix stiffness method (detailed information given in Chapter 2) and internal forces and moments are calculated. These values are used for determining whether the frame design satisfies the design limitations according to the design code LRFD-AISC or not. If the frame design does not satisfy the design constraints, frame weight is penalized by the penalty function given in the Equation (5.16).

$$W_p = W(1 + C)^{\varepsilon} \tag{5.16}$$

where, W_p penalized weight of frame is, C is the total constraint violation and ε is the penalty coefficient. For frame design problem, total constraints violation is defined as follows:

$$C = \sum C_s + \sum C_d + \sum C_{id} + \sum C_{td} + \sum C_{cd} + \sum C_{cc} + \sum C_{bc} \tag{5.17}$$

where, C_s, C_d, C_{id}, C_{td}, C_{cd}, C_{cm}, C_{bc} and C_{bb} are the constraints violations for strength, deflection, inter-story drift, top story drift, column-to-column geometric and beam-to-column geometric constraints functions respectively. In general form, constraints violations can be expressed as:

$$C_i = \begin{cases} 0 & if\ g_i(x_j) \le 0 \quad i = 1,\ldots nc \\ g_i(x_i) & if\ g_i(x_j) \le 0 \quad j = 1,\ldots ng \end{cases} \tag{5.18}$$

where, $g_i(x)$ is i[th] constraints function, x is the design group of frame, nc and ng are the number of constraint functions and design groups defined in the optimization problem respectively.

Step5: After calculating penalized weight one cycle is completed. At the end of the cycle global update scheme is applied. Generally two kinds of global update rule are used for optimization problems. These are ant system and rank ant system. In frame design problem, ranked ant system shows better performance than ant system. Therefore, global update rule with rank ant system is used for frame optimization problems. Global update rule with rank ant system is shown in the following Equation (5.17) [93].

$$\tau_{ij}(t+n) = (1-\rho)\cdot\tau_{ij}(t) + \rho\left[\lambda\cdot\Delta\tau_{ij}^{+}(t) + \Delta\tau_{ij}^{r}(t)\right] \tag{5.19}$$

where, $\Delta\tau_{ij}^{+}(t)$ is the change in the amount of pheromone for the best ant in cycle t. This value is calculated in the Equation (5.20). $\Delta\tau_{ij}^{r}(t)$ is the summation of the change in the pheromone amount for ranked ants in cycle t. $\Delta\tau_{ij}^{r}(t)$ is calculated by using the Equation (5.21). ρ is the global update coefficient and λ is the number of the ranked ant.

$$\Delta\tau_{ij}^{+}(t) = \frac{1}{W_p{}^{+}(t)} \tag{5.20}$$

where, $W_p{}^{+}(t)$ is penalized weight of frame design chosen by the best ant.

$$\Delta\tau_{ij}^{r}(t) = \sum_{\mu=1}^{\lambda}\Delta\tau_{ij}^{\mu}(t) \tag{5.21}$$

where, μ rank of the ant (between 1 and λ). $\Delta\tau_{ij}^{\mu}(t)$ is the change in the pheromone amount of pheromone for ranked ant μ in cycle t. This value is obtained as follows.

$$\Delta\tau_{ij}^{\mu}(t) = (\lambda - \mu)\frac{1}{W_p{}^{\mu}} \tag{5.22}$$

where, $W_p{}^{\mu}$ is penalized weight of frame design selected by the ranked ant μ.

After applying global update rule, new cycle is initiated. This process continues until one of the aforementioned termination criteria is satisfied.

5.3.2 Improvements in ant colony optimization algorithm

5.3.2.1 Static Ants

In large size multistory structures too many geometric constraints are required to be defined. Unfortunately metaheuristic techniques exhibit difficulty of finding feasible designs that satisfy these constraints in their random search. In this study the same problem is also observed in the ant colony optimization algorithm. In order to eliminate this problem, static ant strategy is developed. In ant colony algorithm, certain number of ants is defined. Some of these ants are assigned as static ant in static ant strategy. In frame design problem, geometric limitations between column groups of two consecutive stories and between beam and column groups in the connection are mentioned in the section 5.2.2.3. If these limitations are needed to be satisfied within 100% of probability for each design, some restrictions are required when ants assign sections for their design groups. Static ants use these restrictions and select sections for their design groups to ensure that the geometric constraints are satisfied. Static ants assign section according to following rules. Dependencies vector between member groups is defined at the beginning of the algorithm. If there are geometric constraints defined between two

groups, these groups are depended on each other. These dependencies between for all possible groups are stored in the dependencies vector. Static ants check dependencies vector and use reduced design space for depended groups in selection process. For example, when group number of upper storey column and lower storey column are set as 5 and 6 respectively, unit weight and depth of group 6 should be greater than group 5. Therefore, group 6 depends on group 5 and assigned section number for group 6 should be greater than assigned section number for group 5 from static ants. As a result, geometric constraints are automatically satisfied for the static ants. However, static ants use reduced design space. This can bring stagnation and local convergence in the algorithm. Therefore, the number of static ants is limited in the algorithm. There are three strategies defined in order to determine the number of static ants for any cycle in the algorithm. In the first strategy the number of static ants is determined as constant number for all cycles. In second strategy, the number of static ants is lowered as a dynamic function depending on cycle. This dynamic function is represented in the following Equation (5.23).

$$S(t) = S_{\max} - \left(S_{\max} - S_{\min}\right)\left(\frac{t}{t_{\max} \cdot 0.5}\right)^2 \tag{5.23}$$

where, $S(t)$ is the static ant number in cycle t, $S_{\max}$ and $S_{\min}$ are the maximum and the minimum static ant numbers defined in the algorithm, and $t_{\max}$ is maximum cycle number.

In the third strategy, the number of ants is lowered or increased with respect to whether ant having best design is static ant or not. If ant having the best design is the static ant, the number of static ants is increased; otherwise the number of ants is lowered. This strategy is represented as function in the following.

$$\text{If } Ant_{best}(t) \in \text{static ant, } S(t) = S(t-1) + 1$$
$$\text{Else } S(t) = S(t-1) - 1 \tag{5.24}$$

where, $Ant_{best}(t)$ is the ant has the best weight in cycle t.

Many tests have been done in order to carry out which strategy is better. It is concluded from tests that algorithm is stable when first or second strategy is used. Although good results are obtained in some test by using third strategy, sometimes stagnations are happen in the algorithm. Therefore third strategy is not used in this study.

5.3.2.2 Scaling on pheromone amount

This strategy was inspired by O. Hasançebi et al. [60]. It is observed from numerical experiments that pheromone amounts are concentrated on only a few sections for a design variable in the progressive cycles. On the contrary pheromone amounts of other sections go towards to zero selection probabilities owing to the effect of local update rule. This causes the algorithm convergence to a local optimum. When lower values of local update parameters are tried in order to overcome this problem, the algorithm cannot show the better performance. Since, when local parameter is set too low, algorithm is turned into a random search where convergence cannot be obtained. As a result of these experiments, scaling strategy is developed as a remedy to overcome this problem. Scaling strategy can be described as follows. First, it is determined that whether scaling procedure is required to or not in the algorithm. In order to make this decision, the ratio called pheromone concentration rate ($pcr(t)$) should be calculated. The pheromone concentration rate is the proportion of the sum of pheromone amount of n_p sections with the highest probability and the total pheromone amount of all section described in the following Equation (5.25). In this equation, n_p term represents number of selected top ranked sections obtained from Equation (5.26).

$$pcr_i(t) = \frac{\sum_{j=1}^{n_p} \tau_{i,j}}{\sum_{j=1}^{nof\,\sec} \tau_{i,j}} \tag{5.25}$$

where, $pcr_i(t)$ is the pheromone concentration rate for design variable i in cycle t, *nofsec* is number the of sections defined in the optimization problem for each design variable.

$$n_p = \sqrt{nof\,\sec} \tag{5.26}$$

If the value of pheromone concentration rate is equal or greater than 0.95, scaling procedure will be performed. Otherwise the scaling procedure will continue without scaling. When scaling procedure is performed, pheromone amount is updated by the following Equation (5.27).

$$\begin{aligned} \tau_{ij}^{scaled}(t) &= \tau_{ij} + \frac{\left(\tau_i\right)_{ave}}{2} \\ \left(\tau_i\right)_{ave} &= \frac{\sum_{j=1}^{nof\,\sec} \tau_{ij}}{nof\,\sec} \end{aligned} \tag{5.27}$$

where, τ_{ij}^{scaled} is the scaled pheromone amount of section j for member group i, $\left(\tau_i\right)_{ave}$ is average pheromone amount for group i. Scaling procedure is performed for only one design group at each cycle which has the highest pheromone concentration rate due to the avoid from turning algorithm in to the random search. At the end of the scaling procedure more homogeneous pheromone distribution is obtained and section has zero selection probabilities regain chance to selection.

5.3.2.3 Dynamic local update coefficient

Main reason to use local update rule in ant colony optimization algorithm is that to encourage the following ants in order to choose different sections. Thereby, dissimilar solutions are obtained and intensive search is carried out in each cycle. When the local update coefficient is taken as static, pheromone amount of selections is lowered evenly. This helps that some solutions dominate in the algorithm and can cause stagnation. As a remedy to overcome this problem dynamic local update coefficient strategy is developed by Hasançebi et al [60]. In this strategy, pheromone amount of each selection is reduced based on selection probability which are illustrated in Equations (5.28) and (5.29).

$$\tau_{ij}(t) = \bar{\xi}_{i,j}\, \tau_{ij}(t) \tag{5.28}$$

$$\bar{\xi}_{i,j} = 1 - (1 - \xi_{\min})\sqrt{P_{i,j}} \tag{5.29}$$

where, $\xi_{\min}$ is the minimum local update coefficient defined in the problem. Value of the parameter is set as within the range of 0.7-0.9 values. Dynamic local update strategy helps to set higher local update coefficient values for sections which have low selections probabilities. This increases selection probabilities of these selections for next cycles.

5.3.3 Harmony search algorithm for frame design problem

Harmony search algorithm for the frame design problem has exactly the same steps as the harmony search algorithm for mathematical problems explained in section 4.3 of the previous chapter. Steps of the harmony search algorithm for frame optimization problems are summarized as follows.

Step1: Optimization problem is stated mathematically that was described in Section 5.2. In addition, harmony search algorithm parameters are determined in this step. These parameters are: the number of frame design stored in harmony memory called harmony memory size (HMS), harmony memory considering rate (HMCR), pitch adjusting rate (PAR), and maximum iteration number.

Step2: Then the harmony memory matrix is filled with feasible frame designs which are generated randomly.

Step 3: New frame design is generated based on the three main rules described in Section 4.3.3.

Step 4: The weight and constraint violation value of the new frame design are calculated. If weight of the new frame design is lighter than the frame design having the heaviest weight in harmony memory and the new frame design is feasible, the new frame design is replaced with frame design the having heaviest weight in the harmony memory. The updated harmony memory matrix is then sorted in ascending order of the weight of the frame.

Step 5: Steps 4.2.3 and 4.2.4 are repeated until the maximum number of iterations is reached.

5.3.4 Improvements in the harmony search algorithm

5.3.4.1 Harmony search with adaptive error Strategy (SHSAES)

In regular harmony search method, the unfeasible solution vector is not allowed to put in harmony memory matrix. That causes some difficulties at the beginning of the algorithm. Adaptive error strategy is developed in order to overcome this problem. In this strategy the candidate solution vectors that violate one or more design constraints slightly are also included in the harmony memory matrix in addition to feasible ones. Initially larger error value is selected and this value is adjusted during the design cycles according to the expression given below.

$$Tol(i) = Tol_{\max} - \frac{\left(Tol_{\max} - Tol_{\min}\right) \cdot i^{0.5}}{\left(iter_{\max}\right)^{0.5}} \tag{5.30}$$

where, $Tol(i)$ is the error value in iteration i, $Tol_{\max}$ and $Tol_{\min}$ are the maximum and the minimum error values defined in the algorithm respectively, $iter_{\max}$ is the maximum iteration number until which tolerance minimization procedure continues.

5.3.4.2 Standard Harmony Search with Penalty Function

This strategy is an alternative strategy of the adaptive error strategy for harmony search algorithm. In this strategy candidate vector is included in the harmony memory matrix regardless of whether it satisfies the design constraints or not. However, this solution penalized with penalty function. Penalty function is exactly same as penalty function of ant colony algorithm which is described in Equations (5.16), (5.17) and (5.18).

CHAPTER 6

DESIGN EXAMPLES

6.1 Introduction

Optimum design of six steel space frames is considered in this chapter. Both ant colony and harmony search based optimum design algorithms are used in order to investigate the effect of warping in the optimum design of space frames. The first design example is two-story, two bay irregular steel space frame which consists of 21 members. The second design example is five-story, two bay regular steel space frame with 105 members. Third design example is three-story, three bay 132 members irregular space frame. The fourth design example is twenty stories, three-bay steel space with irregular plan which consists of 460 members. The ten-story four-bay steel space with 568 member sis selected as fifth design example. The last example is the twenty storeys, 1860-member irregular space steel frame. All examples are designed twice by each algorithm developed including and excluding warping deformations in order to investigate the effect of warping on the optimum designs. The modulus of elasticity and yield stress of the steel material are taken as 200GPa and 250MPa respectively. The complete W-section list given in LRFD-AISC [30] which consists of 272 sections are considered as a pool for design variables from which the algorithm presented has selected appropriate W-sections for the frame member groups.

6.2 Two- story, two-bay irregular steel space frame

The two-story, two-bay irregular steel space frame has 21 members that are collected in two beam and three column design groups. The dimensions and member groupings in the frame are shown in the Figure 6.1. The frame is subjected to wind loading of 50kN along Z axis in addition to 20kN/m gravity load which is applied to all beams. The drift ratio limits are defined as 1 cm for inter storey drift 4 cm for top storey drift where *H* is the height of frame. Maximum deflection of beam members is restricted as 1.39 cm.

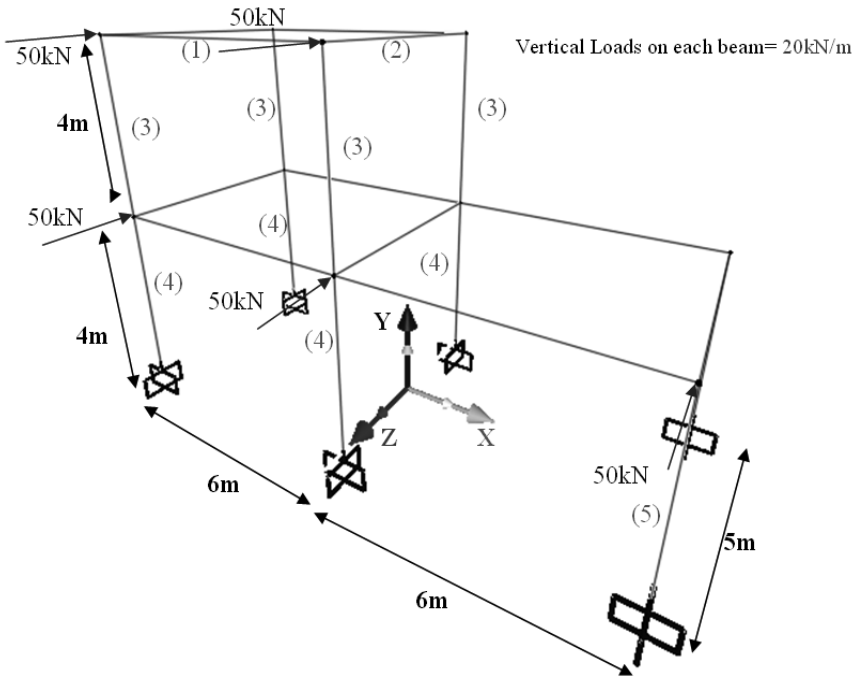

Figure 6.1 Two-story, two bay irregular frame

Table 6.1 Design results of two-story, two bay irregular frame

Group number	Group type	ACO without warping	ACO with warping	HS without warping	HS with warping
1	Beam	W460X60	W460X52	W460X60	W530X66
2	Column	W360X32.9	W360X44	W310X28.3	W410X38.8
3	Column	W460X52	W410X60	W410X60	W410X60
4	Column	W460X68	W530X74	W460X60	W410X60
5	Column	W310X44.5	W460X52	W410X38.8	W310X38.7
Minimum weight (kN)		48.68	53.42	46.63	51.78
Maximum top storey drift (cm)		1.82	1.765	1.917	1.796
Maximum inter- storey drift (cm)		0.95	0.998	0.956	0.932
Maximum strength constraint ratio		0.921	0.969	0.992	0.988
Maximum number of Iterations		10000	10000	10000	10000

This irregular steel frame is designed by using harmony search and ant colony optimization algorithms considering warping and without considering warping cases. In these algorithms, following search parameters are used: number of ants = 100, number of cycles = 100, controlling parameter of visibility (β) = 0.40, minimum local update coefficient (ξ_{min}) = 0.7, strategy of changing in the number of static ant = constant, number of static ant = 30, number of ranked ant= 10, harmony memory size (HMS) = 20, pitch adjusting rate (PAR) = 0.3, harmony memory considering rate (HMCR) = 0.9, error strategy of harmony search = Not Used and maximum iteration number = 10000. The minimum weights, maximum constraints values and steel sections of optimum designs obtained from each of these algorithms and cases are illustrated in Table 6.1. It is apparent from tables that consideration of the warping effect increases the minimum weight 9.74% in ant colony optimization algorithm and 11.04% in harmony search algorithms which are considerable amounts. Moreover, harmony search algorithm finds 3.07% lighter frame for the case where warping is considered and 4.40% lighter frame for the case where warping is not considered with ant colony optimization. Design histories of these solutions are shown in Figure 6.2.

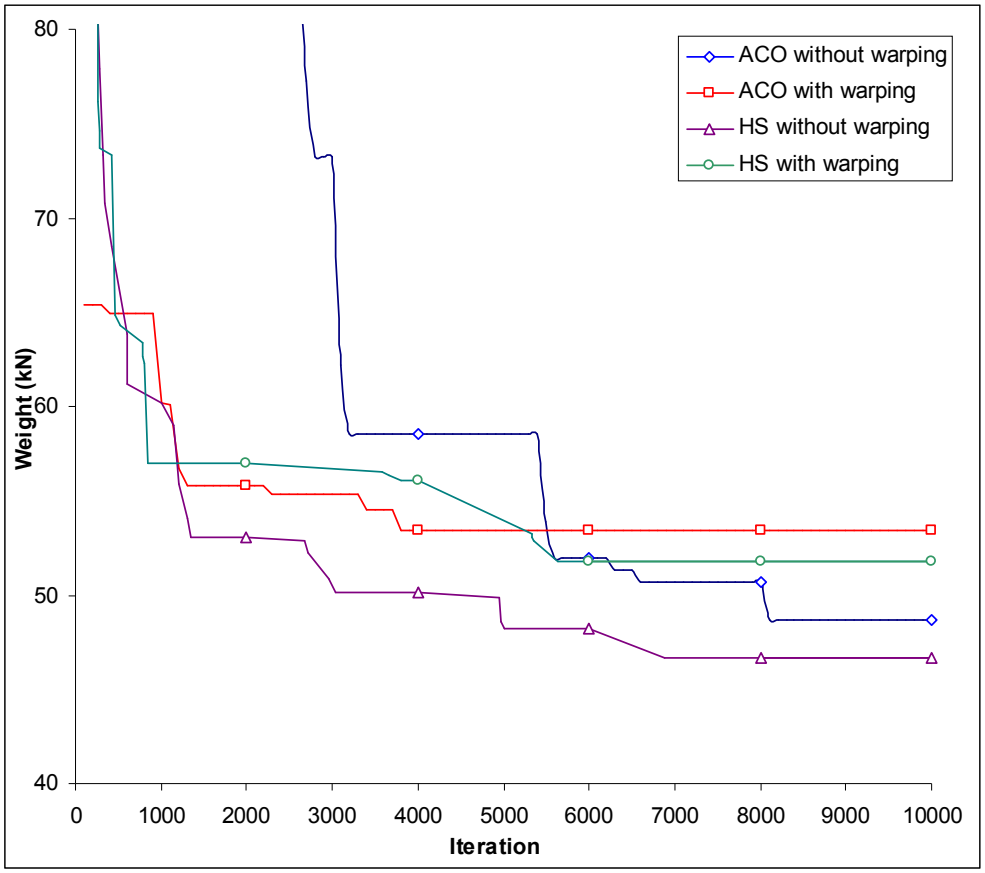

Figure 6.2 Design histories of two-story, two bay irregular frame

6.3 Five-story, two-bay regular steel space frame

The plan and 3D views of the five-story, two-bay steel frame shown in the Figures 6.3 and 6.4 is a regular steel frame with 54 joints and 105 members that are grouped into 11 independent design variables. The frame is subjected to gravity loads as well as lateral loads that are computed as per ASCE 7-05 [129]. The design dead and live loads are taken as 2.88kN/m^2 and 2.39kN/m^2 respectively. The ground snow load is considered to be 0.755kN/m^2 and a basic wind speed is 105mph (65 m/s). The un-factored distributed gravity loads on the beams of the roof and floors are tabulated in Table 6.2. The following load combinations

are considered in the design of the frame according to the code specification. 1.2D+1.6L+0.5S, 1.2D+0.5L+1.6S, 1.2D+1.6W+0.5L+0.5S where D is the dead load, L represents the live load, S is the snow load and W is the wind load. The drift ratio limits of this frame are defined as 1.33 cm for inter storey drift and 6.67 cm for top storey drift. Maximum deflection of beam members is restricted as 1.67 cm.

Table 6.2 Beam gravity loading of the five-story, two bay steel frame

Beam Type	Uniformly distributed load (kN/m)		
	Dead Load	Live Load	Snow Load
Roof Beams	4.78	-	1.508
Floor Beams	4.78	5.76	-

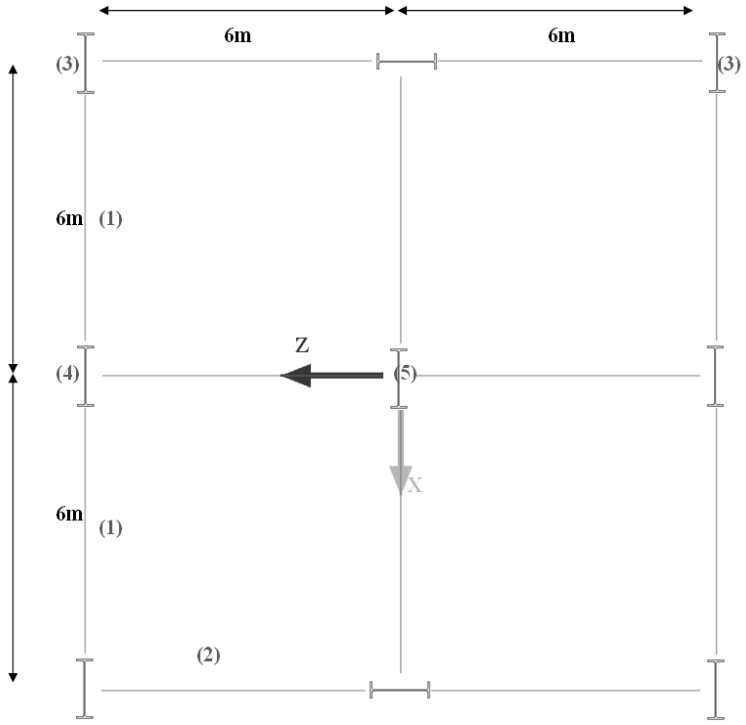

Figure 6.3 Plan view of five-story, two bay steel frame

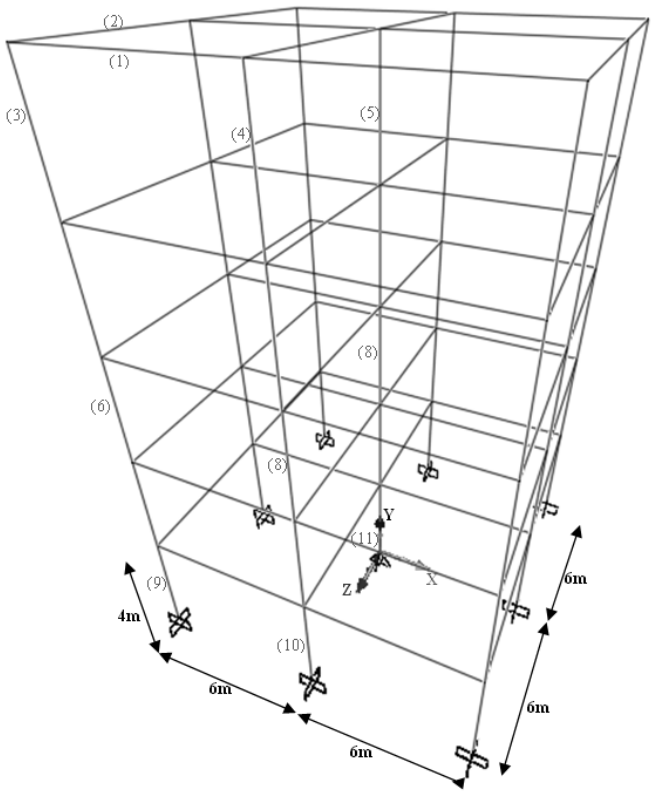

Figure 6.4 3D View of the five-story, two bay steel frame

This regular steel frame is designed by using harmony search and ant colony optimization algorithms without considering warping and with considering warping. The ant colony algorithm and harmony search method parameters are selected as: number of ants = 100, number of cycles = 500, controlling parameter of visibility (β) = 0.35, minimum local update coefficient (ξ_{min}) = 0.7, strategy of changing in the number of static ant = dynamic, the maximum number of static ant in the algorithm = 75, the minimum number of static ant in the algorithm = 5, number of ranked ant = 10, harmony memory size (HMS) = 20, pitch adjusting rate (PAR) = 0.3, harmony memory considering rate (HMCR) = 0.9, error strategy of harmony search = penalty function method and maximum iteration number = 50000. The optimum designs, the maximum constraint values and steel sections

for member groups obtained from each of these runs are given in Table 6.3. Comparison of minimum weights of both cases and both algorithms clearly shows that even in regular steel space frames consideration of warping effect causes 8.4 % increase in the minimum weight of the frame in the case of ant colony optimization algorithm, 10.49% increase in the case of harmony search algorithm. It is interesting to notice that ant colony optimization has obtained 6.86% lighter frame than harmony search algorithm when warping effects are considered and 4.83% lighter frame when warping effects are not considered in this design example. Design histories of these runs are shown in Figure 6.5.

Table 6.3 Design results of the five-story, two bay steel frame

Group Number	Group Type	ACO without warping	ACO with warping	HS without warping	HS with warping
1	Beam	W460X52	W460X52	W530X66	W360X44
2	Beam	W200X35.9	W360X44	W310X38.7	W310X38.7
3	Column	W200X35.9	W200X35.9	W200X35.9	W310X38.7
4	Column	W310X38.7	W360X72	W200X35.9	W310X60
5	Column	W360X57.8	W360X44	W360X44	W610X113
6	Column	W460X52	W310X52	W310X38.7	W530X66
7	Column	W310X86	W360X72	W360X72	W610X101
8	Column	W610X101	W760X161	W610X92	W1000X296
9	Column	W530X66	W530X74	W410X53	W610X82
10	Column	W460X89	W360X72	W360X72	W610X101
11	Column	W690X170	W760X161	W760X147	W1100X433
Minimum weight(KN)		265.38	287.66	278.196	307.384
Maximum top storey drift (cm)		4.983	4.83	4.837	3.362
Maximum Inter-storey drift (cm)		0.569	0.604	1.333	0.475
Maximum strength constraint ratio		0.886	0.969	0.979	0.977
Maximum number of iterations		50000	50000	50000	50000

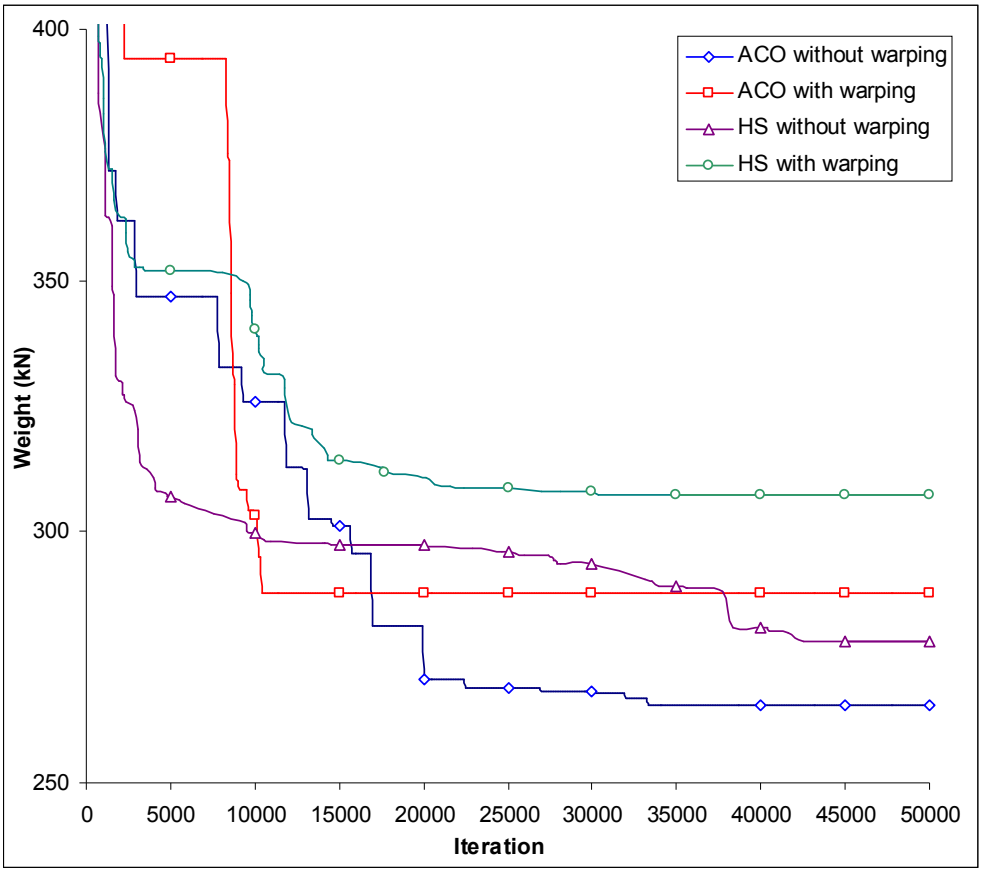

Figure 6.5 Design histories of the five-story, two bay steel frame

6.4 Four-story, three bay 132 members space frame

The third example shown in Figures 6.6, 6.7 and 6.8 is a three dimensional irregular steel frame that are taken from literature [130]. This frame consists of 70 joints and 132 members that are grouped into 30 independent design groups. The frame is subjected to gravity loads and lateral loads, which are computed as per ASCE 7-05 [129] based on the following design values: a design dead load of 2.88kN/m^2, a design live load of 2.39kN/m^2 and a ground snow load of 0.755kN/m^2. The un-factored distributed gravity loads on the beams of the roof and floors are tabulated in Table 6.4 and the un-factored lateral loads are given in Table 6.5. The load and combination factors are applied according to code

specification [33] as: Load case1: 1.4D, Load Case 2: 1.2D+1.6L+0.5S; Load Case 3: 1.2D+0.5L+1.6S; Load Case 4: 1.2D+1.0E+0.5L+0.2S; where D represents dead load, L is live load, S is snow load and E represents earthquake load. In addition, top story drift constraints in *x* and *y* directions are restricted as the 3.89 cm. Inter-story drift is applied as the 1.14 cm to first storey 0.915 cm to other storey. Maximum deflection of beam members is restricted as 2.03 cm.

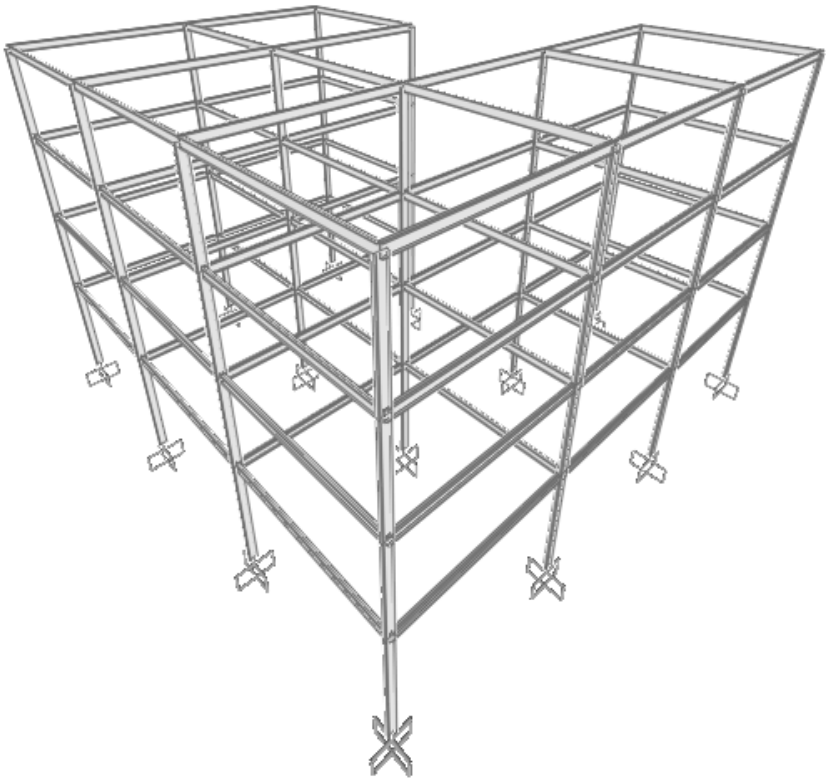

Figure 6.6 3D view of four-story, three bay space frame

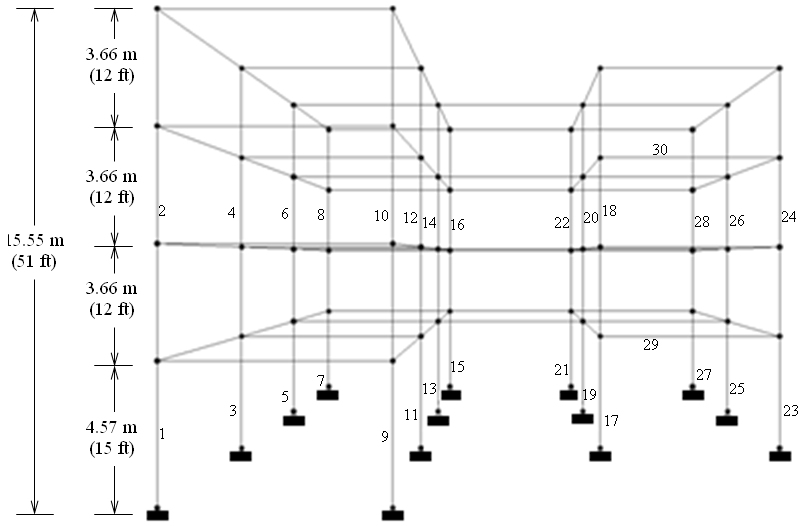

Figure 6.7 Side view of four-story, three bay space frame

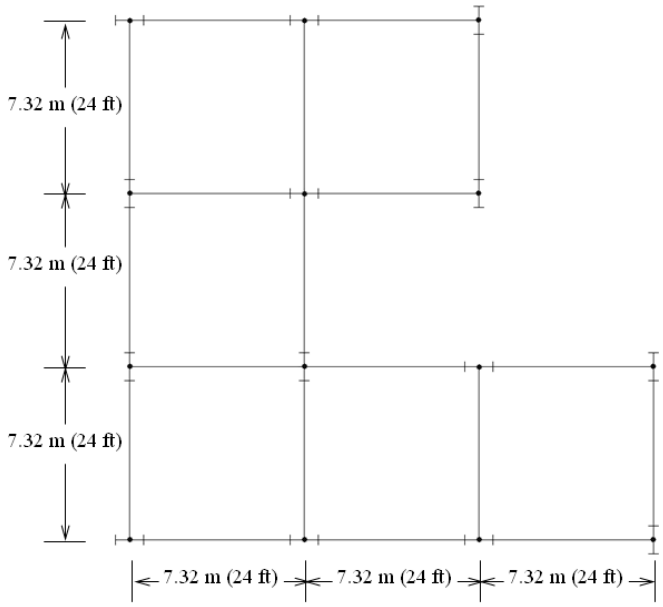

Figure 6.8 Plan view of four-story, three bay space frame

Table 6.4 Gravity loading on the beams of 132-member space frame

	Beam Type	Uniformly distributed load,(kN/m)	
		Outer Span	Inner Span
Load Case 1	Roof Beams	7.01	14.02
	Floor Beams	8.18	16.36
Load Case 2	Roof Beams	7.93	15.87
	Floor Beams	18.26	36.51
Load Case 3	Roof Beams	9.96	19.91
	Floor Beams	10.53	21.05
Load Case 4	Roof Beams	7.01	14.02
	Floor Beams	10.53	21.05

Table 6.5 Lateral loading on the beams of 132-member space frame

Floor Number	Earthquake Design Load (kN)	Floor Number	Earthquake Design Load (kN)
1	29.23	3	82.35
2	55.28	4	110.15

This space frame is optimized by using harmony search and ant colony optimization algorithms with and without considering warping. For the ant colony optimization and harmony search algorithms following search parameters are used: number of ants = 100, number of cycles = 500, controlling parameter of visibility (β) = 0.40, minimum local update coefficient (ξ_{min}) = 0.7, strategy of changing in the number of static ant = dynamic, the maximum number of static ant in the algorithm = 75, the minimum number of static ant in the algorithm = 5, number of ranked ant = 10, harmony memory size (HMS) = 30, pitch adjusting rate (PAR) = 0.3, harmony memory considering rate (HMCR) = 0.9, error strategy of harmony search = adaptive error strategy and maximum iteration number = 50000. The W sections obtained in the optimum designs and the corresponding maximum constraints values for each algorithm are given in the Table 6.6. The harmony search algorithm obtains the optimum design with weights as 560.71kN without considering warping, 617.36kN for considering the warping. The ant colony optimizations yielded the optimum designs with the minimum weights of 568.24kN and 618.38kN without considering warping and considering warping cases respectively. Comparison of these values reveals the fact that consideration

of warping effect causes 8.82 % increase in the minimum weight of the frame in the use of ant colony optimization algorithm, 10.10% increase in the use of harmony search algorithm. In addition, Harmony search algorithm produces optimum designs which are slightly lighter than the ones obtained by using ant colony algorithm for both cases. These differences are only 1.34 % for without considering warping case 0.16 % for considering warping case. Design histories of these runs are shown in Figure 6.9.

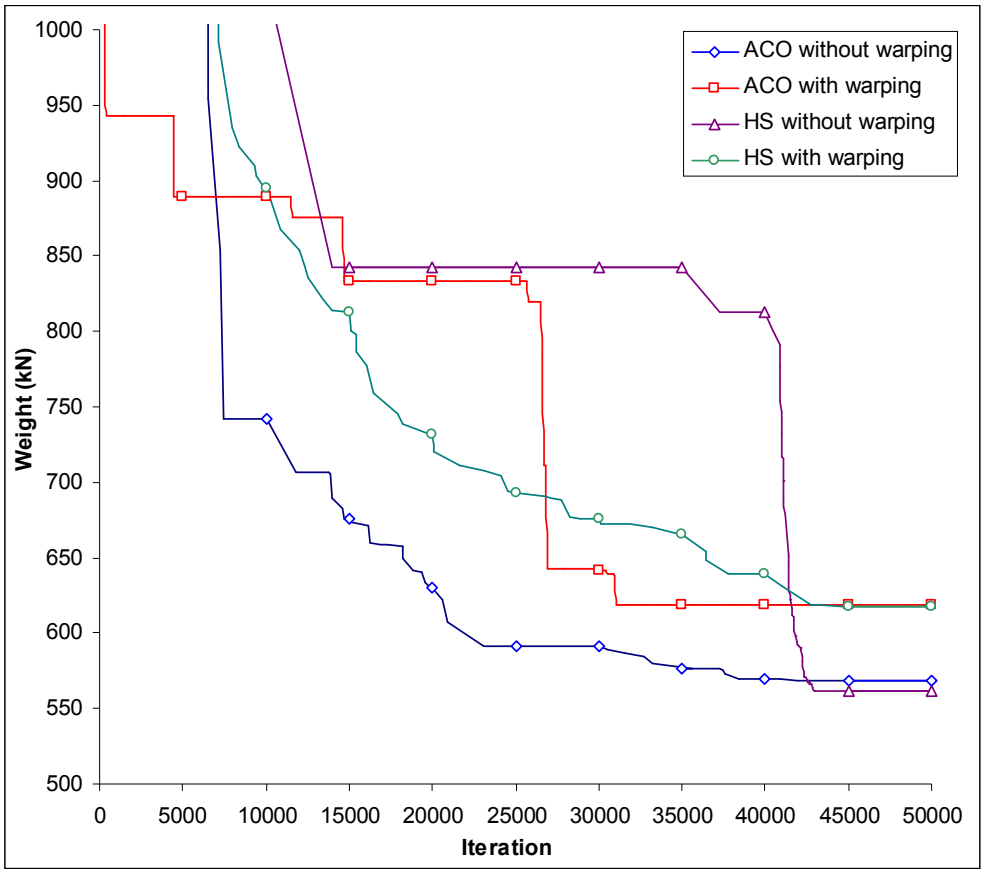

Figure 6.9 Design histories of the 132-member space frame

Table 6.6 Design results of the 132-member space frame

Group Number	Group Type	ACO without warping	ACO with warping	HS without warping	HS with warping
1	Column	W530X74	W310X158	W310X117	W610X155
2	Column	W460X52	W610X195	W460X144	W610X155
3	Column	W310X67	W760X134	W250X58	W690X125
4	Column	W460X74	W760X134	W360X110	W690X125
5	Column	W360X147	W460X82	W310X60	W250X67
6	Column	W360X147	W460X106	W460X89	W250X67
7	Column	W460X74	W610X101	W410X67	W310X86
8	Column	W760X134	W760X134	W410X114	W840X176
9	Column	W250X58	W360X162	W460X144	W360X147
10	Column	W250X58	W760X220	W840X176	W530X150
11	Column	W410X75	W530X182	W410X85	W460X177
12	Column	W530X138	W920X223	W610X155	W690X217
13	Column	W530X196	W310X86	W360X72	W250X89
14	Column	W610X217	W690X125	W530X165	W610X92
15	Column	W460X158	W310X74	W200X59	W360X72
16	Column	W460X158	W460X82	W360X91	W690X140
17	Column	W410X60	W410X149	W460X82	W460X128
18	Column	W610X92	W760X161	W840X176	W760X173
19	Column	W610X82	W610X155	W310X60	W360X147
20	Column	W610X82	W610X155	W460X82	W690X217
21	Column	W530X101	W310X74	W310X74	W460X74
22	Column	W530X101	W460X113	W610X101	W760X134
23	Column	W410X75	W460X128	W310X86	W460X113
24	Column	W410X75	W760X147	W310X117	W760X161
25	Column	W410X60	W250X80	W250X58	W250X89
26	Column	W460X106	W250X80	W460X74	W760X147
27	Column	W690X125	W530X74	W460X74	W460X74
28	Column	W690X125	W460X52	W410X53	W460X52
29	Beam	W250X80	W310X74	W410X100	W410X67
30	Beam	W610X92	W460X106	W690X125	W610X125
Minimum weight(KN)		568.24	618.38	560.714	617.36
Maximum top storey drift (cm)		3.24	3.25	3.54	3.5
Maximum Inter-storey drift (cm)		0.883	0.621	0.857	0.935
Maximum strength constraint ratio		0.986	0.974	0.964	0.989
Maximum number of iterations		50000	50000	50000	50000

6.5 Twenty-story, 460 members irregular space frame

The three dimensional, side and plan views of 20-story irregular steel frame are shown in Figures 6.10, 6.11 and 6.12. This frame is first taken from [114]. The frame consists of 210 joints and 460 members that are grouped into 13 independent design variables. The frame is subjected to a uniformly distributed vertical load of 4.79kN/m^2 on each floor and wind load of 0.958kN/m^2 along the Z axis. The loading of this frame is shown in Figures 6.11 and 6.12. The drift ratio limits of this problem are defined as 1.22 cm for inter storey drift and 24.4 cm for top storey drift. Maximum deflection of beam members is restricted as 2.03 cm.

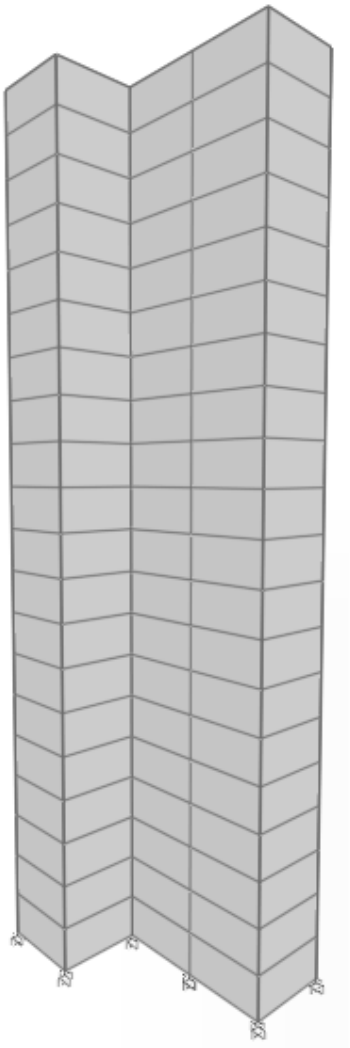

Figure 6.10 3D view of twenty-story, irregular steel frame

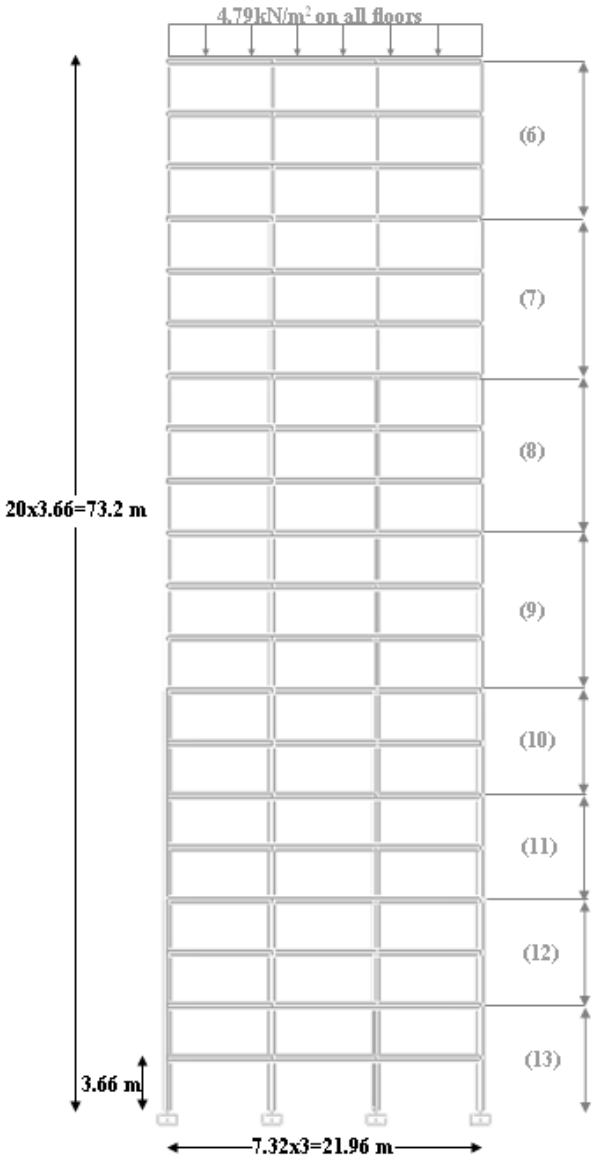

Figure 6.11 Side view of twenty-story, irregular steel frame

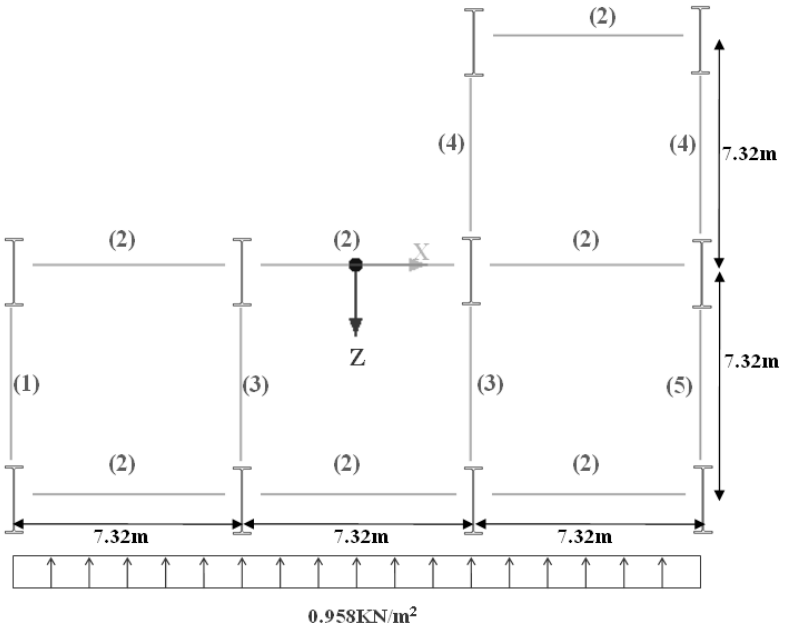

Figure 6.12 Plan view of the twenty-story, irregular steel frame

Optimum design of twenty-story, irregular steel frame problem is solved by using harmony search and ant colony optimization algorithms with and without considering warping. For the ant colony optimization and the harmony search algorithms, following search parameters are used: number of ants = 100, number of cycles = 750, controlling parameter of visibility (β) = 0.30, minimum local update coefficient (ξ_{min}) = 0.7, strategy of changing in the number of static ant = dynamic, the maximum number of static ant in the algorithm = 75, the minimum number of static ant in the algorithm = 5, number of ranked ant = 10, harmony memory size (HMS) = 30, pitch adjusting rate (PAR) = 0.3, harmony memory considering rate (HMCR) = 0.9, error strategy of harmony search = adaptive error strategy and maximum iteration number = 75000. The designation of W-Sections and the maximum constraint values in the optimum designs obtained by each algorithm are given in Table 6.7. The minimum weights determined by ant colony optimization algorithm are 3191.15kN and 3589.73kN without considering

warping and considering warping cases respectively. The harmony search algorithm produces the optimum designs with weights of 2943.81kN without considering warping case and 3452.697kN for considering warping case. It is concluded from table that consideration of warping effect causes 12.50% increase in the minimum weight of the frame in the case of ant colony optimization algorithm and 17.29 % increase in the case of harmony search algorithm. These increases are higher than increases of previous examples because of the fact that the frame has irregular shape and it is taller than the previous frames. Consequently torsional moments become more vigorous. In this design example, the harmony search algorithm shows better performance than ant colony optimization algorithm. In the case where the effect of warping is considered harmony search algorithm reaches 3.96% lighter frame than the ant colony optimizer and 7.7 % lighter frame in the case where the effect of warping is not considered. Design histories of all the runs are shown in Figure 6.13.

Table 6.7 Design results of the twenty-story, irregular steel frame

Group number	Group type	ACO without warping	ACO with warping	HS without warping	HS with warping
1	Beam	W610X92	W610X140	W690X125	W690X125
2	Beam	W310X28.3	W610X101	W460X82	W530X92
3	Beam	W760X196	W760X147	W690X125	W610X113
4	Column	W460X68	W610X101	W610X101	W610X113
5	Column	W530X66	W610X101	W460X89	W460X97
6	Column	W310X202	W360X162	W690X125	W690X125
7	Column	W360X237	W360X162	W760X134	W760X134
8	Column	W360X237	W360X162	W760X134	W760X134
9	Column	W610X262	W610X217	W760X134	W760X134
10	Column	W760X314	W610X262	W760X161	W840X226
11	Column	W760X314	W690X265	W760X173	W1000X249
12	Column	W760X314	W690X265	W1000X222	W1000X249
13	Column	W840X329	W690X265	W1000X272	W1000X272
Minimum weight (kN)		3191.15	3589.73	2943.811	3452.697
Maximum top storey drift (cm)		17.9	19.41	19.64	19.37
Maximum inter- storey drift (cm)		1.133	1.11	1.21	1.2
Maximum strength constraint ratio		0.983	0.876	0.844	0.895
Maximum number of Iterations		75000	75000	75000	75000

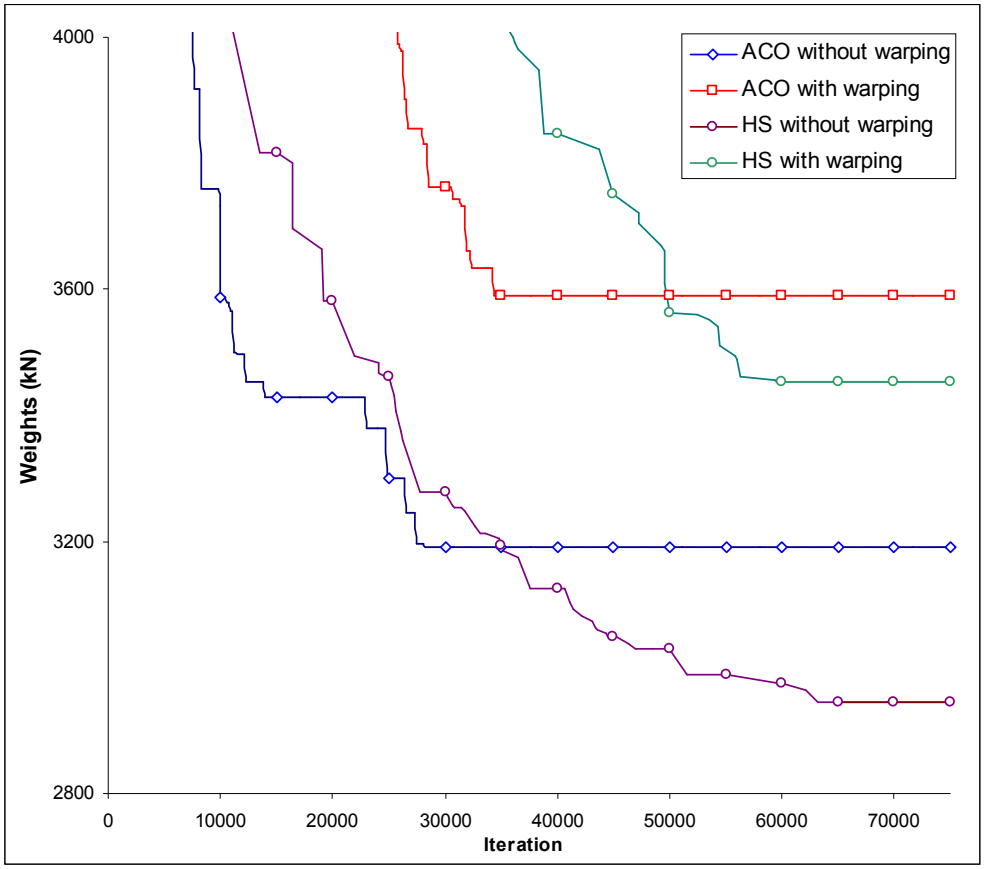

Figure 6.13 Design histories of the twenty-story, irregular steel frame

6.6 Ten-story, four-bay steel space frame

The three dimensional, side and plan views of ten-story four-bay steel frame shown in Figures 6.14 and 6.15 is taken from previous study [114]. This frame has 220 joints and 568 members which are collected in 25 independent design variables. Inner roof beams, outer roof beams, inner floor beams and outer floor beams of this frame are subjected to 14.72kN/m, 7.36kN/m, 21.43kN/m and 10.72kN/m vertical loads respectively. The un-factored lateral loads of this frame are given in the Table 6.8. The drift ratio limits of this frame are defined as 0.914

cm for inter storey drift and 9.14 cm for top storey drift. Maximum deflection of beam members is restricted as 1.69 cm.

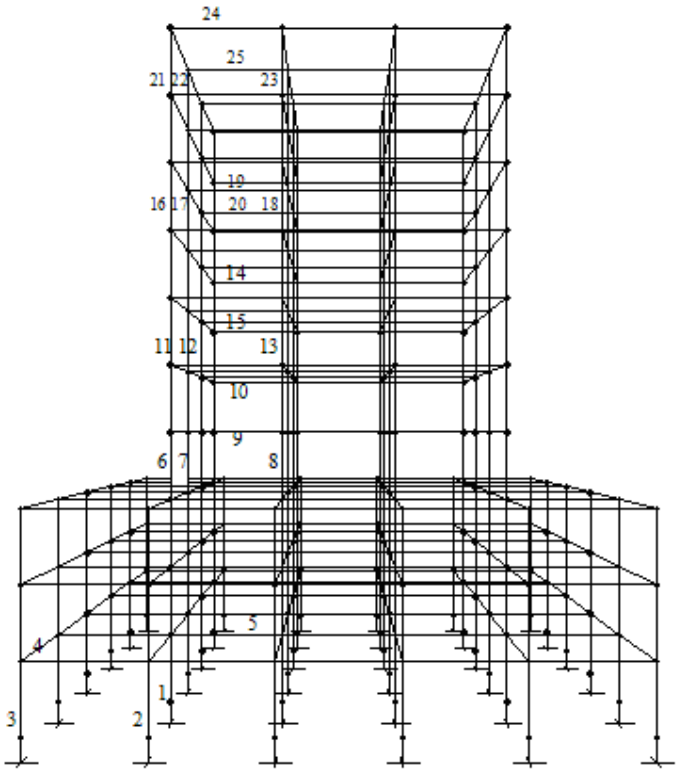

Figure 6.14 3-D view of ten-storey, four-bay steel space frame

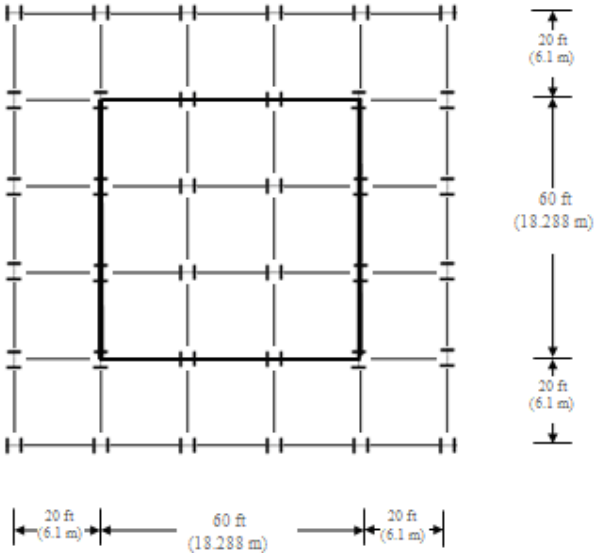

Figure 6.15 Side view of ten-storey, four-bay steel space frame

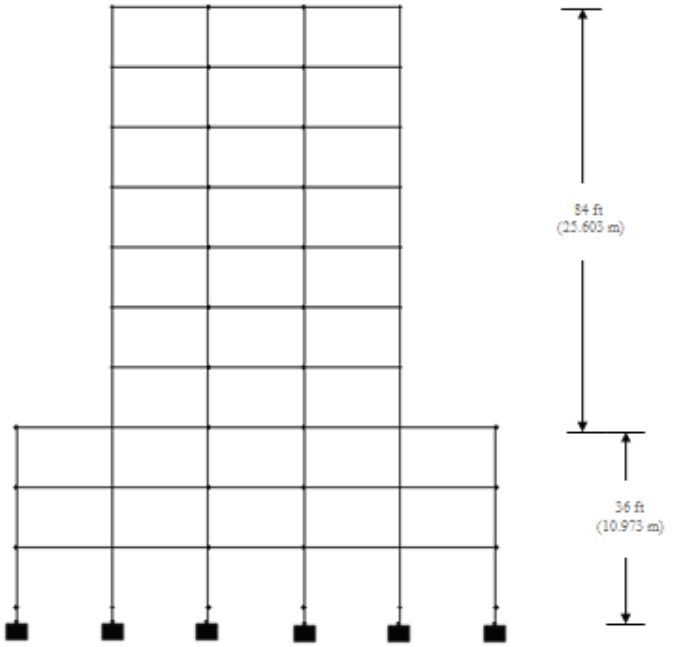

Figure 6.16 Side view of ten-storey, four-bay steel space frame

Table 6.8 Horizontal forces of ten-storey, four-bay steel space frame

Storey No:	Windward		Leeward	
	(lb/ft)	(kN/m)	(lb/ft)	(kN/m)
1	12.51	0.1825	127.38	1.8585
2	28.68	0.4184	127.38	1.8585
3	44.68	0.6519	127.38	1.8585
4	156.86	2.2886	127.38	1.8585
5	167.19	2.4393	127.38	1.8585
6	176.13	2.5698	127.38	1.8585
7	184.06	2.6854	127.38	1.8585
8	191.21	2.7897	127.38	1.8585
9	197.76	2.8853	127.38	1.8585
10	101.9	1.5743	127.38	1.8585

Optimum designs of this regular steel frame is found by using harmony search and ant colony optimization algorithms with and without considering warping effects. The following search parameters are selected for the ant colony optimizer and harmony search method: number of ants = 100, number of cycles = 500, controlling parameter of visibility (β) = 0.40, minimum local update coefficient (ξ_{min}) = 0.7, strategy of changing in the number of static ant = dynamic, the maximum number of static ant in the algorithm = 75, the minimum number of static ant in the algorithm = 5, number of ranked ant = 10, harmony memory size (HMS) = 50, pitch adjusting rate (PAR) = 0.3, harmony memory considering rate (HMCR) = 0.9, error strategy of harmony search = adaptive error strategy and maximum iteration number = 50000. The minimum weights, maximum constraints values and W-sections designations of optimum designs obtained for each of these algorithms are illustrated in Table 6.9. The lightest weights of this regular frame are obtained as 1899.3kN and 2079.2kN by using ant colony optimization algorithm, 1987.2kN and 2107.77kN by using harmony search algorithm for without considering warping and considering cases respectively. It is apparent from results that even in regular steel space frames consideration of warping effect causes 9.47 % increase in the case of ant colony optimization algorithm, 6.07 % increases in the case of harmony search algorithm. These increases are more than increases of second example. In addition, ant colony optimization algorithm attained 4.63 % and 3.75 % lighter frames than harmony

search algorithm without and with considering warping effects respectively. Design histories of these runs are shown in Figure 6.17.

Table 6.9 Design results of the ten-storey, four-bay steel space frame

Group number	Group type	ACO without warping	ACO with warping	HS without warping	HS with warping
1	Column	W250X38.5	W360X64	W130X23.8	W200X26.6
2	Column	W200X86	W310X86	W310X86	W200X59
3	Column	W610X174	W840X176	W840X193	W840X210
4	Beam	W310X23.8	W310X28.3	W310X23.8	W360X39
5	Beam	W410X38.8	W410X38.	W310X44.5	W410X38.8
6	Column	W690X140	W610X285	W460X144	W1100X390
7	Column	W920X201	W690X217	W840X210	W1000X272
8	Column	W840X193	W1000X222	W1000X222	W1000X272
9	Beam	W460X106	W610X113	W460X106	W310X44.5
10	Beam	W610X153	W760X161	W690X152	W610X101
11	Column	W460X128	W610X153	W460X113	W1000X249
12	Column	W460X113	W310X107	W530X123	W610X153
13	Column	W690X170	W690X170	W760X173	W760X220
14	Beam	W360X64	W460X74	W460X60	W410X67
15	Beam	W250X89	W360X101	W610X92	W610X113
16	Column	W360X122	W410X132	W200X86	W690X125
17	Column	W410X114	W310X107	W460X113	W610X101
18	Column	W610X92	W360X91	W460X106	W610X113
19	Beam	W410X38.8	W410X53	W250X32.7	W410X53
20	Beam	W410X46.1	W460X68	W410X53	W410X53
21	Column	W360X72	W310X67	W200X59	W310X97
22	Column	W200X71	W250X58	W250X67	W310X52
23	Column	W460X60	W310X67	W310X60	W360X57.8
24	Beam	W310X28.3	W250X44.8	W200X35.9	W250X32.7
25	Beam	W310X28.3	W310X32.7	W310X38.7	W410X38.8
Minimum weight(KN)		1899.3	2079.2	1987.2	2107.77
Maximum top storey drift (cm)		7.85	6.49	7.14	7.53
Maximum inter-storey drift (cm)		0.901	0.911	0.909	0.895
Maximum strength constraint ratio		0.991	0.956	0.942	0.906
Maximum number of iterations		50000	50000	50000	50000

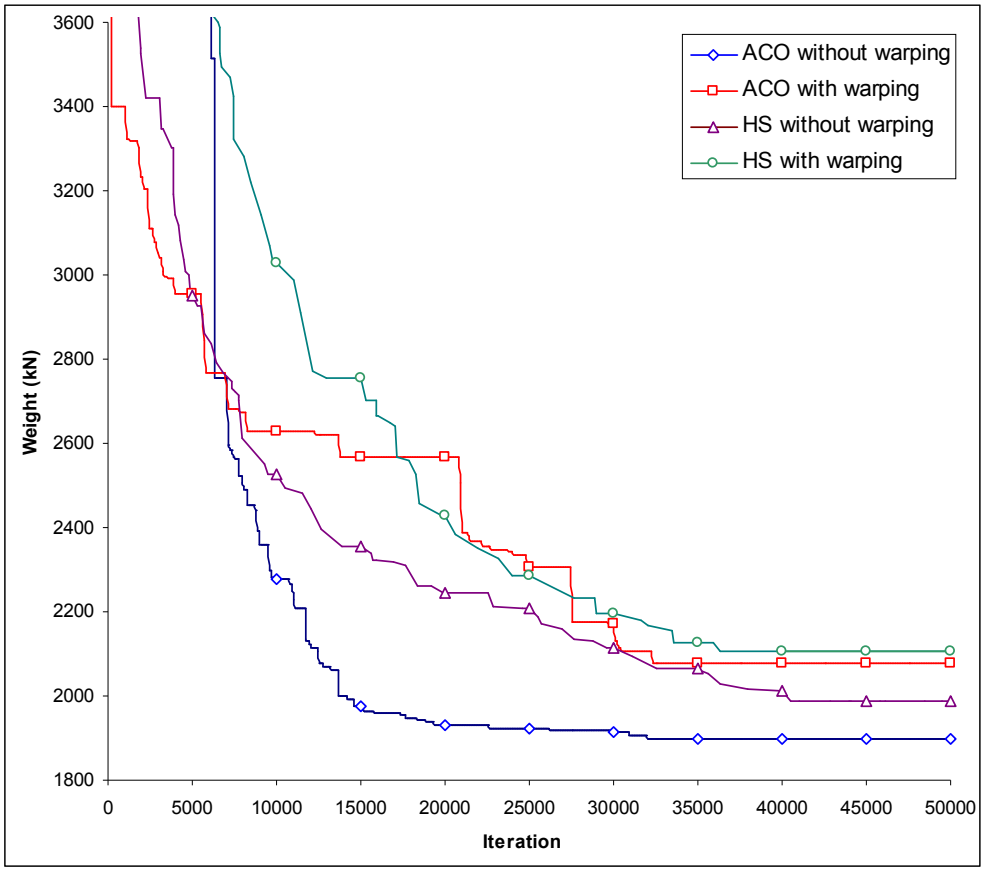

Figure 6.17 Design histories of the ten-storey, four-bay steel space frame

6.7 Twenty-story, 1860–member, steel space frame

The three dimensional and plan views of twenty-story, 1860-member steel space frame are illustrated in Figures 6.18 and 6.19. The frame has 820 joints and 1860 members which are collected in 86 independent design variables. The member grouping of columns is illustrated in Figure 6.19. The frame is subjected to gravity loads as well as lateral loads that are computed according to ASCE 7-05 [129]. The design dead and live loads are taken as 2.88kN/m^2 and 2.39kN/m^2 respectively. Basic wind speed is considered as 85mph (38 m/s). The following load combinations are considered in the design of the frame according to

code specification [33]: 1.2D+1.3WZ+0.5L+0.5S and 1.2D+1.3WX+0.5L+0.5S where D is the dead load, L represents the live load, S is the snow load and WX, WZ are the wind loads in the global X and Z axis respectively. Drift ratio limits for this example are taken as 0.75 cm for inter storey drift where *h* is the storey height and 15 cm for top storey drift where *H* is the height of structure. Maximum deflection of beam members is restricted as 1.67 cm.

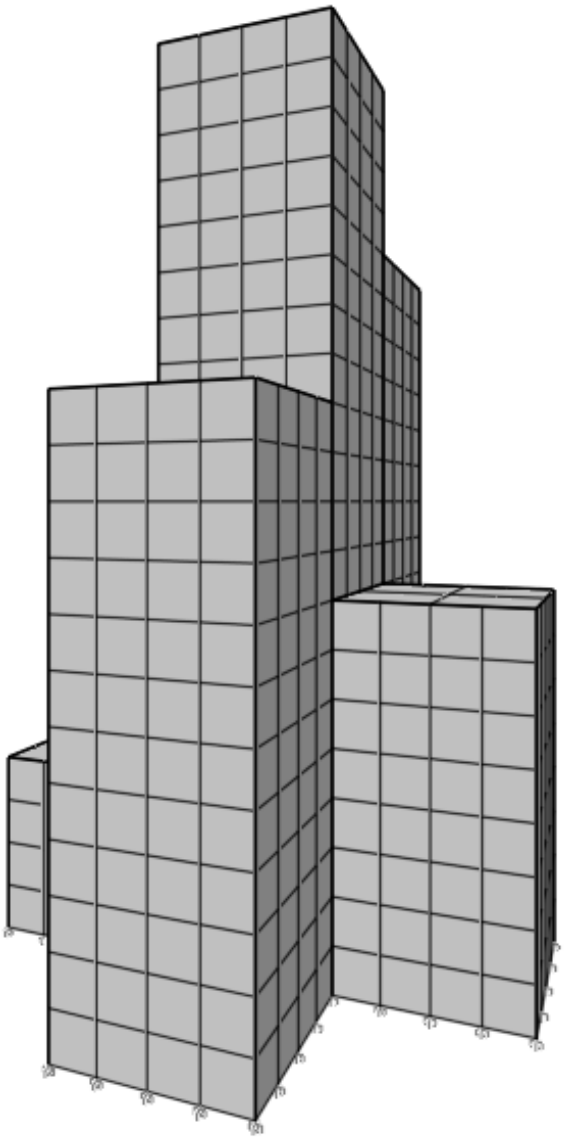

Figure 6.18 3-D view of twenty-storey, 1860 member steel space frame

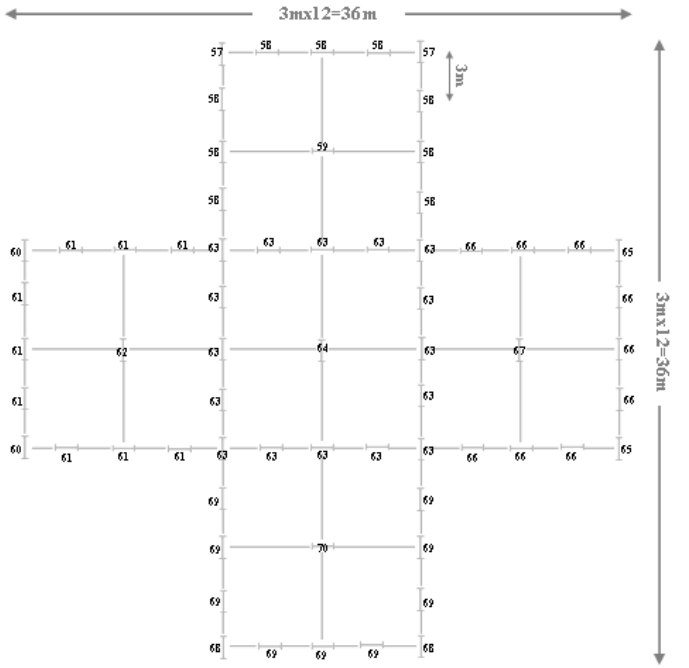

(a) Plan view of 1-4th storey

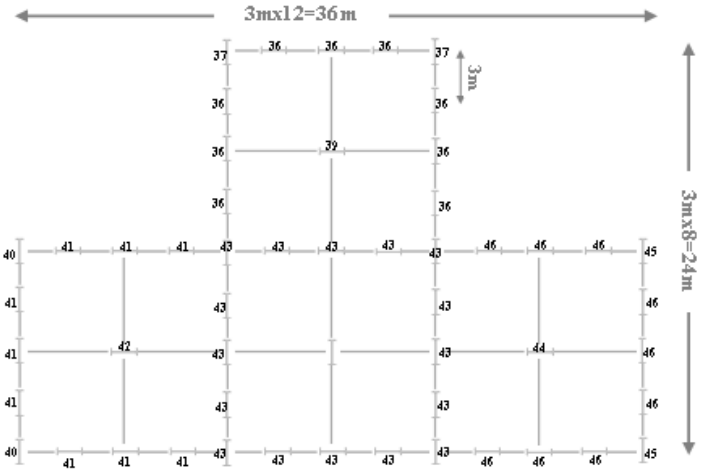

(b) Plan view of 5-8th storey

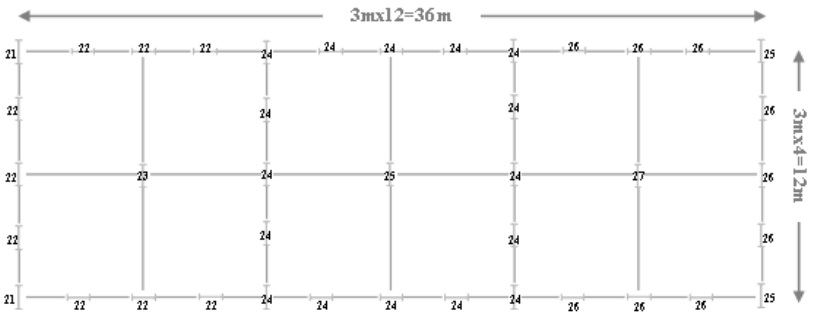

(c) Plan view of 5-8th storey

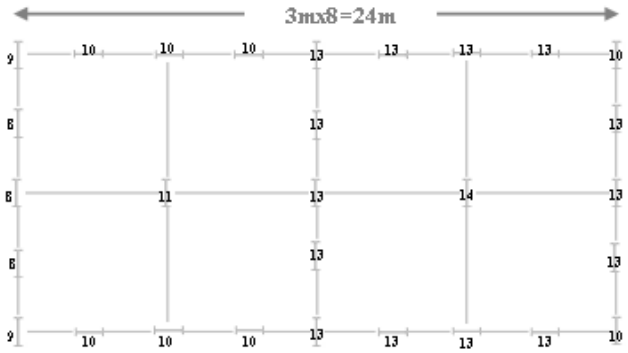

(d) Plan view of 13-16th storey

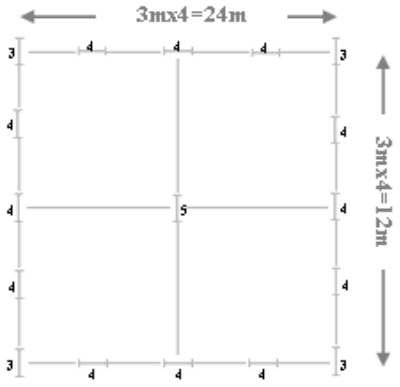

(e) Plan view of 17-20th storey

Figure 6.19 Plan views of twenty-storey, 1860 member steel space frame

Optimum design problem of this irregular steel frame is solved by using harmony search and ant colony optimization algorithms considering warping and without considering warping cases. In these algorithms, following search parameters are used: number of ants = 200, number of cycles = 400, controlling parameter of visibility (β) = 0.30, minimum local update coefficient (ξ_{min}) = 0.7, strategy of changing in the number of static ant = constant, number of static ant = 150, number of ranked ant= 20, harmony memory size (HMS) = 50, pitch adjusting rate (PAR) = 0.3, harmony memory considering rate (HMCR) = 0.9, error strategy of harmony search = adaptive error strategy and maximum iteration number = 80000. The minimum weights, maximum constraints values and W-section designations of the optimum designs obtained from each of these algorithms are illustrated in Table 6.10. It is apparent from tables that the consideration of the warping effect increases the minimum weight of the frame 28.76% in the case of the ant colony optimization algorithm, 25.70% in the case of the harmony search algorithm. These amounts are the highest differences among all examples because geometric shape of the frame is more irregular and the frame is the tallest among all. Moreover, harmony search and ant colony algorithms find optimum designs whose weights are quite close to each other. The differences are only 0.98 % in the case where the effect of warping is not considered (ant colony optimization algorithm is better) and 1.42 % in the case where the effect of warping is considered (harmony search algorithm is better). Design histories of these solutions are also shown in Figure 6.20.

Table 6.10 Design results of the twenty-storey, 1860 member steel space frame

Group number	Group type	ACO without warping	ACO with warping	HS without warping	HS with warping
1	Beam	W250X80	W310X38.7	W250X58	W360X44
2	Beam	W410X85	W310X38.7	W410X53	W360X44
3	Column	W250X80	W410X53	W410X67	W410X85
4	Column	W360X79	W250X32.7	W460X60	W250X32.7
5	Column	W360X79	W760X484	W310X67	W530X138
6	Column	W250X131	W1000X321	W690X125	W1000X272
7	Column	W410X114	W530X92	W610X82	W530X85
8	Column	W410X114	W1000X494	W530X101	W1100X343
9	Column	W200X71	W760X173	W250X73	W410X85
10	Column	W200X71	W250X38.5	W310X60	W250X44.8
11	Column	W410X114	W1100X499	W530X123	W1100X499
12	Column	W250X131	W1100X499	W690X125	W1000X314
13	Column	W530X123	W840X193	W610X113	W530X101
14	Column	W410X114	W1100X499	W610X113	W1100X499
15	Column	W360X72	W1100X390	W530X74	W1000X321
16	Column	W460X74	W410X60	W410X85	W460X144
17	Column	W460X128	W1100X499	W760X134	W1100X499
18	Column	W460X144	W1100X499	W690X152	W1000X314
19	Column	W610X125	W840X226	W690X125	W760X185
20	Column	W410X114	W1100X499	W690X152	W1100X499
21	Column	W360X72	W1100X499	W530X92	W1100X499
22	Column	W760X147	W1000X249	W760X196	W1000X272
23	Column	W610X285	W1100X499	W760X173	W1100X499
24	Column	W610X82	W310X79	W920X238	W410X67
25	Column	W460X193	W610X195	W530X101	W530X196
26	Column	W200X71	W460X97	W360X44	W360X57.8
27	Column	W360X39	W200X71	W360X44	W200X71
28	Column	W410X67	W310X143	W460X52	W250X73
29	Column	W360X72	W1100X499	W610X101	W1100X499
30	Column	W760X147	W1000X249	W760X196	W1000X314
31	Column	W610X285	W1100X499	W1000X272	W1100X499
32	Column	W610X92	W360X79	W920X238	W460X74
33	Column	W460X193	W610X372	W1000X249	W1100X433
34	Column	W250X89	W690X140	W460X68	W610X153
35	Column	W360X39	W760X134	W530X92	W530X85
36	Column	W610X101	W840X251	W610X82	W1000X412
37	Column	W360X44	W250X58	W200X31.3	W690X152
38	Column	W360X44	W360X57.8	W250X38.5	W250X101
39	Column	W360X72	W610X82	W250X32.7	W250X49.1
40	Column	W360X72	W1100X499	W690X152	W1100X499
41	Column	W760X147	W1100X433	W920X201	W1100X343
42	Column	W610X285	W1100X499	W1000X272	W1100X499
43	Column	W610X92	W530X92	W920X238	W530X85
44	Column	W460X193	W1100X499	W1000X249	W1100X499
45	Column	W360X91	W690X140	W610X92	W1100X499
46	Column	W360X39	W1000X314	W610X92	W610X92
47	Column	W610X101	W920X342	W610X92	W1100X433

Table 6.10 Cont.

48	Column	W360X44	W690X240	W530X92	W1100X433
49	Column	W360X44	W530X66	W460X68	W610X113
50	Column	W360X72	W610X307	W610X101	W1100X390
51	Column	W360X72	W1100X499	W690X152	W1100X499
52	Column	W760X147	W1100X499	W920X201	W1100X499
53	Column	W920X342	W1100X499	W1100X343	W1100X499
54	Column	W610X92	W920X201	W920X238	W760X185
55	Column	W460X193	W1100X499	W1000X249	W1100X499
56	Column	W410X100	W1100X499	W610X101	W1100X499
57	Column	W410X114	W1100X343	W610X113	W610X92
58	Column	W610X101	W1100X433	W610X101	W1100X499
59	Column	W410X75	W1100X499	W530X92	W1100X433
60	Column	W360X44	W610X174	W530X85	W690X192
61	Column	W360X110	W1100X433	W610X101	W1100X390
62	Column	W360X72	W1100X499	W690X152	W1100X499
63	Column	W760X147	W1100X499	W920X201	W1100X499
64	Column	W920X342	W1100X499	W1100X343	W1100X499
65	Column	W610X92	W920X201	W920X238	W840X193
66	Column	W460X193	W1100X499	W1000X249	W1100X499
67	Column	W410X114	W1100X499	W610X101	W1100X499
68	Column	W690X125	W1100X343	W610X125	W920X238
69	Column	W610X101	W1100X433	W610X125	W1100X499
70	Column	W310X67	W360X44	W310X67	W410X100
71	Column	W200X71	W410X53	W410X53	W360X44
72	Column	W200X71	W530X150	W410X75	W610X155
73	Column	W410X75	W1100X499	W530X92	W1100X499
74	Column	W360X44	W1000X314	W610X113	W1000X296
75	Column	W530X123	W1100X499	W610X125	W1100X499
76	Column	W360X72	W1100X499	W690X152	W1100X499
77	Column	W760X147	W1100X499	W920X201	W1100X499
78	Column	W920X342	W1100X499	W1100X343	W1100X499
79	Column	W610X92	W920X201	W920X238	W1100X343
80	Column	W610X341	W1100X499	W1000X249	W1100X499
81	Column	W410X149	W1100X499	W1000X249	W1100X499
82	Column	W690X125	W1100X343	W760X173	W1100X343
83	Column	W610X101	W1100X433	W760X173	W1100X499
84	Column	W410X67	W920X223	W610X125	W840X299
85	Column	W360X72	W760X134	W530X66	W530X85
86	Column	W460X82	W920X289	W410X75	W1000X494
Minimum weight(KN)		5570.1	7172	5624.55	7069.9
Maximum top storey drift (cm)		8.56	3	9.54	2.1
Maximum inter-storey drift (cm)		0.461	0.15	0.462	0.15
Maximum strength constraint ratio		0.937	0.9	0.819	0.956
Maximum number of iterations		80000	80000	80000	80000

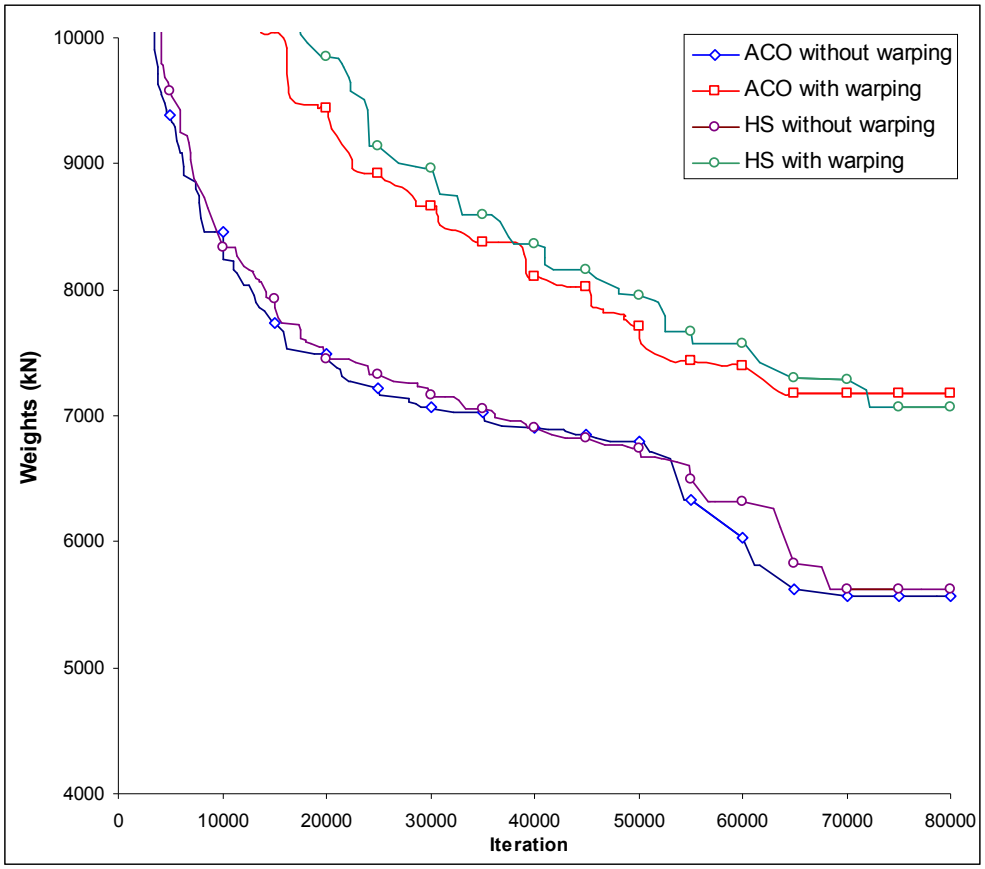

Figure 6.20 Design histories of the twenty-storey, 1860 member steel space frame

6.7 Discussion

In this chapter, six design examples are presented. Among these design examples two of the frames are selected as regular space frames while the remaining four have irregular plans. The reason of selecting some of the frames with symmetrical plans was to find out whether the consideration of the effect of warping in their optimum design is important or not. Furthermore the effect of frame heights to the warping is also investigated. The minimum weights obtained from these examples with and without considering effect of warping by using ant colony optimization and harmony search methods are tabulated in Table 6.11. Relative differences among these weights are also shown in Figures 6.21 and 6.22. It is concluded

that from Table 6.11 that the effect of warping causes considerable amount of increases in the optimum weight of the frame both for regular and irregular structures. This increase varies approximately between 9% and 29% which clearly indicates that the effect of warping should be considered in the optimum design of steel frames where the frame members are made out of thin walled sections. It is interesting to notice that even in frames with symmetrical plans the increase in the optimum weight is around 9%. Another clear conclusion is the height of the frames. In the first and third example where the number of storey is less than five, the effect of warping causes around 10% increase in the optimum weight of the frame. However, these increase rises up to 15 % and 25 % in fourth and last examples respectively where the number of storey is twenty. Both in the second and fifth examples the effect of warping causes around 10% increase in the optimum weight of frame, despite of the fact that number of storey of these frames is different. Hence in the design of tall frames the effect of warping is more serious and needs to be taken in to account in the design process. As far as the efficiency of both metaheuristic techniques is considered it is difficult to make apparent conclusion. In the first, third and fourth design examples harmony search algorithm performs better than ant colony optimization algorithm. However in the second and fifth design examples, ant colony optimization algorithm presents better performance than harmony search method. In the last example, results obtained from these algorithms are close to each other. This is due to the stochastic nature of these algorithms. The values selected for the parameters of the algorithms have an effect in the performance of these techniques. One conclusion can be made regarding this matter that before deciding the optimum design several runs are required to be made with different values of the algorithm parameters to find out which set of values give better result.

Table 6.11 Comparison of the minimum weights (kN) of all design examples

Examples	ACO without warping	ACO with warping	HS without warping	HS with warping	% difference warping causes (ACO)	% difference warping causes (HS)	% difference between methods without warping	% difference between methods without warping
1st example	48.68	53.42	46.63	51.78	9.74	11.04	4.40	3.17
2nd example	265.38	287.66	278.196	307.384	8.40	10.49	4.83	6.86
3rd example	568.24	618.38	560.714	617.36	8.82	10.10	1.34	0.17
4th example	3191.15	3589.73	2943.811	3452.697	12.49	17.29	8.40	3.97
5th example	1899.3	2079.2	1987.2	2107.77	9.47	6.07	4.63	1.37
6th example	5570.1	7172	5624.55	7069.9	28.76	25.70	0.98	1.44

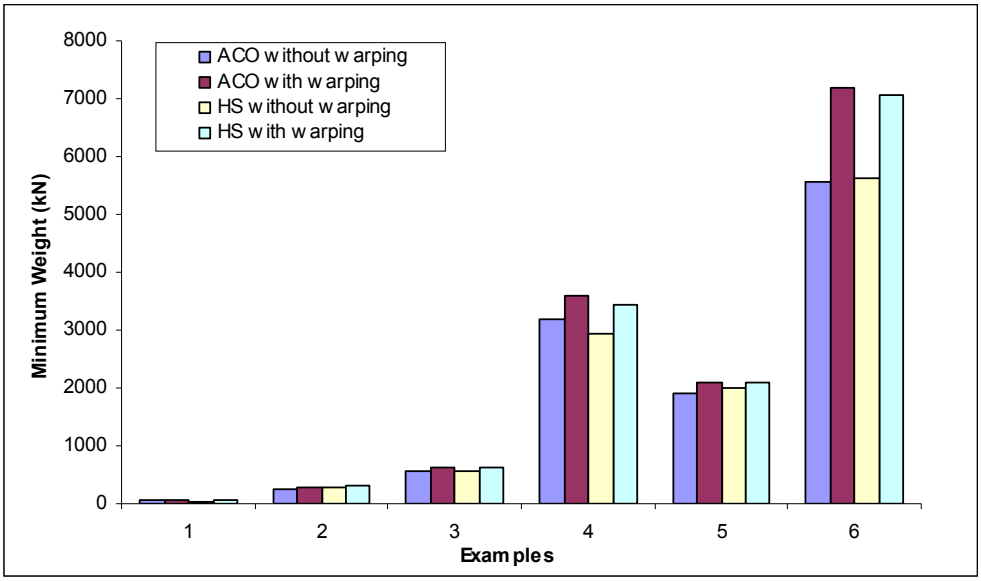

Figure 6.21 The effect of warping in the optimum design of six steel space frames

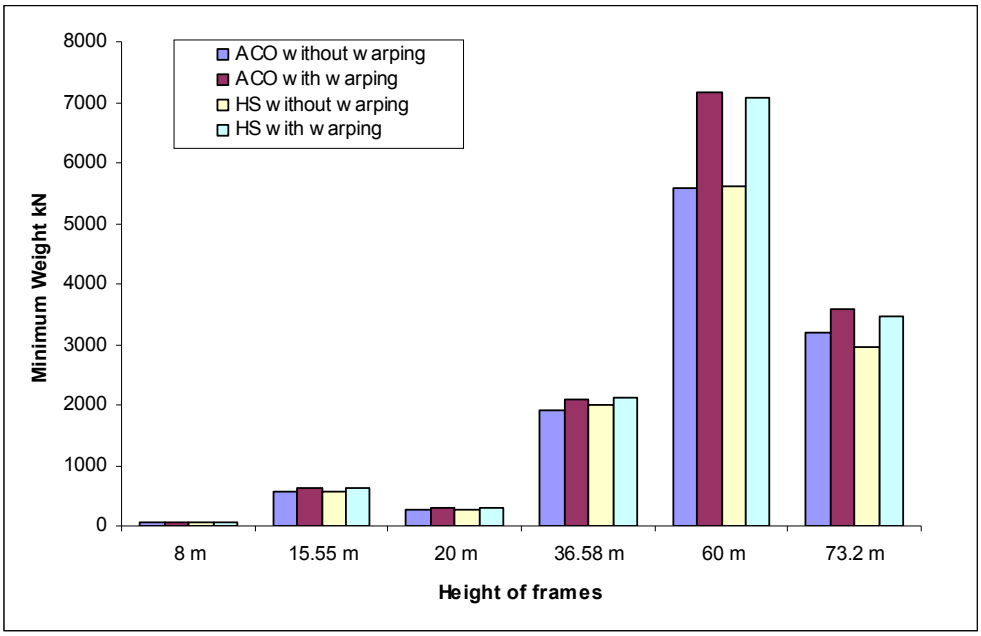

Figure 6.22 Comparison of the effect of warping with respect height of frame

CHAPTER 7

SUMMARY AND CONCLUSIONS

In this thesis, the effect of warping in the optimum design of steel space frame is investigated. This second order torsional effect causes considerable stress increase in thin walled members. This effect even becomes vigorous in tall steel buildings that have unsymmetrical plans. Considering this fact and that the frame members in steel buildings are generally made out of thin walled sections, it becomes apparent that carrying out an optimum design in such buildings without considering the effect of warping in steel structures does not yield realistic results. This thesis involves in developing an optimum design algorithm for steel space frames based on recent metaheuristic techniques of combinatorial optimization so that effect of warping in the optimum design can be investigated. For this reason, a computer program is developed which has the capability of carrying out analysis of space frames under various loading cases provided that steel sections for its members are assigned from W-section list. The program has also ability of carrying out design checks specified in LRFD-AISC. Furthermore it also has the capability of using two metaheuristic combinatorial optimization techniques by which it is possible to determine the optimum W-section designation for the frame members so that the weight of the frame is the minimum and it satisfies all the design limitations described in the steel design code.

The optimum design of steel frames requires selection of steel profiles from the available list for the frame members. This selection should be carried out such that

the design code specifications are to be satisfied and the cost or the weight of the frame is the minimum. Hence in the formulation of the optimum design problem of steel space frames the sequence numbers of W-sections given in LRFD-AISC are treated as design variables. The design limitations that consist of serviceability and strength constraints are implemented from LRFD-AISC. Evaluation of strength constraints necessitates the $P-\Delta$ analysis of the frame which is an iterative process and quite time consuming. Instead LRFD-AISC suggests a short way to determine the magnified values of bending moments. This is included in the program developed as described in the design code. The design problem obtained formulated in this way turns out to be a discrete combinatorial optimization problem. The recent metaheuristic techniques based on natural phenomena are proven to be effective in finding the solutions of such problems. For this reason, the harmony search and ant colony optimization algorithms are selected to determine the solution of the optimum design problem. Although it is shown in the literature that these methods are efficient in finding the solution of discrete optimization problems, in some cases particularly in large scale design problems they may perform not as expected. In the thesis some improvements are suggested for both of these techniques which enhanced their convergence rate as well as finding better results.

Six design examples considered in order to determine the effect of warping in the optimum design of steel space frames revealed one fact clearly. In the optimum design of steel space frame where the frame members are made out of thin walled sections the effect of warping should be considered within its analysis and the design of its members. It is found that even in frames where floor plan is symmetrical and does not change from one storey to another the minimum weight is almost 10% heavier than the optimum design where the effect of warping is not considered. This increase even rises in steel space frames where the floor plan is unsymmetrical and the overall shape of the frame is irregular. This clearly indicates that ignoring the effect of warping in the optimum design of steel space frames does not yield realistic results. Furthermore, the height of frame is another

factor which plays an important role in making the effect of warping more serious. Particularly in tall and irregular steel space frames consideration of the effect of warping yield 25% increase in the minimum weight of the frame. This clearly shows that the effect of warping should certainly be considered in the optimum design of such frames. Two of the metaheuristic techniques namely ant colony optimization and harmony search methods both are effective in finding the optimum solution of the design problem. In some design examples harmony search method found lighter optimum frames while in some other ant colony optimization method reached better optimum frames. Hence it is difficult to conclude that one technique out performs another. Both techniques require selection of values for their parameters initially and their performance is very much dependent upon these initial values as well as type of the optimum design problem under consideration. It is necessary to carry out several runs to find out which set of these parameters can find better solution. This is why in some design problems one technique performs better while in some others the other can reach a better solution. There are some suggestions for the automation of the parameters. However, this topic is currently under investigation and research is being carried out in order to find out how these parameters can be left to the algorithm so that depending on the design problem they can be automatically adjusted during the design cycles. Consequently it is not possible with the results obtained in this study to come up with conclusion which states that among two metaheuristic techniques used one is better than the other.

7.1 Recommendations for future work

In this study, only W shapes of LRFD-AISC are used. However, in some applications especially in large size structures the available steel profiles may not be sufficient to produce the optimum design under the design constraints specified by the design code and steel build up members may be required to be used. The design algorithm developed can be extended to cover the built up sections.

Dimensions of these sections such as the depth, flange width and thickness, web thickness can also be taken as design variables in the optimum design of space frame problems. This adds another practical future to the optimum design algorithm developed.

It is possible to carry out enhancements in the ant colony optimization and harmony search algorithm in order to improve their performance. It is shown that the performance of these techniques is dependent upon the initial values selected for their parameters. Both algorithm can be improved to have adaptive scheme where these parameters are decided and adjusted within the algorithms themselves during the design process so that they have better convergence rate.

Although the minimum weight is an important target to take as an objective function in the optimum design of steel frames, it is known that the minimum weight design is not the minimum cost design. In steel structures the cost is closely related with the weight in transportation and erection of steel members, the member connections such as beam-to-column connection and welding is not related to the weight. Therefore the objective function in the developed algorithm can be extended to include the cost of steel frame.

Both ant colony optimization and harmony search algorithms are found to be capable of finding solutions of large scale tall steel space frames. However they both have some disadvantages. For example, ant colony optimization has a good performance at the beginning of the search but then in later stages it faces stagnation. On the other hand, the harmony search algorithm finds it difficult to fill the harmony memory matrix with feasible solutions particularly in the case of geometric constraints at the initial stages of the design cycles but once the harmony memory matrix is filled then its performance becomes much better towards the final stages of the design iterations. If these techniques are combined together in order to develop a hybrid optimization technique, it may give better results in frame optimization problems.

Shear cores and shear walls are used in the tall building to provide greater stiffness to the building in resisting the lateral loads. These members also decrease the effect of warping. It is interesting to study the effect warping in the optimum design of tall building having shear core or shear wall.

REFERENCES

[1] Krishna, V. (2009). "*Structural Optimization Using Ansys Classic and Radial Basis Function Based Response Surface Models*." MSc Thesis, The University Of Texas At Arlington.

[2] Dantzig, B.G., and Thapa M.N. (1997) . "*Linear programming.*" Springer-Verlag, New York, USA

[3] Bellman, R. (1957). "*Dynamic Programming.*" Princeton University Press. Dover paperback edition (2003), ISBN 0486428095.

[4] Kuhn, H.W., and Tucker, A.W. (1951). "*Nonlinear programming.*" Proceedings of 2nd Berkeley Symposium. Berkeley: University of California Press., 481–492.

[5] Zoutendijk, G. (1960). "*Methods of feasible direction methods.*" Elsevier.

[6] Duffin, R.J., Peterson, E.L., and Zener, C. (1967). "*Geometric programming.*" Wiley, New York.

[7] Caroll, C.W. (1961). "*The created response surface technique for optimizing non-linear restrained systems.*" Oper. Res., 9 2, 169-184.

[8] Fiacco, A.V., and McCormick, G.P. (1968). "*Non-Linear Programming: SequentialUncon- strained MinimizationTechniques.*" Wiley, New York.

[9] Dorigo, M. (1992). "*Optimization, Learning and Natural Algorithms.*" (in Italian), Phd thesis, Dipartimento di Elettronica e Informazione, Politecnico di Milano, IT.

[10] Reeves, C.R. (1993). "*Modern Heuristic Techniques for Combinational Problems.*" Blackwell Scientific Publications, 1993.

[11] Paton, R. (1994). "*Computing with Biological Metaphors.*" Chapman & Hall, USA.

[12] Xie, Y.M., and Steven G.P. (1997). "*Evolutionary Structural Optimization.*" Springer-Verlag, Berlin, Germany.

[13] Van Laarhoven, P.J.M., and Aaarts, E.H.L. (1998). "*Simulated Annealing, Theory and Applications."* Kluwer Academics Publishers, Boston, USA.

[14] Matheck, C. (1998). "*Design in Nature: Learning from Trees.*" Springer-Verlag, Berlin, Germany.

[15] Adami, C. (1998). "*An introduction to Artificial Life.*" Springer-Verlag/Telos,

[16] Flake, G.W. (2000). "*The Computational Beauty of Nature.*" MIT Press, USA.

[17] Mitchell, M. (1998). "*An Introduction to Genetic Algorithms.*" The MIT Press, USA.

[18] Melanie, M. (1998). "*An Introduction to Genetic Algorithms.*" MIT Press, USA.

[19] Goldberg, D.E. (1998). "*Genetic Algorithm in Search Optimization and Machine Learning.*" Addison Wesley Publishing Co. Inc., Reading, MA, USA.

[20] Dasgupta, D. (1999). "*Artificial Immune Systems and Their Applications.*" Springer-Verlag, Berlin, Germany.

[21] Bonabeau, E., Dorigo, M., and Theraulaz, G. (1999). "*Swarm Intelligence: From Natural to Artificial Systems.*" Oxford University Press, U.K.

[22] Dorigo M., Caro G.D., and Gambardella L.M. (1999). "*An Algorithm for Discrete Optimization.*" Artificial Life, 5, 137-172

[23] Flake, G. W. "*The Computational Beauty of Nature*." MIT Press, USA, 2000

[24] Kennedy, J., Eberhart, R., and Shi, Y. (2001). "*Swarm Intelligence*", Morgan Kaufmann Publishers.

[25] Geem, Z.W., and Kim, J.H. (2001). "*A New Heuristic Optimization Algorithm: Harmony Search.*" Simulation, 76, 60-68.

[26] Kochenberger, G. A., and Glover, F. (2003). "*Handbook of Meta-Heuristics.*" Kluwer Academic Publishers.

[27] De Castro, L. N., and Von Zuben, F. J. (2005). "*Recent Developments in Biologically Inspired Computing*." Idea Group Publishing, USA.

[28] Dreo, J., Petrowski, A., Siarry P., and Taillard, E. (2006). "*Meta-Heuristics for Hard Optimization*." Springer-Verlag, Berlin, Heidelberg.

[29] Geem, Z. W. (Editor) (2009). "*Music-Inspired Harmony Search Algorithm; Theory and Applications.* " Studies in Computational Intellige, 191.

[30] Load and Resistance Factor Design. (2001). "*Structural Members Specifications Codes, Third edition, Volume 1*." American Institute of Steel Construction.

[31] TS 648. (1980). "*Çelik Yapıların Hesap ve Yapım Kuralları*." Türk Standardları Enstitüsü.

[32] Haftka, R. T., and Grandhi, R. F. (1986). "*Structural shape optimization*." A survey Computer Methods in Applied Mechanics and Engineering 57(1), 91-106

[33] Saka, M.P. (2007). "*Optimum Design of Steel Frames using Stochastic Search Techniques Based on Natural Phenomena.*" A Review Civil Engineering Computations: Tools and Techniques Saxe-Coburg Publications.

[34] Prager, W., and Shield, R. T. (1967). "*A general Theory of Optimal Plastic Design.*" J. Appl. Mech., 34, 184-186

[35] Lin, C. C., and Liu L. W. (1989). "*Optimal Design Based on Optimality Criteration for Frame Structures.*" Computers and Structures , 24, 375-384

[36] Saka, M. P., (1991). "*Optimum Geometry Design of Trusses by Optimality Criteria Method.*" Computers and Structures, 38, 83-92

[37] Rahsedi, R., and Moses, F. (1986). "*Application of Linear programming to Structural Sysdtem Reliability*" Computers and Structures, 24, 375-384

[38] Rajev, S., and Krishhnamoorty, O.S. (1992). "*Discrete Optimization of Structures Using Genetic Algorithms* ", J. Struct. Eng., ASCE, 118, 1233-1250.

[39] Koumousis, V.K., and Georgious, P.G. (1994). "*Genetic Algorithms in Discrete Optimization of Steel Truss Roofs*", Journal of Computing in Civil Eng'g., ASCE, 8, 309-325.

[40] Adeli, H. and Kumar, S. (1995). "*Distributed Genetic Algorithm for Structural Optimization*", J. Aerospace Eng, ASCE, 8, 156-163.

[41] Camp, C.V., Pezeshk, S., and Cow, G. (1998). "*Optimized Design of Two-Dimensional Structures Using a Genetic Algorithm*", J. of Structural Engineering, ASCE, 124, 551-559.

[42] Pezeshk, S., Camp, C.V. and Clem, D. (2000). "*Design of Nonlinear Framed Structures Using Genetic Optimization*", J. of Structural Eng, ASCE, 126, 382-383.

[43] Kameshki, E.S., and Saka, M.P. (2001). *"Optimum Design of Nonlinear Steel Frames with Semi-Rigid Connections Using a Genetic Algorithm"*, J. of computer and Structures, 79, 1593-1604.

[44] Erbatur, F., Hasançebi, O., Tutuncil, I., and Kilci, H. (2000). "*Optimum Design of Planar and Space Structures with Genetic Algorithms*", J. Computers and Structures, 75, 209-224.

[45] Kameshki, E.S., and Saka, M.P. (2001). "*Genetic Algorithm Based Optimum Bracing Design of Non-Swaying Tall Plane Frames*", J. of Constructional Steel Research, 57, 1081-1097.

[46] Saka, M.P. (2003). "*Optimum Design of Pitched Roof Steel Frames with Haunched Rafters by Genetic Algorithm."* J. Computers and Structures, 81, 1967-1978.

[47] Kameshki, E.S., and Saka, M.P. (2003). *"Genetic Algorithm Based Optimum Design of Nonlinear Planar Steel Frames with Various Semi-Rigid Connections"*, J. of Constructional Steel Research, 59, 109-134.

[48] Saka, M.P. (1998). "*Optimum Design of Steel Grillage Systems Using Genetic Algorithms*", Computer-Aided Civil and Infrastructure Engineering, 13, 233-238.

[49] Saka, M.P., Daloglu, A., and Malhas, F. (2004). "*Optimum Spacing Design of Grillage Systems Using a Genetic Algorithm"*, Advances in Engineering Software, 31, 863-873

[50] Luh, G-C., and Chueh, C-H. (2004). "*Multi-Objective Optimal Design of Truss Structure with Immune Algorithm*", J. Computers and Structures, 82, 829-844.

[51] Bennage, W.A., and Dhingra, A-K. (1995). *"Single and Multi-Objective Structural Optimization in Discrete-Continuous Variables Using Simulated Annealing"*, Int. Jour. for Num. methods in Eng'g., 38, 2753-2773.

[52] Leite, J.P.B., and Topping, B.H.V. (1999) "*Parallel Simulated Annealing for Structural Optimization*", J. Computers and Structures, 73, 545-569.

[53] Xie, Y.M., and Steven, G.P. (1997). "*Evolutionary Structural Optimization*", Springer-Verlag, Berlin, Germany.

[54] Evolution vs. Creationism. (2005). "*An Introduction. Eugenie Carol Scott*." University of California Press, ISBN 0520233913

[55] Goldberg, D.E., (1989). "*Genetic Algorithms in Search, Optimization and Machine Learning.*" Addison-Wesley Publishing Co. Inc

[56] Rechenberg, I. (1973). "*Evolutions strategie, Optimierung technischer Systeme nach Prinzipien der biologischen Evolution.*" Frommann-Holzboog.

[57] Schwefel, H.P. (1981). "*Numerical Optimization of Computer Models.*" Wiley.

[58] Rajasekaran, S., Mohan, V. S., and Khamis, O. (2004). "*The Optimization of Space Structures using Evolution Strategies with Functional Networks.*" Engineering with Computers, 20, 75-87.

[59] Ebenau, C., Rottschäferb J., and Thierauf, G. (2005). "*An Advanced Evolutionary Strategy with Adaptive Penalty Function for Mixed Discrete Structural Optimization.*" Advances in Engineering Software, 36, 29-38.

[60] Hasançebi, O., Çarbaş, S., Doğan, E., Erdal, F., and Saka, M.P. (2009). "*Performance Evaluation Of Metaheuristic Search Techniques In The Optimum Design Of Real Size Pin Jointed Structures.*" Computers and Structures, 87, 284-302

[61] Kirkpatrick, S., and Gelatt, C. D. (1983). "*Optimization by Simulated Annealing.*" Vecchi, M. P. Science, New Series, 220, 671-680.

[62] Balling, R.J. (1991). "*Optimal Steel Frame Design by Simulated Annealing.*" Journal of Structural Engineering, ASCE, 117, 1780-1795.

[63] May, S.A., and Balling, R.J. (1992). "*A Filtered Simulated Annealing for Discrete Optimization of 3D Steel Frameworks*." Structural Optimization, 4, 142-148.

[64] Topping, B.H.V., Khan, A.I., and Leite, J.P.B. (1993). "*Topological Design of Truss Structures Using Simulated Annealing*", Editors: BHV Topping and AI Khan, Neural Networks and Combinatorial Optimization in Civil and structural Engineering, Civil-Comp Press, 151-165.

[65] Hasançebi, O., and Erbatur, F. (2002). "*On Efficient Use of Simulated Annealing in Complex Structural Optimization Problems*." Acta Mechanica, 157, 27-50.

[66] Hasançebi, O., and Erbatur, F. (2002). "*Layout Optimization of Trusses Using Simulated Annealing.*" Advances in Engineering Software, 33, 681-696.

[67] Fourie, P., and Groenwold, A. (2002). "*The Particle swarm Optimization Algorithm in Size and Shape Optimization*." Structural and Multidisciplinary Optimization, 23, 4, 259-267.

[68] Perez, R.E. and Behdinan, K. (2007). "*Particle Swarm Approach for Structural Design Optimization*." Computers and Structures, Doi:10.1016/j.compstruc. 2006.10.013.

[69] Glover, F. (1989). "*Tabu search-part I ORSA."* J Comput 1(3), 190–206.

[70] Wikipedia, the free encyclopedia (2010). http://en.wikipedia.org/wiki/Tabu_search Last accessed date April 16th, 2010.

[71] Degertekin, S. O., Hayalioglu, M. S., and Ulker, M. (2007). "*Tabu search based optimum design of geometrically non-linear steel space frames*",Structural Engineering and Mechanics, 27(5), 575-588.

[72] Degertekin, S.O., Saka, M.P., and Hayalioglu, M.S. (2008). "*Optimal load and resistance factor design of geometrically nonlinear steel space frames via tabu search and genetic algorithm*" ,Engineering Structures , 30(1), 197-205.

[73] Değertekin, S.Ö., Ülker, M., and Hayalioğlu, M.S. (2006). "*Uzay Çelik Çerçevelerin Tabu Arama ve Genetik Algoritma Yöntemleriyle Optimum Tasarımı*", Teknik Dergi-TMMOB İnşaat Mühendisleri Odası, 17(3), 3917-3934.

[74] Değertekin, S.Ö., Hayalioğlu, M.S., and Ülker, M. (2006). "*Geometrik Olarak Lineer Olmayan Uzay Çelik Çerçevelerin Tabu Arama Yöntemiyle Optimum Tasarımı*", Sigma Mühendislik ve Fen Bilimleri Dergisi, 6(1), 107-118.

[75] Değertekin, S.Ö., Ülker, M., and Hayalioğlu, M.S. (2007). " *Uzay Çelik Çerçevelerin Tabu Arama Yöntemiyle Optimum Tasarımı.*" XV. Ulusal Mekanik Kongresi, Isparta.

[76] Schmit, L. and Fleury, C. (1980). "*Discrete-Continuous Variable Structural Synthesis Using Dual Methods.*" AIAA Journal, 18, 1515-1524.

[77] Templeman, A.B., and Yates, D.F. (1983). "*A Sequential Method for Discrete Optimum Design of Structures*." Engineering Optimization, 6, 145-155.

[78] Venkayya, V.B., Khot, N.S., and Berke, L. (1973). "*Application of Optimality Criteria Approaches to Automated design of large Practical Structures*." Second Symposium on Structural Optimization, AGARD-CP-123, 1-3 to 3-19.

[79] Saka, M.P. (1990). "*Optimum Design of Pin-Jointed Steel Structures with Practical Applications.*" Journal of Structural Engineering, ASCE, 116(10),2599-2620.

[80] Grierson, D.E., and Cameron, G.E. (1990). "*SODA-Structural optimization design and analysis*", Released 3.1 User manual, Waterloo Engineering Software, Waterloo, Canada.

[81] Chan, C.-M., and Grierson, G.E. "*An Efficient Resizing Technique for the Design of Tall Steel Buildings Subject to Multiple Drift Constraints.*" The Structural Design of Tall Buildings, John Wiley and Sons Ltd, West Sussex, England, 2(1), 17-32.

[82] Chan, C.-M. (1997). "How to Optimize Tall Steel Building Frameworks", Guide to Structural Optimization, ASCE Manuals and Reports on Engineering Practice No. 90, Ed: J.S. Arora, ASCE, New York, 9,165-196.

[83] Soegiarso, R., and Adeli, H. (1997). "*Optimum Load and Resistance Factor Design of Steel Space-Frame Structures.*" Journal of Structural Engineering, ASCE, 123(2), 184-192.

[84] Arora, J.S. (2002). "*Methods for Discrete Variable Structural Optimization*." Recent Advances in Optimum Structural Design, Ed. S. A. Burns, ASCE, USA, 1-40.

[85] Horst, R., and Pardolos, P.M. (Editors) (1995). "*Handbook of Global Optimization*." Kluwer Academic Publishers.

[86] Horst, R., and Tuy, H. (1995). "*Global Optimization; Deterministic Approaches.*" Springer.

[87] Dorigo, M., Maniezzo V., and Colorni, A. (1991a). "*Distributed optimization by ant colonies.*" Proc., 1st European Conf. on Artificial Life, MIT Press, Cambridge, Mass., 134–142.

[88] Dorigo, M., Maniezzo V., and Colorni, A. (1991). "*Positive feedback as a search strategy.*" Politecnico di Milano, Italy Tech. Rep. No., 91-016.

[89] Dorigo, M., Maniezzo V., and Colorni A. (1992). "*An investigation of some properties of an ant algorithm.*" Proc., 1992 Parallel Problem Solving from Nature Conf., Elsevier, Amsterdam, 509–520.

[90] Dorigo, M., Maniezzo V., and Colorni, A. (1996). "*The ant system:Optimization by a colony of cooperating agents.*" IEEE Trans. Syst.Man Cybern., 26(1), 29–41.

[91] Deneubourg, J.L., Pasteels J., and Verhaeghe, J. (1983). "*Probabilistic behaviour in ants: A strategy of errors*." J. Theor. Biol., 105,259–271.

[92] Deneubourg, J. L., and Goss, S. (1989) "*Collective patterns and decision making*." Ethol. Ecol.. Dipartimento di Biologia Animale e Genetica, Università di Firenze, Firenze, Italy. E, 1, 295–311

[93] Bland J.A. (2001). "*Optimal structural design by ant colony optimization*" Eng. Opt., 33, 425-443.

[94] Camp, C. V., and Bichon, B. J. (2004). "*Design of space trusses using ant colony optimization.*" J. Struct. Eng., 130(5), 741–751.

[95] Camp, C. V., and Bichon, B. J. (2005). "*Design of steel frames using Ant Colony Optimization.*" J. Struct. Eng., 131(3), 369-379.

[96] Geem, Z.W., Kim, J.H., Loganathan, G.V. (2002). "*Harmony search optimization: application to pipe network design.*" International Journal of Modeling and Simulation 22, 125–133.

[97] Lee, K.S., Geem, Z.W. (2004). "*A new structural optimization method based on harmony search algorithm.*" Computers and Structures 82, 781–798

[98] Lee, K.S., and Geem, Z.W. (2005). "*A new meta-heuristic algorithm for continuous engineering optimization: harmony search theory and practice.*" Computer Methods in Applied Mechanics and Engineering 194, 3902–3933.

[99] Geem, Z.W., Lee, K.S., and Tseng, C.-L. (2005). "*Harmony search for structural design.*" In: Proceedings of 2005 Genetic and Evolutionary Computation Conference (GECCO 2005), Washington, USA, 651–652.

[100] Geem, Z.W. (2006). "*Optimal cost design of water distribution networks using harmony search.*" Engineering Optimization 38, 259–280.

[101] Geem, Z. W. (Editor) (2009). "*Harmony Search Algorithm for structural design optimization.*" Studies in Computational Intellige, 219

[102] Saka, M. P., and Hasançebi, O. (2009). "*Adaptive Harmony Search Algorithm for Design Code Optimization of Steel Structures.*" 239, 79-120

[103] Vlasov, VZ. (1961). "*Thin-walled elastic beams.*" National Science Foundation, Washington, USA.

[104] Attard, M.M., and Somervaille I.J. (1987). "*Non-linear analysis of thin-walled open beams.*" Computers and Structures, 25(3), 437–43.

[105] Golturu, B.P. et al (2000). "*Torsion in Thin-walled cold-formed steel beams.*" Thin-Walled Structures, 37,127-145

[106] Chu, X-T, et al (2004). "*The Effect of Warping on the lateral torsional Buckling of Cold formed Zed Purlins."* ASME Journal of Applied Mechanics, 71, 742-744

[107] Tso, W. K., and Ghobarah, A.A (1971). "*Nonlinear non-uniform torsion of thin-walled beams.*" International Journal Mechanical science" 13, 1039-1047.

[108] Pi, Y. L., and Trahair, N. S (1995). "*Plastic-Collapse Analysis of Torsion*." Journal of Structural Engineering (ASCE) 121, 10, 1389-1395

[109] Pi, Y. L., and Trahair, N. S. (1995). "*Inelastic Torsion of Steel I-Beams.*" Journal of Structural Engineering (ASCE) 121, 609-620.

[110] Trahair, N. S., and Pi, Y. L. (1997). "*Torsion, bending and buckling of steel beams*." Engineering Structures, 19, 5, 372-377

[111] Trahair, N. S. (2005). "*Nonlinear Elastic Nonuniform Torsion*" Journal of Structural Engineering, 131, 7

[112] Al-Mosawi, S., and Saka, M. P. (2000). "*Optimum shape design of cold-formed thin walled steel sections*", Advances in Engineering Software, 31, 851-862.

[113] Strand 7 "*Finite Element Analysis FEA software*" Copyright Strand7 Pty Ltd.

[114] Aydogdu, I., and Saka, M.P. (2009). " Ant Colony Optimization of Irregular Steel Frames Including Effect of Warping", Twelfth International Conference on Civil, Structural and Environmental Engineering Computing, Civil-Comp Press. , Stirlingshire, UK, Paper 69

[115] Coates R.C., Coutine, M. G., and Kong, F. K. (1980). "*Structural Analysis , 2nd Edition.*" Vokingham, Berks., Van Nostrand Reinhold.

[116] Saka, M.P., and Aydogdu, I. (2007). "*Yanal yuklerin altinda duzensiz celik cercevelerin analizinde carpilma etkisinin incelenmesi*." XVII. Ulusal Mekanik Kongresi Isparta, 167-175.

[117] Zeng, L.F., and Wiberg, N. E. (1989). "*A Generalized Coordinate Method For The Analysis of 3D Tall Buildings* " Computers and Structures, 33(6), 1365-1977.

[118] AISC Design Guide 9 (2003). "*Torsional Analysis of Structural Steel Members.*" Second Edition.

[119] Saka, M.P., Aydoğdu I., and Hasançebi, O. (2010). "*Evaluation of recent improvements in harmony search based structural optimization algorithms*",

The Tenth International Conference on Computational Structures Technology, 14-17, Valencia, Spain.

[120] Kaveh A., and Shojaee, S. (2007). "*Optimal Design of Skeletal Structures Using Ant Colony Optimization*", Int. Jour. for Num. methods in Eng'g, 70, 563-581.

[121] Dorigo, M., and Gambardella, L. M. (1997a) "*Ant colonies for the traveling salesman problem.*" BioSystems, 43, 73–81.

[122] Dorigo, M., and Gambardella, L.M. (1997b). "*Ant colony system: A cooperative learning approach to the traveling salesman problem.*" IEEE Transactions of Evolutionary Computation, IEEE, NY, 1, Paper 1.

[123] Elshamli, A., Asmar, D., and Elmasri, F. (2003). "*Ant Colony PowerPoint*." Eng614-03-Ant Colony.

[124] Deb, K. (2000). "*An efficient constraint handling method for genetic algorithms.*" Comput. Methods Appl. Mech. Engrg., 186, 311–338.

[125] Homaifar, A., Lai, S.H.-V., and X. Qi (1994). "*Constrained optimization via genetic algorithms.*" Simulation 62 (4),242–254.

[126] Coello, C.A. (2000). "*Use of a self-adaptive penalty approach for engineering optimization problems.*" Comput. Ind. 41(2), 113–127.

[127] HE, S., Prempain, E., and Wu, Q.H. (2004). "*An improved Particle Swarm Optimizer for Mechanical design Optimization Problems.*" Engineering optimization, 36(5), 585-605.

[128] Ad Hoc Committee on Serviceability (1986). "*Structural Serviceability: A critical Appraisal and Research needs*", Journal of Structural Engineering, ASCE, 112(12), 2646-2664.

[129] ASCE 7-05 (2005). "*Minimum Design Loads for Building and Other Structures*".

[130] Çarbas, S., Aydogdu, I., and Saka, M.P. (2009). "*Optimum Design of Steel Frames Using Adaptive Harmony Search Method to LRFD-AISC*" 8th World Congress on Structural and Multidisciplinary Optimization, Lisbon, Portugal

CURRICULUM VITAE

PERSONAL INFORMATION

Surname, Name: Aydoğdu, İbrahim
Nationality: Turkish (TC)
Date and Place of Birth: 31 July 1980 , Burdur
Marital Status: Single
Phone: +90 312 210 44 53
Fax: +90 312 210 44 62
email: wwwfbe@metu.edu.tr

EDUCATION

Degree	Institution	Year of Graduation
BS	Akdeniz University Civil Engineering	2002
High School	Aldemir Atilla Konuk High School, Antalya	1998

WORK EXPERIENCE

Year	Place	Enrollment
2002-Present	METU Department of Engineering Sciences	Research Assistant

PUBLICATIONS

1. Saka, M.P., and Aydogdu, I. (2007). "Yanal yuklerin altinda duzensiz celik cercevelerin analizinde carpilma etkisinin incelenmesi." XVII. Ulusal Mekanik Kongresi Isparta, 167-175.

2. Çarbas, S., Aydogdu, I., and Saka, M.P. (2009). "*Optimum Design of Steel Frames Using Adaptive Harmony Search Method to LRFD-AISC*" 8th World Congress on Structural and Multidisciplinary Optimization, Lisbon, Portugal

3. Aydogdu, I., and Saka, M.P. (2009). " Ant Colony Optimization of Irregular Steel Frames Including Effect of Warping", Twelfth International Conference on Civil, Structural and Environmental Engineering Computing, Civil-Comp Press. , Stirlingshire, UK, Paper 69

4. Saka, M.P., Aydoğdu I., and Hasançebi, O. (2010). "*Evaluation of recent improvements in harmony search based structural optimization algorithms*", The Tenth International Conference on Computational Structures Technology, 14-17, Valencia, Spain.

HOBBIES

Swimming, Basketball, Computer Technologies, Movies, Musi